Peter Bock

The vibrations of lignin

A discussion of the IR and Raman spectra of G-lignins and model compounds

Dissertation

Universität für Bodenkultur

Wien, 2020

ABSTRACT

Raman scattering is a spectroscopic technique which probes laser-induced vibrations of molecules. By rastering the sample, an image with chemical information of the sample can be obtained. Plant cell walls can be probed by Raman imaging with only little sample treatment, allowing for *in-situ* investigations of cell wall chemistry. Beside cellulose as a major wall component, lignin is found in nearly all vascular plants where it provides vessel stability, structural support and a defense against biotic stresses. Although called a polymer, lignin does not have a fixed chain sequence, it is rather composed of monomers linked in several ways. Although many monomers and substructures are known today, only a few are assigned to its vibrational spectra. This work presents a detailed assignment of the Raman and infrared spectra of guaiacyl (G) - lignin. It is shown that the Raman spectrum mainly shows coniferyl aldehyde and alcohol residues, which profit from strong signal enhancement. This amplification, common to all π-conjugated molecules, enables their tracking even at low concentrations, but aggravates the investigation of non-enhanced compounds. In addition, the lasers employed in Raman experiments can cause chemical changes in the sample which reveal details on the chemical structure of lignin. Infrared spectra are complementary to Raman spectra, less affected by π-conjugated molecules and therefore required for a detailed investigation of lignin. The assignment tables given herein enable researchers to interprete their spectra according to the latest findings of lignin research. Raman imaging will see more and more applications in science and society, as instrumentation gets smaller and cheaper. This work contributes to a better understanding of the vibrational spectra of aromatic compounds.

KURZFASSUNG

Mittels Ramanspektroskopie können Molekülschwingungen untersucht werden, die typischerweise durch einen Laser angeregt werden. Durch das Abtasten entlang mehrere, nebeneinander liegender Linien kann ein Bild erzeugt werden, dass sämtliche chemische Information der Probe enthält. Die Methode erfordert vergleichsweise wenig Probenvorbereitung, sodass die Chemie pflanzlicher Zellwände *in-situ* untersucht werden kann. Neben Zellulose ist Lignin eine der Hauptkomponenten der Zellwand. Es kommt in fast allen Gefäßpflanzen vor und bietet neben Schutz gegen Pflanzenfresser, Pilze und andere Schädlinge vor allem strukturelle Festigkeit der Gefäße. Obgleich Lignin als Polymer bezeichnet wird, hat es im Unterschied zu solchem keine feststehende Abfolge von Einheiten, es ist vielmehr aus den immer gleichen Untereinheiten aufgebaut, die auf verschiedene Weise miteinander verbunden sein können. Trotz der Fülle der heute bekannten Unterstrukturen des Lignins ist sein Schwingungsspektrum relativ schlecht beschrieben. In dieser Arbeit wird eine detaillierte Beschreibung der Raman- und Infrarotspektren von Guaiacyl (G) – Lignin präsentiert. Im Zuge der Untersuchung hat sich herausgestellt, dass das Ramanspektrum von Lignin hauptsächlich Coniferylaldehyd und –alkoholgruppen zeigt, da diese stärkeres Signal liefern. Diese Signalverstärkung, welche allen Molekülen mit konjugierten π-Elektronensystemen gemein ist, erlaubt die Detektion selbst geringer Mengen dieser Substanzen, erschwert jedoch die Untersuchung von Molekülen, denen diese Verstärkung nicht zuteil wird. Darüber hinaus wurde beobachtet, dass die verwendeten Laser die Probe beschädigen und dadurch die Messung verfälschen können. Dies kann jedoch auch ausgenutzt werden, um genauere Information über die chemische Natur von Lignin zu gewinnen. Infrarotspektren zeigen komplementäre Information zu Ramanspektren, sind weniger durch π-konjugierte Moleküle beeinflusst und daher für eine genaue Untersuchung von Lignin unabdingbar. Die mitgelieferten Bandenzuordungstabellen beinhalten die neuesten Erkenntnisse der Ligninforschung und sollten für zukünftige Forschung hilfreich sein. Durch die Verringerung von Preis und Größe von Ramangeräten wird diese Technik in Zukunft vermehrt in Wissenschaft und Gesellschaft angewendet werden. Diese Arbeit trägt dazu mit einem tieferen Verständnis der Schwingungsspektren von Aromaten bei.

Doktorarbeit, vorgelegt am Department für Nanobiotechnologie der Universität für Bodenkultur, Wien, zur Erlangung des Titels *Doctor rerum naturalium technicarum* (Dr. nat. techn.)

Betreuer:

Assoc. Prof. Dr.rer.nat. Notburga Gierlinger

Berater:

Univ.Prof. Dr. José Luis Toca-Herrera

Univ.Prof. Dipl.-Chem. Dr.rer.nat. Antje Potthast

Ich erkläre eidesstattlich, dass ich die Arbeit selbständig angefertigt habe. Es wurden keine anderen als die angegebenen Hilfsmittel benutzt. Die aus fremden Quellen direkt oder indirekt übernommenen Formulierungen und Gedanken sind als solche kenntlich gemacht. Diese schriftliche Arbeit wurde noch an keiner anderen Stelle vorgelegt.

Diese Arbeit wurde aus Mitteln des

Fonds zur Förderung der wissenschaftlichen Forschung im Rahmen eines START-Projekts mit der Nummer Y-728-B16

und des

Europäischen Forschungsrats im Rahmen eines ERC-Consolidator grants mit der Nummer 681885

finanziert.

LIST OF PUBLICATIONS

This thesis is based on the following publications:

Paper I

Martin Felhofer, Batirtze Prats-Mateu, Peter Bock and Notburga Gierlinger

Antifungal stilbene impregnation: transport and distribution on the micron-level

Tree Physiology 2018, Volume 38, Issue 10, Pages 1526–1537.

DOI: 10.1093/treephys/tpy073

Paper II

Batirtze Prats-Mateu, Peter Bock, Martina Schroffenegger, José Luis Toca-Herrera and Notburga Gierlinger

Following laser induced changes of plant phenylpropanoids by Raman microscopy

Scientific Reports 2018, Volume 8, Article number 11804.

DOI: 10.1038/s41598-018-30096-3

Paper III

Peter Bock and Notburga Gierlinger

Infrared and Raman spectra of lignin substructures: Coniferyl alcohol, abietin and coniferyl aldehyde

Journal of Raman Spectroscopy 2019, Volume 50, Pages 778-792.

DOI: 10.1002/jrs.5588

Paper IV

Peter Bock, Paula Nousiainen, Thomas Elder, Markus Blaukopf, Hassan Amer, Ronald Zirbs, Antje Potthast and Notburga Gierlinger

Infrared and Raman spectra of lignin substructures: Dibenzodioxocin

Journal of Raman Spectroscopy 2020, Pages 1 – 10.

DOI: 10.1002/jrs.5808

Introduction 1
1.1. Perspective 1
1.2. Lignin 2
1.3. Raman spectroscopy and imaging 7
1.4. Aim and Objectives 9
Methods 10
2.1. Spectroscopic Experiments 10
2.1.1. Reference substances 10
2.1.2. Raman spectroscopy and imaging 10
2.1.3. Infrared spectroscopy 11
2.1.4. UV-Vis spectroscopy 12
2.2. Quantum chemical simulations 12
2.3. Interpretation of vibrational spectra 12
Results and Discussion 16
3.1. Factors affecting Raman intensities 16
3.2. Laser influence on lignin band intensities 21
3.3. Lignin substructures and linkages from the spectral perspective 27
3.3.1. The aromatic ring 27
3.3.2. β-O-4' and free G-rings 28
3.3.3. β-5' 28
3.3.4. 5-5' and DBDO 29
3.3.5. 4-O-5' 29
3.3.6. β-β' 30
3.3.7. β-1' (spirodienones) 30
3.3.8. Cinnamyl alcohols 30
3.3.9. Cinnamaldehydes 30
3.3.10. Cinnamyl acids and esters 31
3.3.11. α-Carbonyls 31
3.3.12. Stilbenes 32
3.3.13. Flavonoids 32
3.4. IR and Raman spectra of G-lignin and their assignment 36
3.5. The extrapolation to non-G-lignins 53
Conclusion and Outlook 55
Literature 58
Appendix 69

Vnd dich züme io

das ien° icht e kome wen du

So magstu wol bestan

recht vor eyne~ gute~ man

Johannes Liechtenauer

gewidmet

Wilhelm Böhm

(19.04.1935 – 07.07.2019)

1

Introduction

The fundamental cause of the trouble is that
in the modern world the stupid are cocksure
while the intelligent are full of doubt.

Bertrand Russell

1.1. PERSPECTIVE

The ongoing severe forest fires in Australia illustrate once again the severity of climate change and its impact on our society. Policy makers have realized that the traditional ways our society and economy run, cannot be longer sustained. The increasing pressure from nature as well as from society has been reflected in political efforts to accomodate economy to a better environmental compatibility.

Very recently, the European commission proclaimed "The European Green Deal" by which Europe will take leadership in becoming the first climate neutral region of the world by 2050[1]. To achieve this, at least one trillion euros should be invested to the transformation into a green economy[2]. This project is by far not the only one. China has announced in the last five-year plan, that it wants a green developement, including transformation to sustainable energy production, reduction of water usage, and end employment of "functional zones" to protect arable land and ecological areas. Three hundred and twenty billion dollars have been budgeted for this project[3]. Furthermore, in South Korea, sustainability goals to transform the country's economy into a green economy within the next 60 years were proclaimed in 2008[4]. In the US, a resolution regarding a "Green New Deal" was introduced into the 116th Congress (H.Res.109) last year. It demands that in a ten-year effort, several goals and projects should be acchieved, including "spurring massive growth in clean manufacturing"[5].

According to the United Nations environment programme, a green economy is characterized as an economy where "growth in employment and income are driven by public and private investment into such economic activities, infrastructure and assets that allow reduced carbon emissions and pollution, enhanced energy and resource efficiency, and prevention of the loss of biodiversity and ecosystem services"[6].

Plants play a key role in such approaches, as they are the resource for many biomass conversion and biorefining technologies. Up to one third of plant biomass consists of lignin[7,8], which is the second most abundant polymer on earth[7,9,10]. Many recent reviews are therefore concerned with valorization of lignin[11-16]. Up to now, lignin has mostly been a by-product of the pulp and paper industry and burned for energy generation, although it would be an attractive raw material for synthetic building blocks, pharmaceutical precursors and polymer composites[17,18]. Spectroscopy can play an important role in characterizing both lignin in-situ as well as in the process stream of manufacturing processes. Furthermore, the high variability of lignin demands comprehensive approaches to study lignin in its natural environment. This can be achieved by Raman imaging[19], where a laser is used to obtain chemical information. The present work strenghtens the understanding of aromatic vibrational spectra and is an invaluable asset for anyone working with vibrational spectra of lignin.

1.2. LIGNIN

Around 450 million years ago, soon after plants conquered the continents, a new unbranched aromatic polymer entered the stage. This plant polymer is believed to be the common ancestor of three aromatic polymers: Cutin, suberin and lignin[20]. In the beginning, it could not be degraded by organisms and became a carbon sink, which in turn increased the oxygen/carbon dioxide ratio in the atmosphere[21]. It was hypothesized that this led to the concomitant appearance of giant insects[22]. The advantage for plants having lignin was manifold: The stability of plants is mainly based on maintaining pressure in a hydrostatic skeleton[23]. Water-conducting elements, the defining element of vascular plants, transport water from the roots to the shoot and are exposed to high negative pressures. They would simply implode without lignin[24]. Lignin therefore occurs in all vascular plants[10] and strong primary wall lignification was shown to correspond to weak hydraulic response and vice versa, meaning that highly lignified vessels maintained their conductance also under unfavorable conditions[25]. Furthermore, lignin hydrophobizes the cell wall, plays a major role in structural support and therefore also occurs in non-conducting tissues. In addition, it plays a defensive role in plants, as it is hard to digest for herbivores, inhibits growth of microorganisms and is often synthesized as wound response. Lastly, it glues different cells together and prevents wood decay. It is therefore not surprising, that this muli-purpose polymer is the second most abundant natural substance on earth and roughly one third of a plants biomass consists of lignin[7-10,26].

Lignin can occur in all layers of the cell wall. The highest lignin content is found in the S_3 layer, where it probably acts as a defense layer against microbial attacks often originating from the lumen. However, by volume, the main fraction of lignin is encountered in the S_2 layer[10].

Lignin is polymerized in a process called lignification, where the individual monomers are coupled together by a radical polymerization process[27]. Lignification starts in the corners of the primary cell wall, continues after cellulose and hemicellulose deposition in the S_2 and peaks after cellulose deposition in the S_3-layer of the cell wall. Monolignols are synthesized in the cell membrane, whereas the polymerization takes place in the cell wall[10]. The transport mechanism is still subject to debate. There is evidence for simple diffusion as well as for active transport[28]. Lignification is iniated by laccases and peroxidases, which are located in the cell wall. They seem to be rather

immobile, so that the monolignols somehow have to make their way to them[29]. *In-vivo* experiments demonstrated that artificially introduced monolignols were successfully incorporated into lignin[30] and lignin-oxidizing enzymes were even found to be active in dead cells. Lignification can therefore also occur postmortem[31] and it is therefore possible that suitable monomers "accidentially" get incorporated, if they occur at lignification sites[32]. Studies showed no preference or temporal pattern regarding the incorporation of H or G-units (see below) and there is a polarization in the lignification process observed, where the tangential cell wall oriented to the inner of the stem lignifies first[30]. While the monolignol synthesis and activation is under tight biological control[33], the actual polymerization step is not. It is only controlled by chemical means, however it is not random in a statistical sense, as the outcome of previous reactions as well as the chemical environment influence the ongoing process. "Random" as used in literature refers to the sequence not being predetermined. However, the plant can control the outcome by the spatial and temporal availability of monomers[27]. There are no sound arguments that indicate a process control by proteins as proposed by some scientists[34].

During the actual bond forming step, two chiral carbons (α and β) are formed per unit with no preference for one enantiomer over the other. Only the environment can influence the direction from which the second monolignol or water is attached to the quinone methide in the re-aromatization step (see Fig. 1B). The stereochemistry therefore seems to be entirely controlled by reaction kinetics. It is therefore absolutely unlikely that two lignin chains have exactly the same structure[27]. Nevertheless, stereochemistry can severly affect the resulting geometry and thus physiochemical properties, as shown in a computational study[35]. The grid-like synthesis pathway with many different routes toward the final monolignol allows the plant to cope with genetic mutations or other pathway obstructions[32].

During secondary wall formation, lignin and hemicelluloses are both deposited[36]; the dominating hemicellulose in dicots is xylan, in gymnosperms it is galactoglucomannan[37]. Lignin can cross-link with hemicelluloses both via ferulate residues (which also can undergo radicalization) or via bonding to sugar hydroxyl groups during quinone methide re-aromatization[36]. Direct NMR evidence for an alpha-ether linkage between lignin and carbohydrates[38] is opposed by a study, which did not find indication of covalent bonding, instead, electrostatic interactions are established by hydrophobic surfaces between xylan and lignin[39]. The reason might be that instrument sensitivity is not high enough to yet detect such rare covalent linkages[39,40]. In mature maize stems, no indication for pectin - lignin interactions was found[39].

In contrast to other polymers, lignin has an irregular sequence of structural units[27]. The reason for this irregularity is based on the formation process of the polymer: The first step is the homolytic cleaveage of hydrogen from the aromatic hydroxyl group. The unpaired electron can delocalize over almost the whole molecule, which is normally shown as several resonance structures (Fig. 1A). Electron distribution calculations support this picture[35]. In contrast to other polymerization reactions, the monomer radicals couple with each other at any of the positions and thus, a lot of different linkages can be created, as shown in Fig. 1C. Lignin structures are therefore highly variable. This structural variability is further increased by the plant's ability to introduce many different compounds into the polymerization process. Up to now, 35 different monomers could be identified

in natural lignins[32], these are the "classical three", p-coumaryl- (H), coniferyl- (G) and sinapyl (S) alcohol[41]; furthermore caffeoyl (C) and 5-Hydroxyconiferyl alcohol (5H)[42-44] as well as aldehyes and esters of the aforementioned. Even stilbenes[45], flavones[46-48] and ferulic acid amides[49] can be regarded as monomers. The number is further increased by acetylation of some of these, however not all of them are incorporated as inter-chain units, so only act as nucleation sites, that is as chain starters[32]. A survey on chemical structures showed that suitable structures contain a phenol unit with hydroxy groups *ortho* to it and have side chains with alcohol, aldehyde, amide or carboxylate ester functional groups[50]. Furthermore, energy barriers have to be in the same range as for the traditional monolignols, which could be shown for piceatannol to be the case[51]. It is therefore likely that the list has to be expanded in the future as research goes on[32]. Apart from phenolic units, glucosides can also be incorporated into the structure, but only if the precursor substance has a ring with two hydroxy groups (one for the glycosidic linkage, one for the radical generation)[52]. Despite this "anabolic plasticity"[10], the bulk of lignin in normal plants is still made up of the classical three monomers and their esterified analouges[32].

Given that the exact structure of the polymer is not defined, elucidation of lignin structures is even more important[27]. This is mostly done by analyzing the linkages. Fig. 1C shows possible linkages, the resulting structures and their relative distribution within a "typical" spruce lignin (which is a simplication as there is no "typical" lignin due to the high variance[10,32].

As can be seen from Fig. 1A, while there are several bond forming possibilites, certain linkages are chemically preferred over others (indicated as a higher percentage in the resulting polymer). It is also important to note that there is a difference between monomer - monomer and monomer - oligomer coupling. Monomers favor β-O-4' or β-β' coupling with each other (dehydrodimerization), precursors with unsubstituted 5-position have furthermore the possiblity to couple via β-5. In contrast to some texts, they do not 5-5' or 4-O-5' couple. This is limited to oligomers which often couple that way as there are no free β-carbons remaining on such units. This way is not open for S-units, so that β-O-4 linkages prevail in S-lignins. They are therefore less condensed and easier to cleave during pulping[27]. β-β' dimers are linked over 4-O-5' to the polymer[53]. While the discussed linkages result in dimers, specific trimers exist - dibenzodioxocin and spirodienone. Dibenzodioxocins (DBDO) are substructures where two 5-5' joined rings are both connected over a third coniferyl alcohol, this creates a characteristic 8-membered ring[54-56]. Given their nature, they cannot be generated from S-units. Contrary to popular belief, dibenzodioxocins are not branching points for lignin, neither are 4-O-5' linkages so that lignin should be regarded as an unbranched, linear polymer[57,58]. In spirodienones, one quinone methide is trapped by β-1 bonding. This prevents the final re-aromatization step normally occuring in the polymerization process and creates a hexadienone structure[59,60].

In spruce (*Picea abies*) lignin, the prevalent linkage form is β-O-4' (38-65%), followed by β-5' (9-25%) and β-β' (2-11%) structures. 4-O-5' (3-5%) and DBDO-linkages (2-8%) are found to a lesser extent. Coniferyl aldehydes (2-4%), -alcohols (1-4%) and spirodienonens (~2%) occur only in small amounts[60-67] (see Fig. 1C).

The monomeric composition of lignin differs between plant species. Softwood lignins are characterized by consisting mainly of G-units, whereas hardwood lignins are mixtures of S- and G-

units. Grasses additionally incorporate considerable amounts of H-units into their lignins[7,10,68]. Beside that, the composition also varies between tissues. Stress-induced lignins contain more H-units as do compression wood lignins and are therefore more condensed. Higher H-unit counts are probably caused by fast response of monomer synthesis which doesn't allow the full monomer synthetic pathway to be completed. Infected tissues can also show enrichment of S-units[69]. However, plants can sustain considerable variation of the S/G ratio, which shows the flexibility of the polymerization pathway[27]. Recently discovered C-lignins were found in seed coats. They are solely based on caffeoyl alcohol[43] and have different physiochemical properties due to their different chemistry[20]. In the subfamily of *cactoideae*, researchers found that not all genera use this novel lignin. While the majority of species had C-lignin in their seed coats, six species used 5H-derived lignins and many did not use these uncommon lignins at all, instead relied on traditional S/G-mixtures. In three species, no lignin could be detected. This was taken as evidence, that the evolution of lignin was not finished within this subfamily of *Cactacea*[70]. A great deal of lignin research has been performed by spectroscopic approaches (mainly nuclear magnetic resonance) requiring isolation of lignin fractions by various means, which was identified as an issue when transferring insights over to native lignin[27]. Ball milling was especially identified as a cause for undesired changes in the samples[71,72]. Raman spectroscopic imaging is a way, which can help in the elucidation of lignin and its distribution *in planta* and does not require ball milling or extraction procedures.

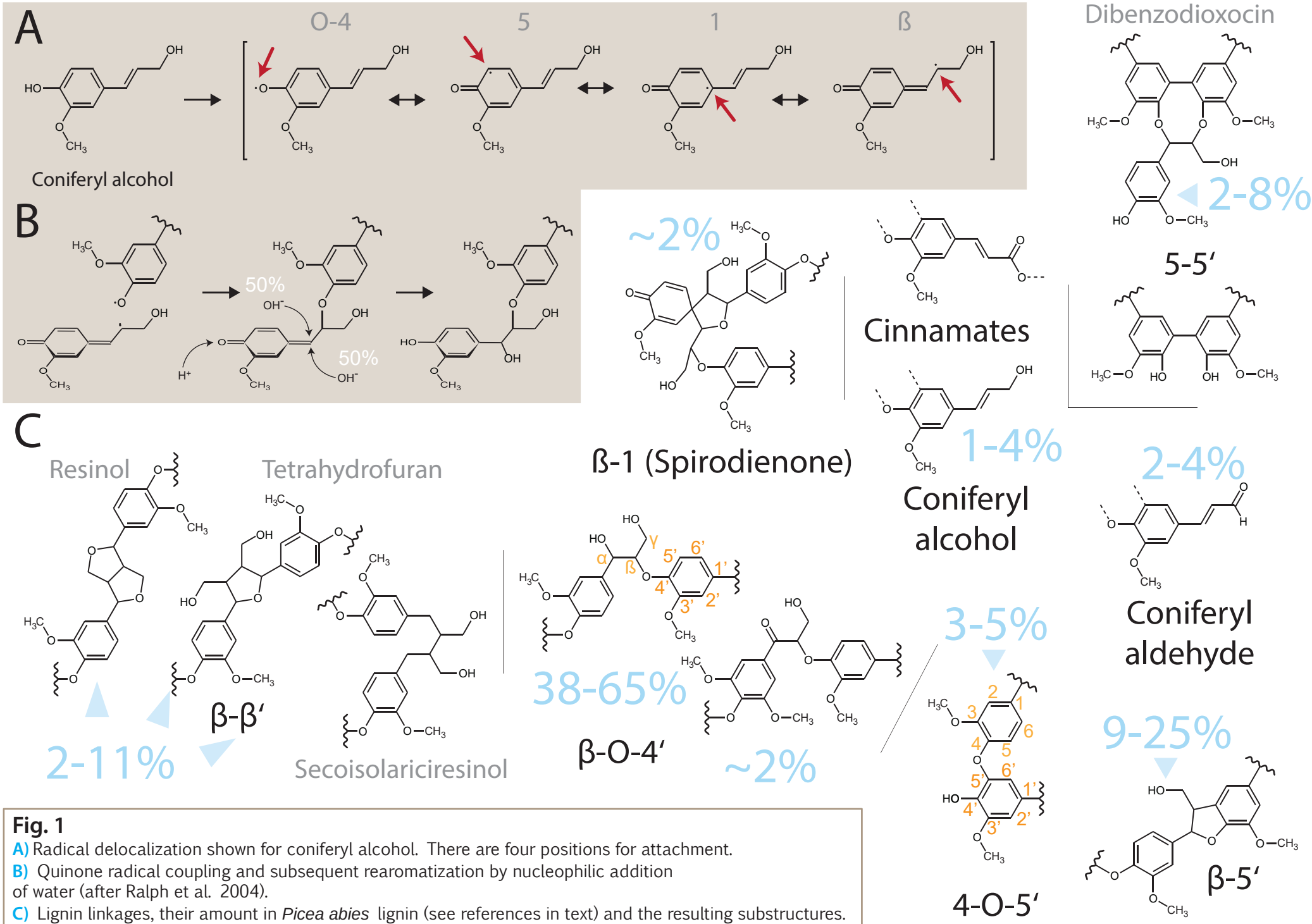

Fig. 1

A) Radical delocalization shown for coniferyl alcohol. There are four positions for attachment.

B) Quinone radical coupling and subsequent rearomatization by nucleophilic addition of water (after Ralph et al. 2004).

C) Lignin linkages, their amount in *Picea abies* lignin (see references in text) and the resulting substructures.

Bock. P., 2020. The vibrations of lignin. Doctoral thesis. Vienna.

1.3. RAMAN SPECTROSCOPY AND IMAGING

Raman spectroscopy probes chemical information encoded in molecular vibrations[73]. It can be employed in imaging systems, where a spectrum is obtained at every pixel of the image. This spectrum contains all chemical information of that point[74]. A typical system uses a laser to irradiate the sample and records the inelastic backscattering of the sample. This way, samples can be probed with little preparation, thus making Raman a non-invasive technique[75]. Consequently, Raman (imaging) has seen application in many fields of science, including materials sciences, where defects[76] or orientation in 3D[77] of materials were successfully probed. Also the degradation of lithium-ion batteries during charge cycles[78] was evaluated. Especially carbon nanotubes and other nano-carbon materials can be probed very well with Raman spectroscopy[79]. Individual carbon nanotubes were measured[80] as well as sheets of graphene, where stress and functionalization can be determined by Raman[81-84]. Raman imaging is used in pharmaceutics to determine distribution, concentration and state of a drug in addition to other characteristics, as reviewed by [85] and shown by [86] and [87]. The method is also employed in the analysis of minerals and rock[88-91] and is inarguably a valuable tool in medicine, where the advantage over traditional protocols/methods is that no labelling is required. Furthermore, information can be acquired live at the time of diagnosis or surgery and there is no radiation burden to the patient (cf. x-ray-based methods). In histology, malignant tissue can be discriminated from healthy tissue without chemical treatment before any cut is made – providing precise guidance for the surgeon[92]. This makes Raman imaging interesting to many fields of medicine and a lot of work has been undertaken to identify malignant tissue in different parts of the body, e.g. the *in-vivo* inspection of the gastrointestinal system by an endoscopic Raman probe[93]. Live-imaging of brain tissue with hand-held Raman instruments during cancer surgery greatly helps reducing the risk of missing infected tissue which would cause the cancer to reccur[94]. Similarily, in cardiology, attempts are made to help the surgeon to better assess the myocardial viability at the time of surgery[95] and to evaluate the degree of atherosclerosis[96-98]. Lung-tissue has been screened[99] as well as the surface of tooth enamel[100,101] and measurements have been undertaken on the living eye[102] showing that Raman spectroscopy will be part of future medical treatment.

Historical paintings on the ceiling of the Alhambra complex were studied[103] and the provenance of old banknotes could be clarified using Raman imaging[104]. Hand-held Raman spectrometers proved useful in studies of paintings and other exhibits[105]. Raman microscopes also entered forensic analysis, where gunshot residues, paint, blood and semen stains are investigated[106-110].

The Raman process has even been utilized to understand Raman quantum memory for computing applications[111] and Raman imaging played a part in identifying red blood cells in wound tissue of the 5300 year old Oetzi mummy[112]. The 3D-structure of a 53 million year old ant trapped in amber could also be resolved by x-ray Raman scattering[113].

Consequently, the potential of this method has also been applied to plant sciences[19,75,114-116] and a wide variety of plant material, including *Arabidopsis*[117-119], cereals[120,121], miscanthus[119,122], hemp[123], bamboo[124], fruits and vegetables[125-129] was studied. Flower[130], stem[131,132],

cuticles[117,133], leaves[121,132,134-136], roots[121,132,137,138], follicles[139,140], buds[141], pollen[142-144] and plant DNA were also studied[145] and attempts were made to detect plant stresses by Raman spectroscopy[146,147].

Specifically for wood, researchers have used Raman spectroscopy and imaging to investigate the cellulose microfibril angle orientation[148], to study heart wood formation[149-151] and to follow the decay by bacteria and fungi[152,153]. The effect of mechanical stress[154,155], (genetic) modification and functionalization on wood was studied[156-161] as well as the characteristics of thermomechanical wood pulps[162-165].

Especially lignin, which shows strong Raman signal[162] attracted attention of researchers. Several studies explored the variation of lignin content[118,166], the deposition within the cell wall[167,168] and its quantification[169]. The influence of the lasers used in the experiement on lignin was recognized early on[170,171] and subsequently utilized for laser delignification[163,172].

More specifically, attempts were made to characterize lignin by Raman spectroscopy, namely to assess the ratio of its syringyl and guaiacyl units[119,173-179] and to track cinnamyl alcohols and aldehydes within the cell wall and throughout lignification[157,180-182]. It was discovered that ethylenic (conjugated) residues exhibit much stronger Raman scattering[171]. Therefore, conjugated lignin substructures were extensively researched[183,184] and their spectral dominance was used as an advantage for quantification[165]. With the advances in instrumention and therefore a wider application of the method came the need for more detailed analysis of the vibrational behavior of lignin units[185]. This process, which continues to date, includes the recording of spectra of lignin-like molecules and substructures[163,164,167,179,183,184] as well as the computer-assisted interpretation of bands[186-192]. Interestingly, Raman spectra of the classical lignin monomers were not investigated in detail, although they were the only lignin substructures appearing in the assignment tables[163,185,193,194] and hence served as the main targets for lignin analysis in most studies[125,156,157,168,180,181,195]. In contrast, infrared (IR) assignment tables, which can also be used for interpretation of Raman spectra, include more features of the lignin polymer[196,197], although these assignments have never been transferred to the Raman tables. Taken together and given the number of possible lignin substructures (see section 3.3), the current assignments are not satisfying. It was therefore time to reassess the current assignments, close gaps of reference structures and incorporate new findings of lignin research into the tables. This might come also handy for cellulose research, as aged cellulosics also contain lignin-like aromatics as chromophores[198].

1.4. AIM AND OBJECTIVES

This work aims to

1) Increase the number of available reference spectra

2) Increase the vibrational understanding of the aromatic ring, which is the central group of lignin

3) Translate new findings of lignin structure research into assignment tables

2

Methods

Sô die bluomen ûz dem grase dringent
Same si lachen gegen der spilden sunnen
In einem meien an dem morgen fruo
Und diu kleinen vogellîn wol singent
In ir besten wîse die si kunnen
Waz wünne mac sich dâ gelîchen zuo?

Walther von der Vogelweide

2.1. SPECTROSCOPIC EXPERIMENTS

2.1.1. Reference substances

The majority of reference substances was purchased from Sigma Aldrich/Merck (Darmstadt, Germany). A few compounds are from Carl Roth (Karlsruhe, Germany) or were synthesized in-house or by collaborators.

2.1.2. Raman spectroscopy and imaging

The Raman microscope used in this work is an alpha 300RA system by WITec GmbH, Ulm, Germany.

The instrument can be equipped with various objectives, but most of the spectra presented here were acquired with either a 20x (NA 0.4) or 100x (NA 0.9) objective from Carl Zeiss, Jena, Germany. Two linear polarized lasers were available and used: A 532 nm laser (Sapphire SF, Coherent, USA) and a 785 nm laser by Toptica Photonics, Germany. Scattering was directed by an optic multifiber (50 µm for 532 nm, 100 µm for 785 nm experiments) to the spectrometer (UHTS 300, WITec, Ulm, Germany). This was equipped with blazed gratings and CCD cameras. For 532 nm experiments, a 600 g/mm and a 1800 g/mm blazed grating together with an DV401 BV CCD camera by Andor, Belfast, Northern Ireland was used, 785 nm measurements had a 600 g/mm and a 1200 g/mm blazed

grating with a CCD camera of the same manufacturer (DU401 DD) available.

The laser was coupled into the microscope and passed through the objective onto the sample. The backscattering was collected with the same objective and passed through a band pass filter to cut off the Rayleigh scattering. Both laser and Raman radiation polarization could be controlled by polarizers.

Measurements were conducted as single point measurments, as line scans and as mapping. Point distances, distribution, laser power and integration time were all set (often iteratively) to optimize the Raman signal.

Almost all reference substances were tested against laser-induced spectral artifacts and positive testing resulted in careful selection of measurement parameters to get the most unaffected spectrum possible.

For samples prone to laser degradation or fluorescence, water was used as a quenching agent.

Samples were typically available as powders or liquids and were mounted either on standard microscopic glass slides or in an aluminum dish. No enhancement effects by the aluminum (SERS) were observed. The sample amount mostly followed sample-handling-considerations. In most cases, a spatula tip, resulting in a volume of approximately 1 x 3 x 0.5 mm was used.

All polarizers were used to obtain information on polarized Raman modes as well as on orientation of the sample.

During the work period, a temperature controlled stage (PE120, LINKAM Scientific Instruments, Epsom, UK) was purchased and made available to the lab. This enabled the recording of Raman spectra in a temperature span of 268 - 393 K. If reference substances had a melting point (most were solid at room temperature) within this span, the spectra of the melt were also recorded. This proved useful to disrupt crystal order and accompanying effects on the Raman spectrum. Prior to the availability of this stage or in cases where this was not applicable, solvents (ethanol, acetone, isopropanol, DMSO) were used.

Spectra without artifacts, little fluorescence and a good signal to noise ratio were cut and baseline corrected (polynomial fit, normally 1-3 steps) in OPUS 7.0/7.5 software from Bruker (Billerica, USA).

2.1.3. Infrared spectroscopy

Infrared spectra were obtained using a Vertex 70 FT-IR spectrometer by Bruker with an ATR sampling unit. Solid stamples were measured with the pressure stamp (position 1) and subsequently dissolved in ethanol or aceton to break crystal structure and measured again without stamp. In most cases, this resulted in a thin film on the ATR crystal which gave better intensity than the pressed crystal sample.

Liquids were measured without stamp.

For every substance and condition (pure, with ethanol, ...), five spectra were recorded and averaged using OPUS 7.0/7.5 software from Bruker.

2.1.4. UV-Vis spectroscopy

Absorption spectra were recorded on a Hitachi U-2900 double-beam spectrophotometer (Hitachi High-Technologies, Japan). A spatula tip (<1 mg) was dissolved in ethanol (>99,5%) and measured in QS-cuvettes.

2.2. QUANTUM CHEMICAL SIMULATIONS

Vibrational analysis was performed with GAMESS and GAUSSIAN.

GAMESS[199,200]

Calculations were performed with gamess.2016-pgi-linux-mkl.exe on a work station with Microsoft Windows 10, 64-bit version. All calculations were done using the SCF-DFT functional B3LYP together with a 6-311G basis set. Structures were optimized in the programm to minimum energy and then used for vibrational analysis. The resulting local coordinates were visualized with the wxMacMolPlt program[201].

GAUSSIAN[202]

All calculations were performed by Thomas Elder (US Forest Service, Auburn, USA) using the Extreme Science and Engineering Discovery Environment (XSEDE), supported by the National Science Foundation grant number ACI-1548562, using the Stampede 2 supercomputer at the Texas Advanced Computing Center (TACC) via MCB-090159, Gregg T. Beckham as PI.

Optimization of the structures was carried out in Spartan '16 (Wavefunction Inc. USA) by performing a 1000 step Monte Carlo search with MMFF minimization. Unique conformations were further refined by a PM6 semi-empirical optimization in the same programm. GAUSSIAN 16, Revision A.03 was then applied to the 10 lowest energy conformations from the previous step. The B3LYP functional, the 6-311G basis set and a GD3 empirical dispersion correction as well as default values for optimization and grid size were used. The lowest energy conformation was used for spectral interpretation.

Calculations with both methods were always performed on single molecules in vacuo. No frequency scaling was applied. Most of the reference substances were calculated by GAMESS, some by GAUSSIAN, a few with both methods. This is because the possibility to calculate spectra with the latter method became available late in the course of this work.

2.3. INTERPRETATION OF VIBRATIONAL SPECTRA

There are several aspects for successful spectral interpretation.

The first aspect is knowledge about molecular vibrations, which can be found in classical books on this topic. For this work the following sources were mainly used: Varsanyi[203], Colthup et al.[73], Mayo et al.[204] and Harris and Bertolucci[205].

The second aspect is the spectroscopic experiment itself. Vibrational spectra reflect the molecule in its current conformation and environment[73]. It is therefore helpful to vary the conformation as well as the environment. While the former is often not directly controllable, it can be a consequence of

the latter, which is easy to vary. Changing temperature or adding solvents are easy ways of accomplishing this. Substances can change their state of matter or internal hydrogen bonds may be broken, both being useful for spectral interpretation. Polarization experiments are another way of obtaining information about a compound. Polarized Raman modes, which indicate vibrational symmetry[206] or overall sample orientation[207] are two ways of getting more information about the sample for interpretation.

The third aspect is the availability of good spectral library. There are commericial libaries available but it is generally useful to have a library developed for the specific research goals. This work is based on a library built around lignin-specific substructures with a focus on G-units.

The fourth aspect is the availability of local coordinate calculations. Nowadays, this is very easily done, as normal personal computers can calculate the vibrational spectrum of a small molecule within hours. Although such calculations are often performed on single molecules in vacuum (to save computation time), the calcualted spectrum often matches the experimental spectrum very well. Furthermore, up to the present time, this was the only method for investigating the normal modes of a molecule. Recent advances might provide an experimental approach in the future[208]. Getting an idea which atoms are involved in a mode is useful in designing follow up experiments to experimentally test the calculation. Lastly, a huge advantage of computational methods is that experiments can be simulated that cannot be carried out in the lab. Molecular conformations not testable in reality can be designed to understand how certain normal modes behave, for example, if angles are changed.

Additionally, three things have to be noted:

First is the assumption that *it is possible to measure lignin and model compounds by vibrational spectroscopy.*

Although vibrational spectroscopy is generally thought to be non-invasive, sample alterations can still occur (e.g. by multi-photon absorption[209]). Samples showed no degradation during IR-measurements as was checked by comparision to literature reference spectra.

Many samples were prone to photodegradation caused by the lasers used in the Raman experiments. This was seen as as strong increase in fluorescence and subsequent loss of signal (sample vaporized) or occurrence of carbon peaks indicating condensed carbon structures (sample burnt). Immersing a substance in water often allowed for increased measurement time before the sample was degraded. Furthermore, some compounds showed signs of laser degradation. Therefore, time-series experiments were always the first measurements on reference substances. These were a series of subsequent Raman measurements on the same spot. The conclusion that can be drawn is that vibrational spectroscopy is suited to measure lignin and lignin model compounds, however care has to be taken that no laser-induced spectral artifacts are recorded. See section 3.2 for details.

Second is the assumption that *there is no coupling between individual rings in lignin.*

If this assumption is true, then single ring reference compounds can be used to describe the spectrum of a polymer containing many rings. There is theoretical evidence that no coupling between ring modes exists in lignin. The reason is that mechanical coupling requires both bonds to have similar force constants[73]. This is not the case in the majority of the lignin structure, as can be seen by simple inspection of Fig. 2. Rings (with bond order 1.5) are well separated from each other

by carbon single bonds (bond order 1.0). The only exceptions are biphenyl substructures, where coupling can also be seen in their spectra (see **Paper IV** for details).

Second, IR spectra of lignin monomers and dimers match the polymer spectrum of lignin very well. This is shown in Fig. 2A. In the case of mechanical coupling new bands arising from the interaction would be expected (progression bands)[210].

The assumption therefore seems to hold.

Third is the approximation *that it is possible to describe the lignin spectrum by mainly considering aromatic normal modes*.

The reason for this simplification is that aromatic rings have 30 different normal modes, meaning that they contribute to virtually every wavenumber region in the spectrum. In addition, a number of these modes include substituents attached to the ring, so that the ring mode can be considered as a substituent mode instead. As can be seen later, even substituents of 2nd and 3rd order have an influence. Considering the lignin structure (Fig. 2B), it is evident, that in most cases the residual parts which do not have any atoms attached to the ring are quite small and surprisingly uniform. These are mainly methyl groups, ethanol-like and ethylenic residues. Their spectral footprint is expected to be rather small, because all of them contain C-H, C-C and C-O groups, which will occur in a rather narrow wavenumber region. Nevertheless, their band intensities can be quite strong, especially seen in the IR spectrum.

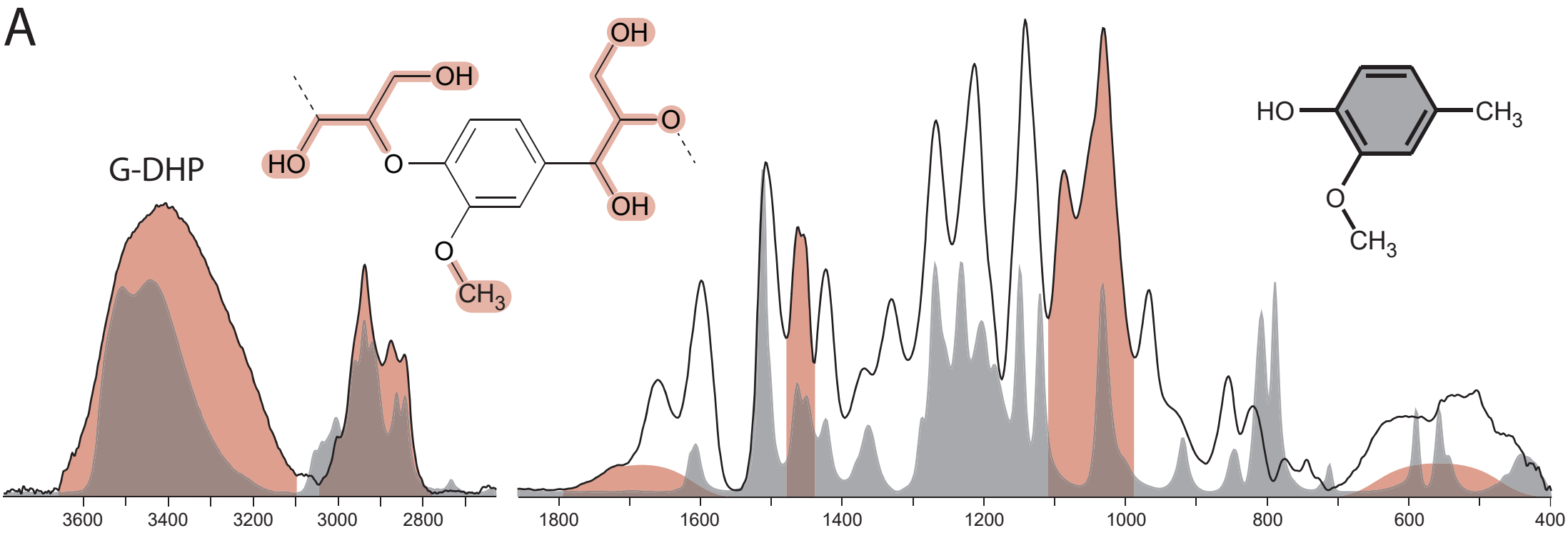

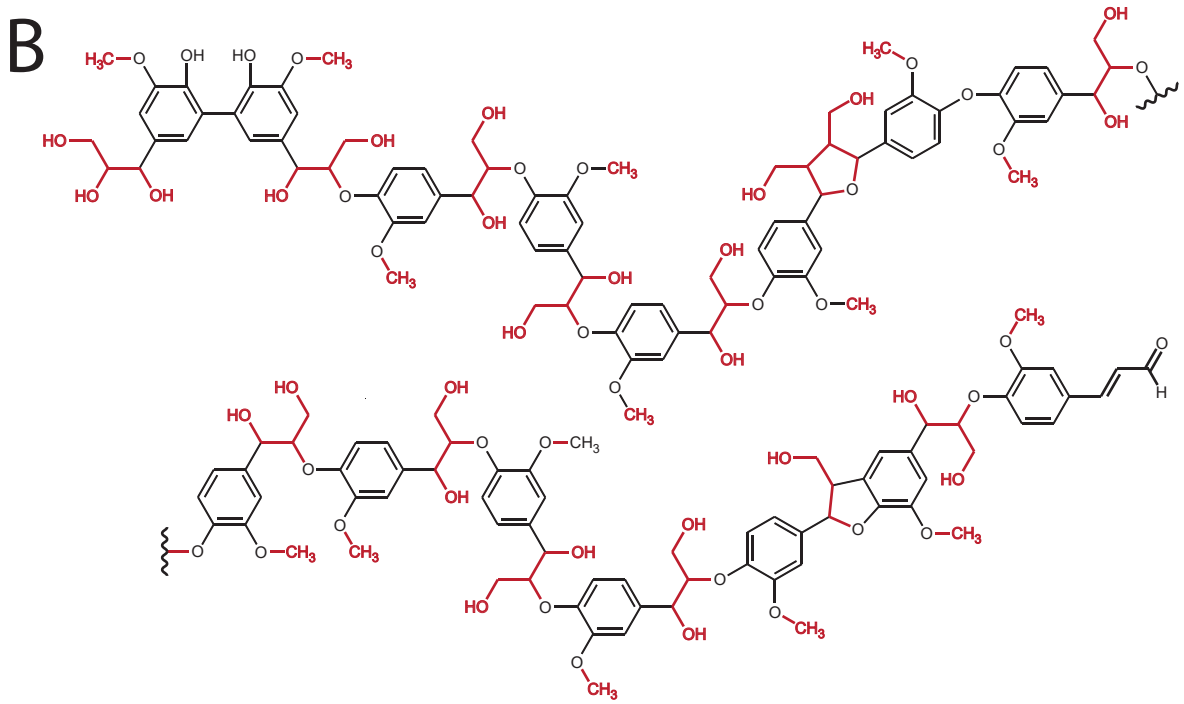

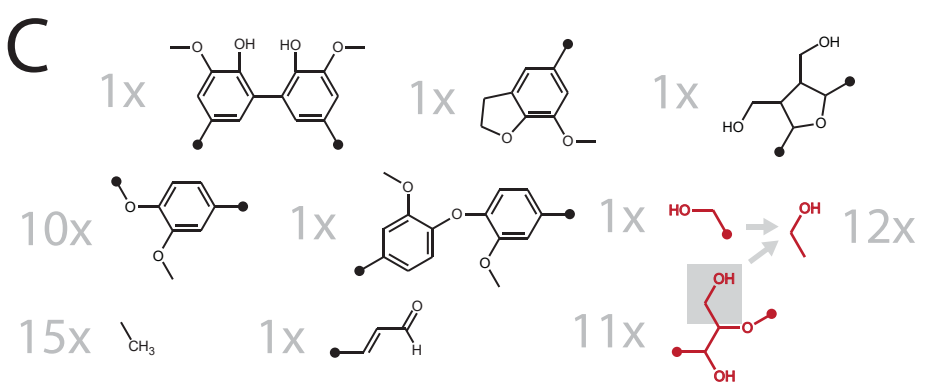

Fig. 2

A) IR spectra of G-DHP and 2-methoxy-4-methylphenol. Both spectra match well and many bands can already be explained with this simple model compounds. **B)** An example lignin structure. Aliphatic oscillators not being part of ring modes are highlighted in red. **C)** Dissection of the lignin chain into vibrational subgroups shows that the aliphatic oscillators are very similar, meaning that their contribution to the spectrum will occur in rather narrow band regions.

Bock. P., 2020. The vibrations of lignin. Doctoral thesis. Vienna.

3

Results and Discussion

Labor omnia vincit improbus.

Vergil

3.1. Factors affecting Raman intensities

Fig. 3A shows IR and Raman spectra of several lignin model compounds. While it is observed that the IR spectra look quite similar, there are two groups of Raman spectra. The reason is that certain enhancement effects act on some aromatic compounds.

It is therefore worth reiterating the factors affecting Raman intensity here:

The Raman intensity of Stokes scattering is given by Eq. 1.,

$$I_{Stokes} = konst \cdot I_0 \cdot \left(\omega_0 - \omega_{0,p}\right)^4 \cdot |\alpha|^2 \quad \textbf{(1)}$$

where I_o is the intensity of the incident light, $(\omega_0 - \omega_{o,p})$ is the frequency of the incident light and α the polarizability of the molecule[211].

Ways to increase Raman scattering are therefore to 1) increase the laser power, 2) decrease the excitation wavelength and 3) increase the polarizability of the molecule.

In a Raman experiement on the cell wall, all chemical compounds on the surface experience the same radiataion wavelength and intensity. It is therefore the individual polarizability of a molecule which governs the contribution to the recorded signal. This polarizability is a measure how easy an electron cloud can be deformed or displaced[206]. The polarizability increases with π-conjugation[212]. Considering the chemical structures occuring in lignin (see Fig. 1C) one can already expect that cinnamyl alcohols, cinnamyl aldehydes and other aromatic rings with ethylenic residues have higher polarizabilities and contribute more to the Raman signal.

Approaching an electronic transition with the excitation wavelength will increase the polarizability as well. This is called pre-resonance Raman scattering and is a gradual effect, meaning the closer the transition gets the larger the effect (Fig. 4A, D). If the excitation energy matches that of an electronic transition, it is called resonance Raman scattering[213]. Both effects are summarized in this work under "resonance enhancement". Conjugation decreases the HOMO-LUMO gap and redshifts the absorption of the pi-orbitals[205]. Conjugated compounds are thus more likely to exhibit stronger

Raman signal.

Another signal enhancing effect is observed when aromatic rings participate in π-electron conjugation and is often refereed to as conjugation enhancement. It is manifested in the spectrum as an intensification of two ring modes at 1600 cm^{-1} (Φ8a and Φ8b). It does not depend on the excitation wavelength (see Fig. 4D). This was explained as the polarizability change of a certain normal mode being distributed over the whole molecule while the normal coordinate is localized on the benzene ring[214-219].

Both effects were known to Bond[171], who studied these enhancement effects on model compounds, He found that the intensity of Φ8b decreased in the order coniferyl aldehyde > (α-, 4-dihydroxy-3-methoxyacetophenone ≈ coniferyl alcohol) > guaiacyl propanol at excitation wavelengths of 514.5, 647 and 1064 nm.

He further calculated the contribution of preresonance enhancement at 514.5 nm to be 68%, 37%, 30% and 8% respectively, for the substances listed above. Absorption experiments showed that a carbonyl or a carbon-carbon double bond red-shifted the absorption maxima and that a combination of both groups as in coniferyl aldehyde increased this shift even more. He therefore concluded that the preresonance enhancement was related to the length of the conjugation path, which was the longest in coniferyl aldehyde that therefore had the highest Raman intensity at 514.4 nm. He also related the intensity ranking at 1064 nm to the conjugation pathlength and assumed no preresonance enhancement at this wavelength.

Bond concluded that in wood, it must also be possible to measure the amount of conjugated compounds based on the intensity. He also expressed his surprise about the magnitude of enhancement in coniferyl aldehyde and about the fact that all compounds under study were able to absorb 514.5 nm photons although they had no absorption bands at or close to this wavelength (a solution to this is presented in section 3.2).

Around the same time as Bond published his work, researchers encountered problems when trying to explain strong Raman bands in compounds featuring extended π-conjugation. This intensification was also observed at excitation wavelengths far off-resonance and also the corresponding IR bands were strongly enhanced. Zerbi and Gussoni[220] proposed an explanation based on intramolecular charge transfer focussing on electron-phonon coupling. Up to this time, intramolecular charge transfer was seen as part of the conjugation enhancement effect[219]. Zerbi and Gussoni observed, that polyenes featuring an intramolecular charge transfer had those normal modes enhanced in IR and Raman, where the vibrational displacement mimic the geometry change induced by the charge transfer. Specifically, a charge-transfer results in a bond length change, because double bonds are shorter than single bonds. Going back and forth between both geometries (see Fig. 4D) changes the molecular geometry similar to a vibrational mode. Normal modes having the same displacement pattern can therefore couple to the electron-induced geometry change. Such modes, representing a bond-alternation-oscillation strongly coupled to the first allowed electronic transition, are called Я-modes. They are very strong in the Raman spectrum and "are also strongly activated in the infrared because of polarization of the molecular backbone by polar end groups." (see Figs. 3C,D and 4C)[221]. The effect is imagined as an internal electric field acting on the apolar charge distribution of the molecule. Cinnamaldehydes are Donor-π-Acceptor molecules which have an aromatic ground state but a quinoidal charge-transfer state[222]. Я-coordinates for two

cinnamaldehydes were defined and large internal fields were found[223,224].

Interestingly, although coniferyl alcohol and aldehyde contribute so strongly to the spectrum and are the only substructures of lignin which appear in the assignment tables, their spectra were never investigated in detail. Furthermore, athough the strong Raman bands of conjugated structures were repeatedly noted[163-165,171,183-185], the most affected band remained assigned to the aromatic ring stretch of lignin in general[163,185,193,225].

Paper III therefore aimed to re-evaluate previous findings on the Raman intensity with regard to wood spectra and to supply a detailed vibrational investigation of coniferyl alcohol, abietin and coniferyl aldehyde.

Surprisingly, in coniferyl alcohol crystals, the molecules were found to be arranged in a sheet-like fashion and Raman spectra showing different "sides" of the molecule could be obtained. This proved invaluable for the assignment process, which was otherwise based on literature and DFT calculations. It was therefore possible to present a detailed assignment for this molecule.

Spectra of abietin, which is the glycosylated form of coniferyl alcohol, showed the janiform nature of its spectra regarding its structural elements. While the Raman spectrum was insignificantly different from that of coniferyl alcohol, the IR spectrum showed a strong signal of the sugar moiety. This was the first experimental proof that in lignin, conjugated parts of a molecule can effectively render non-conjugated parts invisible in most regions of the spectrum.

Coniferyl aldehyde served as the model compound for cinnamaldehydes. H-bending of the aldehyde could be assigned to the spectrum as new marker band (1400 cm^{-1}) and the well-known 1135 cm^{-1} band was shown to originate from the aldehyde-specific C-C stretch. In addition, a controversy[164,226] regarding the C=O/C=C stretch assignment could be resolved.

Most important, it could be shown that the contribution of conjugated substructures of lignin extends beyond the previously recognized intensification of the ring stretch at 1600 cm^{-1}. As it turned out, most bands in the Raman spectrum stem from such conjugated moieties which leads to an underrepresentation of the bulk lignin structure. This implies two things:

1) Conjugated molecules can be studied very well using Raman spectroscopy owing to several signal enhancing mechanisms. This was used as an advantage in **Paper I** for tracking pinosylvins in wood.

2) These mechanisms are responsible for a stark overrepresentation of such molecules in the Raman 532 nm spectrum. The majority of unconjugated structures can best be estimated by the band around 800 cm^{-1}, although even their contribution of coniferyl aldehyde and similar compounds is present.

With four mono-substituted phenyl compounds it could be shown (Fig. 3C) that the charge-transfer enhancement acts on all those bands which represent normal modes involved in the charge transfer pathway. In contrast, conjugation enhancement only intensifies the members of ring stretch Φ8. The effect was also very pronounced in the IR spectrum, raising the question of how biased IR is towards Я-coordinates of lignin structures.

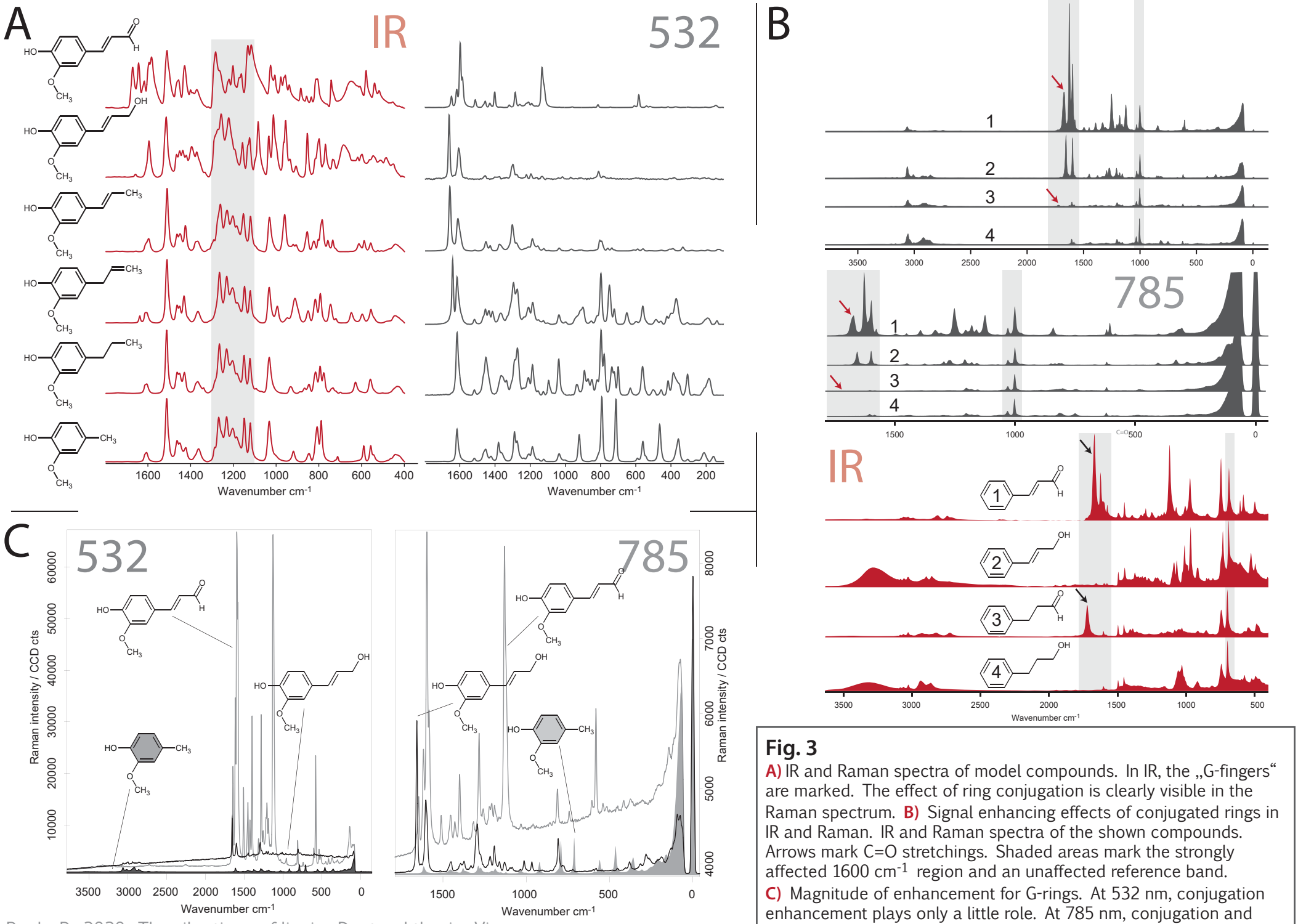

Fig. 3

A) IR and Raman spectra of model compounds. In IR, the „G-fingers“ are marked. The effect of ring conjugation is clearly visible in the Raman spectrum. **B)** Signal enhancing effects of conjugated rings in IR and Raman. IR and Raman spectra of the shown compounds. Arrows mark C=O stretchings. Shaded areas mark the strongly affected 1600 cm^{-1} region and an unaffected reference band.

C) Magnitude of enhancement for G-rings. At 532 nm, conjugation enhancement plays only a little role. At 785 nm, conjugation and charge-transfer enhancement have roughly the same magnitude.

Bock. P., 2020. The vibrations of lignin. Doctoral thesis. Vienna.

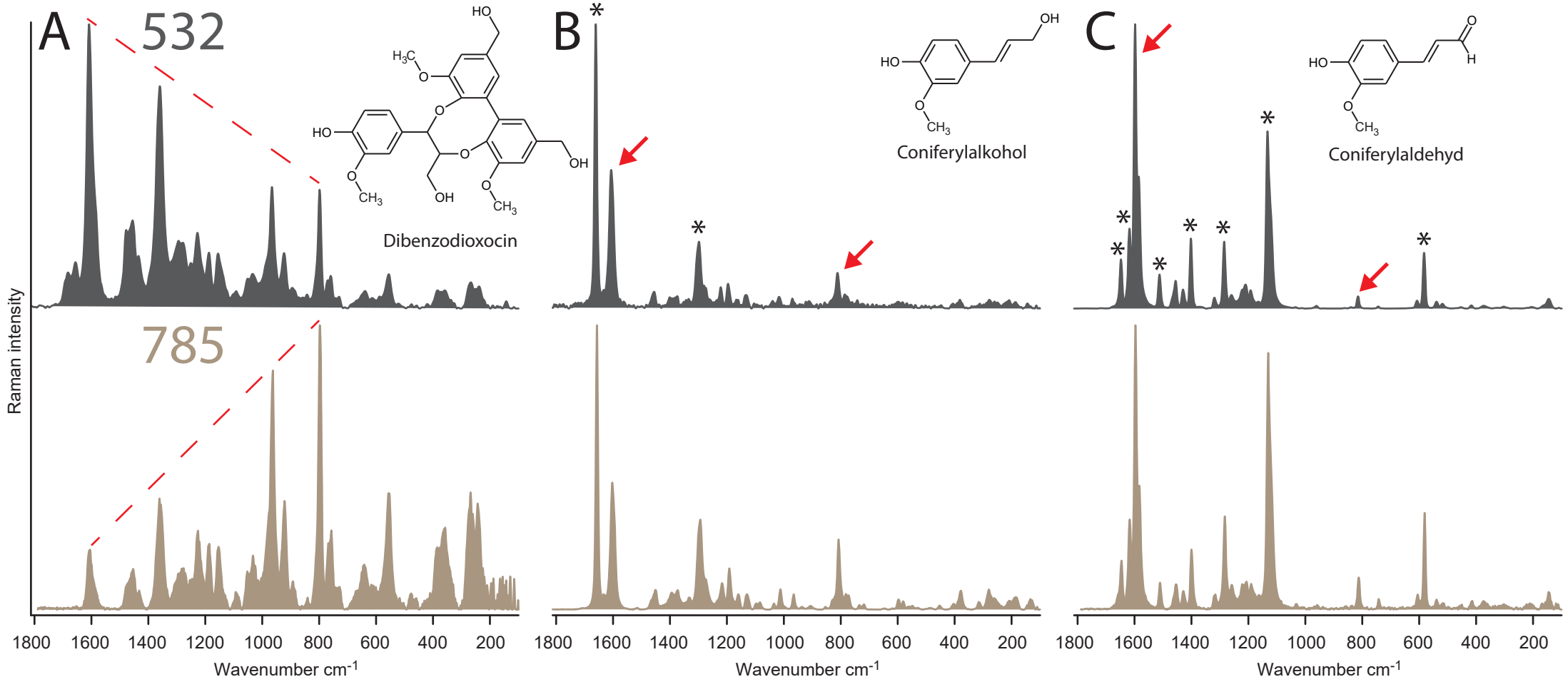

Fig. 4

A) Raman spectra of dibenzodioxocin recorded at 532 (upper panel) and 785 nm (lower panel). The difference in the ratio between 1600 and 800 cm^{-1} is visualized by the dashed line. This indicates preresonance enhancement being the only contribution to the signal. **B)** Spectra of coniferyl alcohol. At both excitation wavelengths, the ring stretch Φ8b at 1600 cm^{-1} is stronger than ring stretch Φ1 at 800 cm^{-1}. Beside this, only two modes of the C=C bond (marked by an asterisk) are intensified. This is a clear sign for conjugation enhancement. **C)** Spectra of coniferyl aldehyde. Φ8b at 1600 cm^{-1} is again stronger than Φ1 at 800 cm^{-1}. Additionally, all bands representing vibrations involved in the bond-length-alternation-oscillation (Я) are intensified too (marked by an asterisk). Preresonance enhancement has a lower share than in coniferyl alcohol.

D) Depiction of preresonance enhancement: The laser energy is close to an electronic transition. **E)** Charge-transfer resonance forms of coniferyl aldehyde. With numbers: The bond-length-alternation-oscillation (Я) coordinate (Bond designation and formula adapted after Castiglioni et al. 1993). Respective Я-bands are annotated.

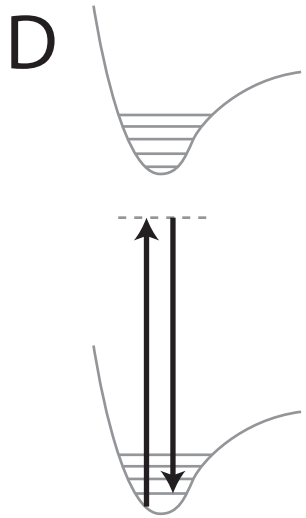

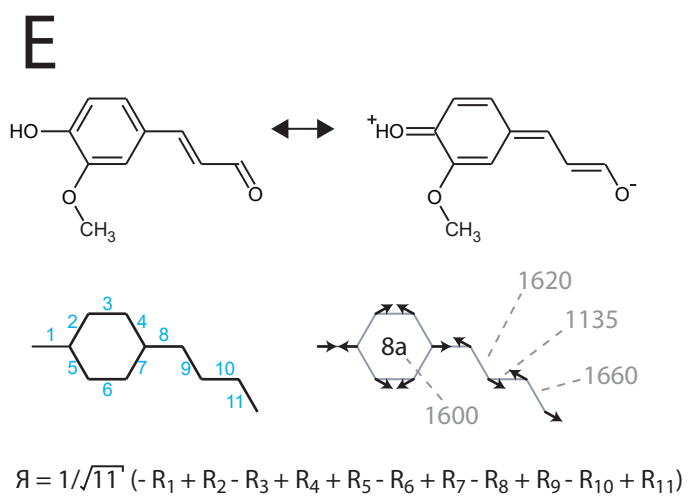

$$Я = 1/\sqrt{11}\,(-R_1 + R_2 - R_3 + R_4 + R_5 - R_6 + R_7 - R_8 + R_9 - R_{10} + R_{11})$$

Bock. P., 2020. The vibrations of lignin. Doctoral thesis. Vienna.

3.2. LASER INFLUENCE ON LIGNIN BAND INTENSITIES

Parallel to the several factors influencing intensity on the molecular level, it was also recognized early that measuring with high-powered lasers could introduce spectral artifacts at best and destroy the sample in the worst case. In one of the pioneering studies on Raman spectroscopy of wood, Bond[171] observed that the Raman bands decay over time when samples were measured in water. The decay followed an exponential pattern and was faster at 514.5 nm than it was at 647.1 nm. In contrast, measuring in dry atmosphere (air, O_2, N_2) did not result in band decay. Although he could not elucidate water's role in the decay process, he noted that it was an essential prerequisite. Consequently, he sought for ways to stabilize lignin against photodegradation. None of the treatments by acid chlorite or sodium borohydride alone, combinations of both, acetone washing followed by diethylenetriaminepentaacetic acid, methylation or quenching by potassium iodide or oxygen affected the decay process. The conclusion drawn was that either the treatment was not 100% effective or other structural features unaffected by his treatment are responsible for the decay. Only copper (II) chloride and immersion in glycerol proved successful in preventing decay of the 1600 cm^{-1} band, but both methods produce unwanted side reactions preventing their use. In summary, his attempts to stabilize native-state lignin to laser radiation were not successful. Furthermore, based on higher intensity of the 1600 cm^{-1} on dry samples, he concludes that: "These data suggest that a very rapid modification of the lignin macromolecule occurs in an aqueous environment." and that "water appears to be intimately involved both in lignin decay and reduction of background fluorescence".

After the extensive studies on laser effects by Bond[171], only one study exploited his findings in order to remove lignin by a laser[163]. The topic was not studied for 25 years until my colleagues Batirtze Prats-Mateu and Martin Felhofer rediscovered it. They noted that when restarting a Raman mapping with the same coordinates several times, the intensity of the 1600 cm^{-1} band complex (including the shoulder at 1620 cm^{-1} and the band at 1660 cm^{-1}) decreased. Furthermore, the decay of the band at 1660 cm^{-1} appeared to be much faster than that of the 1600 cm^{-1} band. This observation remained unnoticed in Bond's study, probably because his time series were in the range of hours, whereas our measurements in the range of seconds. He also did not study the decay behavior of lignin model compounds.

His results attributing spectral changes mainly to the 532 nm excitation, could be confirmed, as excitation at 785 nm did not affect the sample. A survey was therefore conducted on how the spectra of reference substances react to prolonged laser exposure (see **Paper II**). Since the decay was predominantly seen in the 1660 cm^{-1} band (see Fig. 5A), which is assigned to coniferyl alcohol and aldehyde structures, they were the compounds of choice. As it turned out, only 4-hydroxy-cinnamyl alcohols showed a decay behavior similar to that observed in wood after repeated measurements and the curves were similar to Bond's data, who already proposed that two processes are involved. Interestingly, among all substances, only those having both an arylic and aliphatic hydroxy group were prone to laser induced effects. Cinnamaldehydes were not affected. Moreover, the decay occured only in air, H_2O, D_2O and DMSO (attributed to its water content due to hygroscopicity). Ethanol, isopropanol and acetone seemed to prevent the photoreaction. The susceptibility of coniferyl alcohol was recognized earlier in UV-VIS absorption studies and since no radicals could be detected in the reaction, an alternative pathway was proposed[227,228]. In this process, a highly reactive quinone methide[229] is formed by addition of a proton to the aliphatic hydroxyl group. Two

results support the reaction mechanism:

1) A proton donor is needed, which is in line with the observation by Bond[171] and our experiments, that water is needed in the process. Air moisture or traces of water are sufficient. Acids should also work. It also explains, why isoeugenol is not susceptible: There is no OH-group to add the proton.

2) For the formation of the quinone, an aryl-hydroxy group is required. This explains why cinnamyl alcohol, abietin and eleutheroside B do not show a reaction. The oxygen is absent or obviously not capable of participating in the electron rearrangement.

However, studies of wood and DHP (dehydrogenation polymer) immersed in ethanol were not succesful in stopping photodegradation. It could be that hydroxyl groups of lignin sidechains or carbohydrates were still available for the reaction. Beside this, a band at 1630 cm^{-1} appeared and its origin could not be explained.

Also the reaction products could not be elucidated. Raman spectra indicate that addition reactions on the α- and/or β-carbons occur. This could be, for example, a dimerization reaction. A comparison of the 785 nm spectrum of secoisolariciresinol, a coniferyl alcohol dimer with coniferyl alcohol after prolonged laser exposure neither supports nor refutes a laser-induced polymerization reaction.

Another puzzling observation is the obvious absorption of 532 nm photons. Bond[171] was surprised about this fact and our own measurements validated previous absorption studies showing that there is no absorption at or close to this wavenlength. In **Paper II**, we discussed briefly some features of energy transfer to the molecules. A mechanism over an excited electron state was ruled out due to lack of absorbance at the excitation wavelengths. Moreover, calculations showed that the energy provided by both lasers were not sufficient to dissociate bonds, but may be enough to oxidize them, but surprisingly, only 532 nm radiation caused experimentally observed changes, whereas 785 nm radiation did not.

However, an important fact slipped our and Bond's[171] attention, which could explain the experimental results.

All studies so far have reported second order kinetics of the band decay. Consequently, all authors concluded that there must be a fast (polymerization) reaction and a slow degradation process involved. Laser-induced degradation of acrylic polymers was investigated in detail by Dyumaev et al.[230,231]. They used radiation of 530, 690 and 1064 nm to investigate laser damage after short pulses (ns range). PMMA does not have an absorption band anywhere near these wavelengths[232]. Their investigations showed that the laser damage threshold (LDT) was strongly dependent on temperature and could be strongly increased by adding low-molecular additives like water, butanol, propanol or hexanol. Mixtures of small amounts of water (1%) with these alcohols resulted in an even higher LDT. The proposed explanation was based on an initial inclusion or defect being responsible for absorption of light and creation of vibrationally excited radicals. Newly generated radicals absorb even more radiation, thus an "absorption wave" is propagating from the intial damage spot which will eventually create cracks in the matrix. Alcohol molecules will participate in energy-transfer reactions with radicals, this reaction increases the vibrational state of the solvent and lowers the vibrational state of the radical, thus decreasing its lifetime. The requirement for this quenching is effective vibrational cross-coupling between the radical and the quencher. In PMMA, the hydrogen-bonded OH-stretch has twice the frequency of the acrylic C=O stretch, therefore coupling occurs.

A similar process can be constructed for lignin by adding two pieces of information.

First, laser flash photolysis studies showed that irradiation of α-(p-methoxyphenoxy)-p-methoxyacetophenones (similar to structure **V** in Fig. 5C) produces ketyl- and phenoxyl radicals. It was therefore speculated that α-ketone substructures play a role in paper yellowing[233-235]. These studies employed a laser wavelength of around 330 nm.

Second, beside single photon events there exists the possibility for multi-photon absorption. This is when two photons are absorbed at the same time, their energy is added. Multi-photon absorption cross sections of most materials are small[236].

In conjunction with the Dyumaev model[230,231], the process appears to be as following (Fig. 5C):

Multiphoton absorption is responsible for energy transfer from the laser to the sample, because no lignin structure is known to have absorption bands at the common Raman excitation wavelengths (532, 785, 1064 nm), as inferred from UV-absorption studies[237]. Also dihydrochalcone has all absorption bands lower than 360 nm[238]. Taking multiphoton absorption into account, it can be seen that two 532 nm-photons (266 nm), three 785 nm-photons (261.7 nm) and four 1064 nm-photons (266 nm) can combine to fall into the absorption range of coniferyl/sinapyl alcohol (Fig. 5B). However, multiphoton absorption gets less likely the more photons are involved. This makes 532 nm the primary wavelength for causing such absorptions.

Multiphoton absorption is therefore proprosed to lift coniferyl alcohol **I** from the ground to the first excited state **II** (Fig. 5C). In the presence of protons, highly reactive quinone-methide **III** is formed, which subsequently reacts to structures having much less Raman intensity (due to release of ring conjugation, eg. **IV**) and are therefore hard to identify in the Raman spectrum (compare the intensity in Fig. 5A). It is proposed that energy is also transferred from coniferyl alcohol **I** to α-carbonyl structures **V** in the form of

$$\mathbf{I}^* + \mathbf{V} \rightarrow \mathbf{I} + \mathbf{V}^* \qquad (2)$$

which causes α-carbonyl structures to break at the β-carbon. While quinone methide has its absorption at 350 nm[227], the carbon-centered radical **VI** has a broad absorption at 540 nm[239]. Therefore, only one photon is required for absorption, making energy transfer far more efficient. This increases fluorescence in the Raman spectrum and causes subsequent sample burning.

This is consistent with the observation that lasers of all three wavelengths will ultimately burn a sample, although the longer the wavelength, the more time is required. Furthermore, only 532 nm radiation can efficiently transfer energy over the ketyl radical to lignin and it can be speculated that other radicals have similar absorption bands.

Experimentally it has been found that decreasing integration times, reducing laser powers and increasing the step width (point-to-point distance) can ameliorate the problem. In light of the above discussion, decreasing the laser power will just reduce the likelihood for such a two-photon absorption, but considering the high photon flux of modern lasers, this seems to be the least effective counter measure. Much more useful is decreasing the integration time or increasing the step width, because both effectively move away the laser from the spot which already is directly absorbing radiation due to laser damage. This also explains the fluorescence drag ("Fluoreszenzverschleppung") which is manifested in the observation that once fluorescence

increases, it will continue to do so for all subsequent pixels of the measurement. Since the absorbing species are already created, any attempts to "let the sample relax or cool down" will not be successful. The only solution is to create sufficient distance between the measurement spot and such light absorbing species. The long used practice to add water to the samples to decrease fluorescence can also be understood in the framework of the Dyumaev model. The broad OH-stretch of water ranges from 3700 to 3100 cm^{-1}, this is sufficient to capture all overtones of C=O, C=C and Φ8 ring stretches, which are shared by molecules also having absorptions in reach of the 532 nm two-photon absorption. Energy can therefore be transferred from vibrationally excited molecules back to water, decreasing the lifetime of excited species.

Additionally, the reaction of lignin monomers to laser irradiation can also be clarified. As has been noted previously, only 4-hydrxoxy cinnamyl alcohols showed decay of Raman bands (predominantly the 1660 cm^{-1} band). Although the reaction mechanism involving water for creatin of the quinone methide could be reproduced, involvement of an excited state was rejected based on no absorption bands being present. We wondered however, why 532 nm radiation caused a reaction, whereas 785 nm did not. With the concept of multiphoton absorption, a new perspective opens up.

As can be inferred from the absorption spectrum of coniferyl alcohol in Fig. 5C, both laser wavelengths are well removed from any absorption bands. Invoking two-photon absorption, it can be seen that two photons of the 532 nm laser match almost perfectly with one of the absorption bands (263 nm). Doubling the frequency for the 785 nm laser however does not result in a match, in fact, the photon energy is still too low for any absorption. This is in perfect agreement with our experimental results, where recently also (2E)-3-(8-methoxy-2,3-dihydro-1,4-benzodioxin-6-yl)-prop-2-enol and ethyl-4-hydroxy-3-methoxycinnamate were found to react to laser exposure due to having absorption bands accessible for two-photon absorption (unpublished).

Both processes observed in the intensity decay curves can now be explained by the fast reaction of mostly 4-hydroxy-cinnamyl alcohols and slower degradation of lignin itself. The implications are manifold:

1) Lasers can induce photochemical reactions during Raman measurements. Although the 532 nm-laser is desired in Raman imaging for its high-signal to noise ratio (see Eq. 1) and good spatial resolution, it is prone to causing laser damage. By comparison with reference spectra, it seems, that mainly 4-hydroxycinnamyl alcohols are responsible for this absorption (see Pew[237] and Fig. 5C). 785 and 1064 nm can be considered as "safe" during normal measurement conditions.

2) Measuring an area which had previous laser contact should be avoided. The extent to which the laser effect is distributed over the area, meaning the spatial distance between subsequent measurements is yet to be determined.

3) Laser susceptibility checks (e.g. time series) are advised to be conducted prior to measurement.

4) Laser retention times (e.g. integration time) should be as short as possible.

5) The process can be used to laser-delignify a sample spot. This removes the strong spectral contribution of lignin chromophores and (literally) sheds light onto buried structures.

6) Some coniferyl alcohol units seem to be present in lignin either as "free" monomer, i.e. totally unbound or in a linkage form that retains both hydroxyl groups (which is only 4-O-5, since 5-5' coupling does not occur[58]). This is because neither abietin nor eleutheroside B were susceptible to

laser damage, hence excluding β-O-4-linked alcohols.

7) Water can vibrationally cross-couple with stretch overtones of C=O, C=C and rings (Φ8). This reduces the lifetime of excited species.

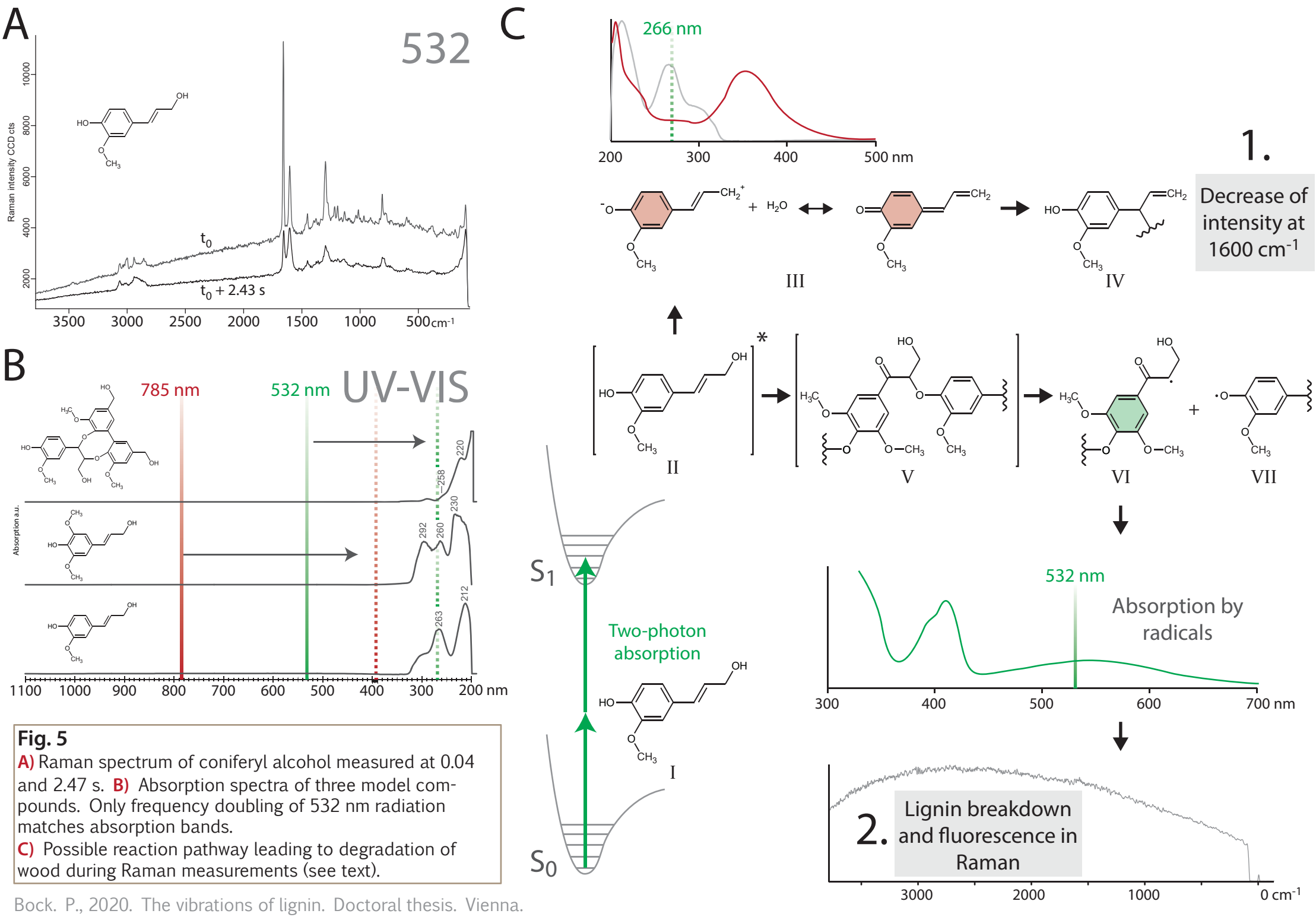

Fig. 5
A) Raman spectrum of coniferyl alcohol measured at 0.04 and 2.47 s. **B)** Absorption spectra of three model compounds. Only frequency doubling of 532 nm radiation matches absorption bands.
C) Possible reaction pathway leading to degradation of wood during Raman measurements (see text).

Bock. P., 2020. The vibrations of lignin. Doctoral thesis. Vienna.

3.3. LIGNIN SUBSTRUCTURES AND LINKAGES FROM THE SPECTRAL PERSPECTIVE

It is apparent that a succesful interpretation of the spectroscopic experiment requires knowledge about the underlying principles. From a structural perspective, the normal modes of vibrations have to be understood in infrared (IR) and Raman experiments.

Non-linear molecules have 3N - 6 normal modes of vibration, which can be excited by absorption (IR) or inelastic scattering (Raman) of a photon. Normal modes are nuclear displacements which do not change the center of mass. They involve stretching, bending and torsion of bonds[74,206,240]. They oscillate at a frequency which is determined by the force constant of the bond and the involved masses. Eq. 3 shows the relationship in the case of a harmonic oscillator,

$$\nu = \frac{1}{2\pi}\sqrt{F\left(\frac{1}{m_1}+\frac{1}{m_2}\right)} \qquad (3)$$

where ν is the frequency, F the force constant and m the atomic mass.

It can be derived from this relationship, that

1) strong bonds oscillate at higher frequencies than weak bonds

2) high masses oscillate at lower frequency than low masses on the same bond.

Vibrational spectra of a molecule are characterized by many bands relating to different normal modes which often also relate to different chemical groups that is that C-H bonds oscillate at higher frequencies than C-O bonds due to hydrogen being much lighter than oxygen. It has therefore been customary to ascribe so-called group frequencies to certain regions of the spectrum, acknowledging that chemically similar bonds will also have similar vibrational frequencies.

It is furthermore important to note that the actual molecular geometry plays a crucial role when determining the normal modes of a molecule. This is because the geometry influences mechanical coupling as well as electron distribution of the molecule and both will affect the vibrational frequency. The vibrational spectrum of a molecule therefore depends on its conformation; thus a substance can display many different spectra. Therefore, structural considerations have to be taken into account for spectral interpretation. Furthermore, hydrogen bonding, isotopes, pH and chemical environment affect mechanical coupling and electron distribution and therefore the spectrum as well[73,204,205,241,242].

3.3.1. The aromatic ring

The aromatic ring is the identifying chemical group of lignin. As can be seen from Fig. 1C, at least half of the carbon atoms is involved in the ring structure of a classical monomer. The aromatic ring is regarded as the biggest and most complex group in vibrational spectroscopy[73]. It has 30 normal modes of vibration, where 12 are C=C modes and 18 are C-H modes. The latter are converted in C-X modes upon ring substitution (X: substituent). This drastically lowers the frequency of these modes and shifts them below 1400 cm^{-1}. These substituent-sensitive modes are valuable for determining the pattern of ring substitution[203,243]. It has to be noted that "substituent-sensitivity" has to be

taken literally as some vibrational modes even react with frequency shifts to second- and third-order substituents (see Fig. 6B). The choice of an appropriate molecular structure suitable for representing a certain lignin substructure is therefore challenging. The actual choice depends on the type of question. If the ring substitution is to be investigated, than care should be taken on proper substitution (including second order etc). If the focus is on aliphatic C-H stretches, then they should be modeled as close to the original structure as possible. Furthermore, peculiarities of molecular vibrations further complicate the process. This is illustrated in Fig. 6A, where spectra of two similar compounds are shown, only differing in the second-order substituent. Although methyleugenol is better suited from the substitution perspective (the oxygen in the prevalent β-O-4' linkage does not bear a hydrogen), molecular symmetry causes a band shift and intensification (Φ14) which is only due to both methoxy groups being in-plane with the ring and pointed away from each other. Furthermore, the spectral contribution of the second methoxy group (non-existent in lignin) interacting with the first one also contributes to the spectrum. Unfortunately, availability or the price of reference compounds often additionally limits the choices of the spectroscopist.

In the following, spectral considerations regarding the individual linkage patterns of a guaiacyl (G)-lignin are presented. G-lignins are well suited for such a discussion, because G-rings occur in the lignins of grasses and hard- and softwoods, in the latter they constitute a majority[10]. Furthermore, a G-ring has three substituents: One carbon at position 1 and two oxygens at positions 3 and 4. This leaves position 5 free for condensation reactions resulting in a wide range of structural possibilities. Results are therefore transferable to other lignins within spectroscopical limits.

Atoms are abbreviated by element symbol and designation as shown in Fig.1C. Ring modes are denoted in Wilson/Varsanyi notation[203,244]. Tables for these modes can be found in the appendix, Fig. A2..

3.3.2. β-O-4' and free G-rings

β-O-4' linkages do not alter the substitution pattern of the original guaiacyl ring. Only the hydroxyl group at C4 is replaced by an ether group, linking C4 by O4 to Cβ of the next monomer. Idealized band positions and intensities for a G-ring are shown in Fig. 6C. A diagnostic band complex caused by C-X stretches and C-H bendings is shown in Fig. 3A. All G-Rings have this feature to a certain degree. The band at 1270 cm^{-1} sees wide use in the literature[176-178,245] as diagnostic band of G-rings and as far as the reference structures tell, this is correct. Other typical bands are shown in Fig. 7.

3.3.3. β-5'

In β-5-linkages, C5 does not bear a hydrogen and instead is connected to Cβ of the neigboring monomer. This makes the ring asymetrically-tetrasubstituted with all the consequences for its vibrational modes. The S-ring should serve as our reference system for this substitution pattern. Its all-in-phase-C-X-stretch has a frequency of 1335 cm^{-1} and is good marker band because of its good IR and Raman intensities. Replacing one oxygen by a carbon atom should increase the frequency (cf. equ.2), this is also observed in 5-5' structures (vide infra). Furthermore, the hydrofuran ring that is generated creates strain in the aromatic ring. Based on orbital considerations[246,247], this is expected to increase the p character of the C4-C5 bond, thus increasing its length. Contrary to this, the DFT calculation shows a shortening of this bond (compare Fig. 6D). The concomitant change of the exocyclic angles should decreases the frequency of those modes which involve C4-O4 stretching, which is also reproduced by calculations.

In the case of Φ20a, this leads to an interesting result: While the lowered mass (O replaced by C) upshifts the mode, the angle deviation from 120° downshifts it. Both effects appear to have the same strength, so overall the frequency is not shifted. When comparing with literature spectra of β-5' compounds[184,248], a band can be found at 1330/1338 cm^{-1}. This sets the β-5' ring well apart from G-rings (at 1270 cm^{-1}). It can however, mislead S/G ratio interpretations based on ratioing the 1330/1270 cm^{-1} band, because pure G-lignins would be incorrectly assigned as having S-units and in GS-lignins, the S-content would be overestimated. Meanwhile, a different method for quantifying S-units was published[173,174], which circumvents the problem.

3.3.4. 5-5' and DBDO

Except for diferulate crosslinks in grasses[249,250], no other lignin substructure has two rings directly joined together[27,41,58]. This makes these structures highly interesting for vibrational spectroscopy. **Paper IV** was dedicated to such a structure. In biphenyls, C5 of one ring is linked to C5 of another ring. The substitution situation is similar as in β-5' rings, however, the ring strain is not present. This will make the frequency change by the overall lowered substituent mass the dominant factor and upshifts the all-in-phase-C-X stretching mode (Φ20a) to 1365 cm^{-1}. As far as could be told from reference substances, this mode is not affected by linkages on the C4. This seems logical, as it is mainly the heavy-loaded triangle of the ring (C1-C3-C5) which is involved in the vibration. The intensity characteristics remain unchanged and the band can serve as a marker as well. The only other useful band for identifying such structures is the band at 967 cm^{-1}. However, in IR, this is also the frequency of the C=C hydrogen wag of phenyl propenoids, so their contribution has to be taken into account.

Biphenyl structures can occur in an open form, where the C4s bear hydroxy groups or in a closed ring structure, as dibenzodioxocin (DBDO)[27]. In DBDO, a third monomer joins the two rings linking their O4s to its Cα and Cβ, respectively (compare Fig. 1C). Our calculations show that in open 5-5' structures, both rings adopt a more or less orthogonal conformation that is minimizing steric repulsions and lowering the overall energy. In DBDO however, this conformation is not possible. The α-O-4' and β-O-4' linkage forces both rings into a conformation which was calculated to be 48.2°. This increases overlap of π-orbitals and is expected to increase the Raman intensity (see section 3.1). However, inspection of Raman spectra at 532 and 785 nm leads to the conclusion, that conjugation enhancing effects play only a minor role (Note the difference of the Raman spectra in Fig. 4A) and that the intensification at 532 nm is due to preresonance enhancement. The consequence is that in contrast to phenyl propenoids, overproportional signal contribution by planar biphenyls can be avoided by using excitation wavelengths of 785 nm or higher.

3.3.5. 4-O-5'

This is the third linkage type where the G-ring is substituted on C5, making it asymmetrically-tetrasubstituted. Altough from ring substitution, this is a close match to a real S-ring, the substituent modes are still G-like. The reason is that the 4-O-5'-linkage is shared by two rings, which means that the O3-CH_3 stretch cannot couple with the symmetry-equivalent O4-CΦ' of the second ring. This affects all those modes which involve the C-O-C bonds (e.g. Φ7a, 7b), while others remain at S-ring frequencies (e.g. Φ20a)

3.3.6. β-β'

This linkage type includes three motifs: Resinol-type, tetrahydrofuran-type and secoisolaricinol structures[27]. In contrast to monomers, Cβ and Cγ carbons are no longer sp^2-hybridized in β-β'-linkages - the aromatic ring is no longer conjugated. Moreover, β-β'-structures were found to be 4-O-5'-linked to the remaining polymer[53]. This excludes any Raman enhancing effects and makes the intrinsic Raman cross sections rather small. In addition, these linkages only have C-O, C-C and sp^3-C-H vibrations. By diagnostic means, this is problematic, because these modes are shared by most of the substructures and also appear in carbohydrates. While in Raman spectra, their signal is swamped by (conjugated) aromatic modes, in IR the C-O/C-C region is crowded by many modes originating from different moieties. It is therefore no wonder that none of these structures appears in assignment tables.

3.3.7. β-1' (spirodienones)

In spirodienones, the quinone-moiety is the most interesting part because it possesses sp^2-carbons. This removes both C-H and C=C/C=O modes away from the crowded regions. Bond[171] tried to remove quinones by trimethylphosphite. Contrary to expectation, the 1600-band's intensity increased after treatment. He therefore could not clarify the contribution of quinones to the Raman spectrum. Reference measurements on similar structures suggest that their Raman cross section is smaller than that of conjugated aromatic rings (they do not benefit from conjugation enhancement). Prednisolone showed only one strong band appearing at 1654 cm^{-1}, while a substituted cyclohexadienone showed a band at 1667 cm^{-1}. This region has already considerable overlap of bands (see below). The situation in the IR is not any better. Overall, based on their spectral features and their low occurrence in lignin, spirodienones can hardly be identified in lignin's vibrational spectra.

3.3.8. Cinnamyl alcohols

Cinnamyl alcohols are unsaturated end groups of lignin. They are monomers linked over the ring to the polymer. The C=C bond is in conjugation with the ring and enhances the Φ8 stretches. Its electrons however seem to be fairly localized in the bond, because the frequency is not or only slightly shifted from the reference frequency of single C=C bonds, 1660 cm^{-1}. The bond is non-polar, as a result, the strong Raman band faces almost no signal in the IR. Nevertheless, the spectrum is typical for phenylpropenoids (compare Fig. 3A) Cinnamyl alcohols can be thought as being present either in a free (non-bonded) state or linked by β-O-4', β-5' or 4-O-5' to the rest of the polymer. The unsaturated side group is never depicted as involved in linkages[27,41,58]. They are identified mainly by their C=C stretch at 1660 cm^{-1} in Raman. The Raman band at 1275 cm^{-1} was found to exclusively represent β-O-4' bound coniferyl alcohol. Other bands are less useful due to strong overlap and the fact that many of them depend on ring substitution. In IR, the ethylenic-all-in-phase-out-of-plane-wag (967 cm^{-1}) is shared with cinnamaldehydes, acids and esters.

3.3.9. Cinnamaldehydes

In terms of Raman intensity, cinnamaldehydes are probably the most useful structures of lignin. This is also reflected in their early identification and assignment[163,171] and subsequent use of their characteristic bands for Raman studies[157,165,180-182]. The reason is that the propenal side chain has

strong and characteristic bands which are easy to identify, but can also be partially attributed to the fact that they can relatively easy be eliminated by $NaBH_4$-treatment to study their spectral contribution. Cinnamaldehydes benefit from all Raman enhancing effects and therefore show a strong Raman signal. Their IR signal is also increased. Based on measured intensities (see Fig. 3C) it can be speculated that a large part of the Raman spectrum at 532 nm is caused by these structures only. At 785 nm, their contribution is less.

In **Paper III**, the band assignments of cinnamaldehydes were reviewed and updated with new findings. To date, they are the only compounds which can be identified by several bands, because the whole propenal side group is characterized. The main marker bands in the Raman spectrum are the C=C and C-C stretches at 1620 and 1135 cm^{-1}, respectively. Beside that, the aldehyde group has useful modes both in IR and Raman: The C=O stretch (1665 cm^{-1}) and several C-H modes (~2850, 2750, 1400, 967 cm^{-1}).

3.3.10. Cinnamyl acids and esters

Similar to aldehydes, cinnamyl acids and their esters feature aromatic rings conjugated with a C=C-C=O group. In lignins, ferulates, p-coumarates and feruloyl amides would fall in this category. Despite similar configuration, the ester carbonyl's frequency is affected by inductive and resonance effects. While the second oxygen raises the frequency by induction, its lone pairs also enable additional resonance forms[204]. This resonance competition increases the frequencies. The C=C bond is only slightly upshifted to 1630 cm^{-1} and the C=O stretch frequency is increased to 1700 cm^{-1}. They can be seen in both Raman and IR.

Similar to cinnamaldehydes, enhancement effects increase the signal of the whole cinnamyl acid/ester molecule. The C=C stretch of esters was recently used for identifiying these structural motifs in Raman spectra of transgenic poplar samples[251]. There is potential overlap with C=C stretches of β-O-4'-linked coniferyl aldehyde (4-Acetoxy-3-methoxycinnamaldehyde 1628 cm^{-1}) and stilbenes.

Care has to be taken when measuring reference spectra of acids: They often form dimers which increases molecular symmetry and creates dimer bands in the spectrum!

3.3.11. α-Carbonyls

In native lignin, p-hydroxybenzoates are structures having α-carbonyls and in extracted lignins, they could also be induced by ball milling[252]. In these structures, Cα is involved in a carbonyl group, which is in conjugation with the ring, therefore enhancement effects operate. Furthermore, since Cα is a first-order substituent, ring modes are affected. Beside geometrical effect, the carbonyl frequency is subject to the electron density distribution[73,204], which is affected by ring substitution. As deduced from acetophenones, the C=O strech in α-ketones is found in the range of 1680 - 1655 cm^{-1}. The Cα-Cβ stretch is located at 980 cm^{-1} and has weak to medium Raman-intensity. (The Raman band at ~1090 cm^{-1} is caused by methyl rocking and therefore not relevant.)

The reference structure for p-hydroxybenzoates, ethylparaben has useful Raman bands, because it is an H-unit, so its signal differs with respect to G- and S-units and it can be detected due to signal enhancement. Most notable are the C-H bend (Φ9a, 1176 cm^{-1}) and a ring stretch (Φ1, 873 cm^{-1}). The C=O stretch (1667 cm^{-1}) and two other ring modes (Φ8a, 1610 cm^{-1} and C-X stretch, 1283 cm^{-1}) are less

useful due to overlap with other bands. The situation in IR is more complicated and only one strong band appears in a region not covered by G- and S-units (Φ4, 696 cm^{-1}).

3.3.12. Stilbenes

Stilbenes are genuine lignin monomers[32,45] and can appear in lignin spectra due to co-localization of extractives with lignin[149,151]. Their inter-ring C=C bond is responsible for a strong Raman signal at 1630 cm^{-1}, the IR intensity is very low. Their other bands strongly depend on substitution of the two phenyl rings. In case of mono-, meta- or 1,3,5-trisubstitution of at least one of the rings, a strong Raman band at 1000 cm^{-1} can be found (Φ12). This is more extensively discussed in **Paper I**. 5-5 coupling into the lignin polymer[52] creates a conjugated system involving the DBDO moiety. This will further boost the Raman intensity of the DBDO bands.

3.3.13. Flavonoids

Flavonoids comprise a diverse group of molecules with a similar backbone structure. At present, one flavone (tricin) has been shown to act as lignin nucleation site[32,46-48]. It is likely that others will be discovered in future. They should therefore not be dismissed from such a review. From the vibrational perspective, the main distinction will be between flavonoids, where the π-systems of the rings are connected (chalcones, aurones, anthocyanins, flavones) and others, where this is not the case. The former group benefits from various signal enhancing effects in Raman, but suffers from increased fluorescence, especially when measured at 532 nm. The latter group will have Raman cross sections not different from common lignin units and therefore hard to detect. The situation in the IR is comparable. Spectra in the literature[253-258] show that many flavonoids possess a Raman band between 1580 - 1540 cm^{-1}, sufficiently strong and set apart from other ring stretches to be used as a marker band. Judging from IR spectra[259], this band is less useful in the IR; there is also overlap with ring stretch Φ8. It is not straightforward to discuss other marker bands, as this depends on the specific setup of the molecule. Strong coupling and interaction even cause structural similar flavones to feature very different vibrational spectra[259].

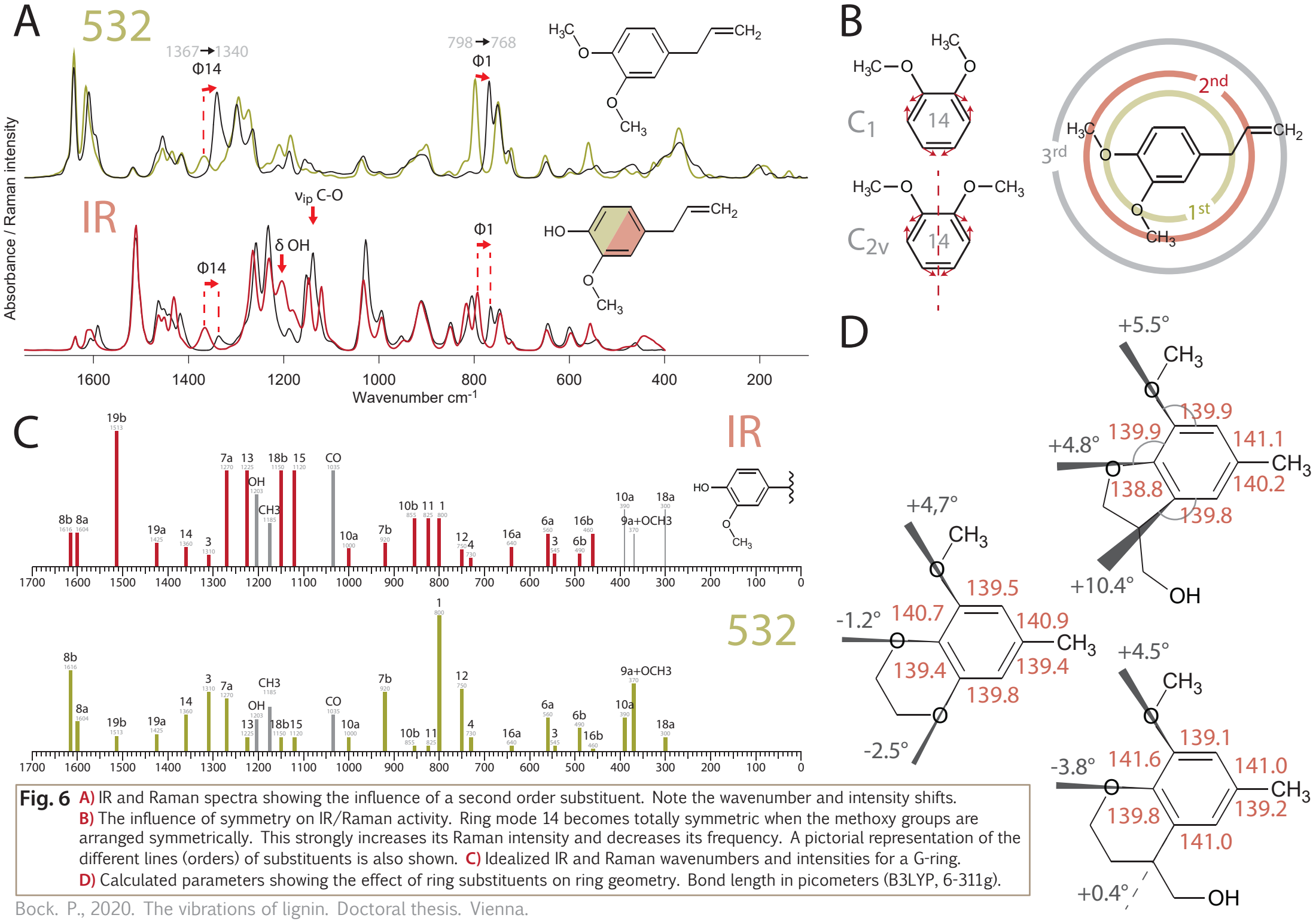

Fig. 6 **A)** IR and Raman spectra showing the influence of a second order substituent. Note the wavenumber and intensity shifts. **B)** The influence of symmetry on IR/Raman activity. Ring mode 14 becomes totally symmetric when the methoxy groups are arranged symmetrically. This strongly increases its Raman intensity and decreases its frequency. A pictorial representation of the different lines (orders) of substituents is also shown. **C)** Idealized IR and Raman wavenumbers and intensities for a G-ring. **D)** Calculated parameters showing the effect of ring substituents on ring geometry. Bond length in picometers (B3LYP, 6-311g).

Bock. P., 2020. The vibrations of lignin. Doctoral thesis. Vienna.

1365 (IR)
1310 (Ra)
1265
1230 (IR)
1205 (IR)
1150 (IR)
1125 (IR)
1030 (IR)
930
855 (IR)
825 (IR)
800
730 (IR)

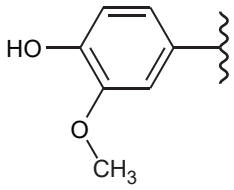

1330 (IR)
1310 (IR)
1265 (IR)
1215 (IR)
1150 (IR)
1125 (IR)
1030 (IR)
930
855 (IR)
825 (IR)
780
730 (IR)

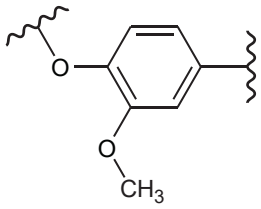

1335 (Ra)
1215 (IR)
1145
1115 (IR)
960
800
730 (IR)

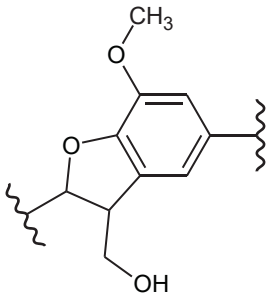

1630 (Ra)
1310 (Ra)
967 (IR)

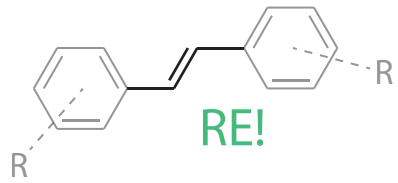

1660 (Ra)

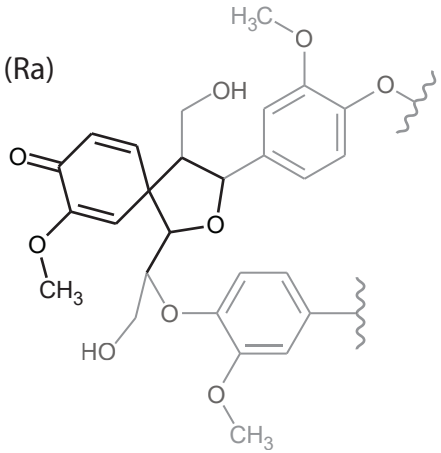

1365 (Ra)
1275 (IR)
1140 (IR)
1085 (IR)
1048 (IR)
967 (Ra)
930 (Ra)
750 (IR)
555 (Ra)

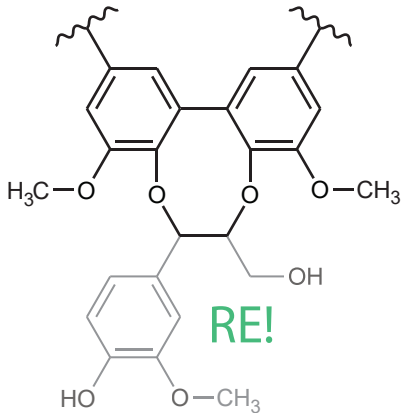

1365
1275 (IR)
1140 (IR)
1085 (IR)
1048 (IR)
967 (Ra)
930 (IR)
555 (Ra)

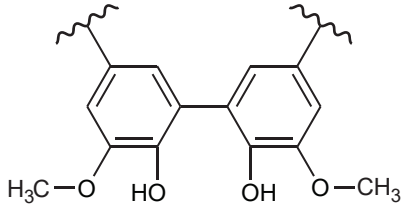

1335 (Ra)
1230 (IR)
1150 (Ra)
1090 (IR)
930
800

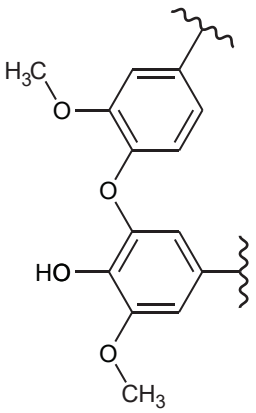

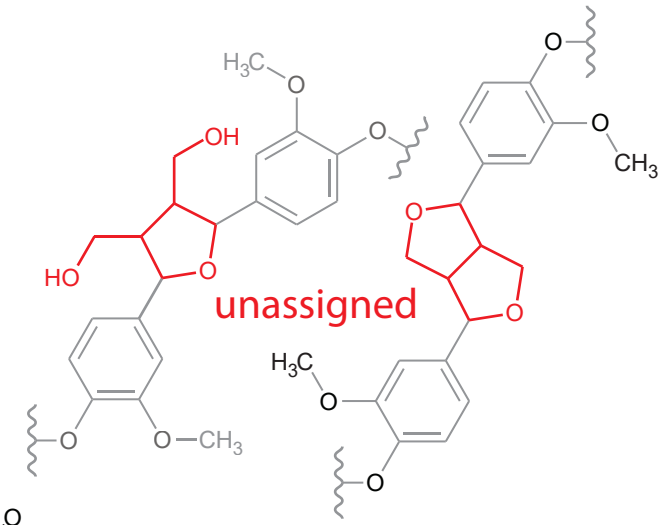

1700 (IR)
1630 (Ra)
1290 (Ra)
967 (IR)

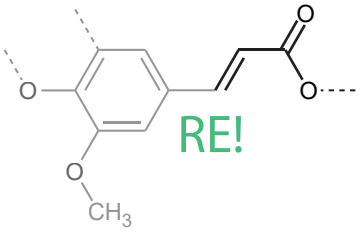

2850 (IR)
2750 (IR)
1660 (IR)
1620 (Ra)
1400 (Ra)
1290 (Ra)
1130
967 (IR)

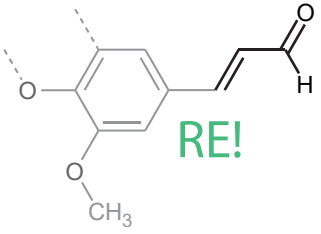

1660 (Ra)
1290 (Ra)
1085 (IR)
1012 (IR)
967 (IR)

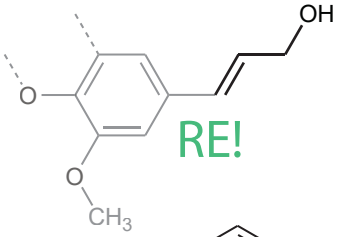

1580 - 1540

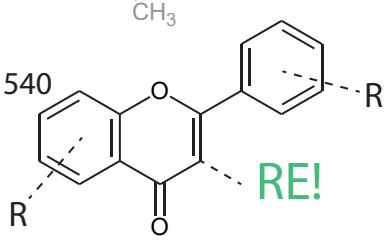

1176 (Ra)
873 (Ra)

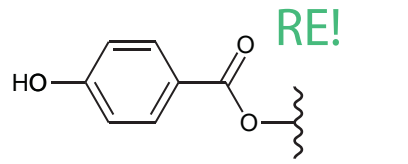

1660 (Ra)

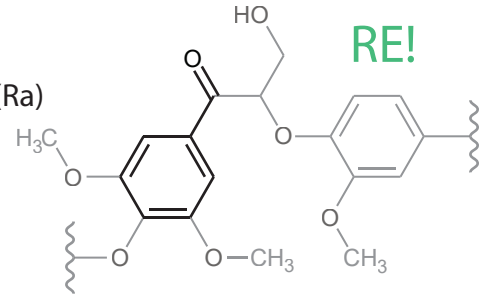

Fig. 7
Strong bands of lignin substructures useful for their identification. Listed are only general bands of the moieties shown. There are no currently known assignments for ß-ß‘ structures.
RE = Raman enhancement (Resonance-, conjugation-, and or charge-transfer enhancement).

Bock. P., 2020. The vibrations of lignin. Doctoral thesis. Vienna.

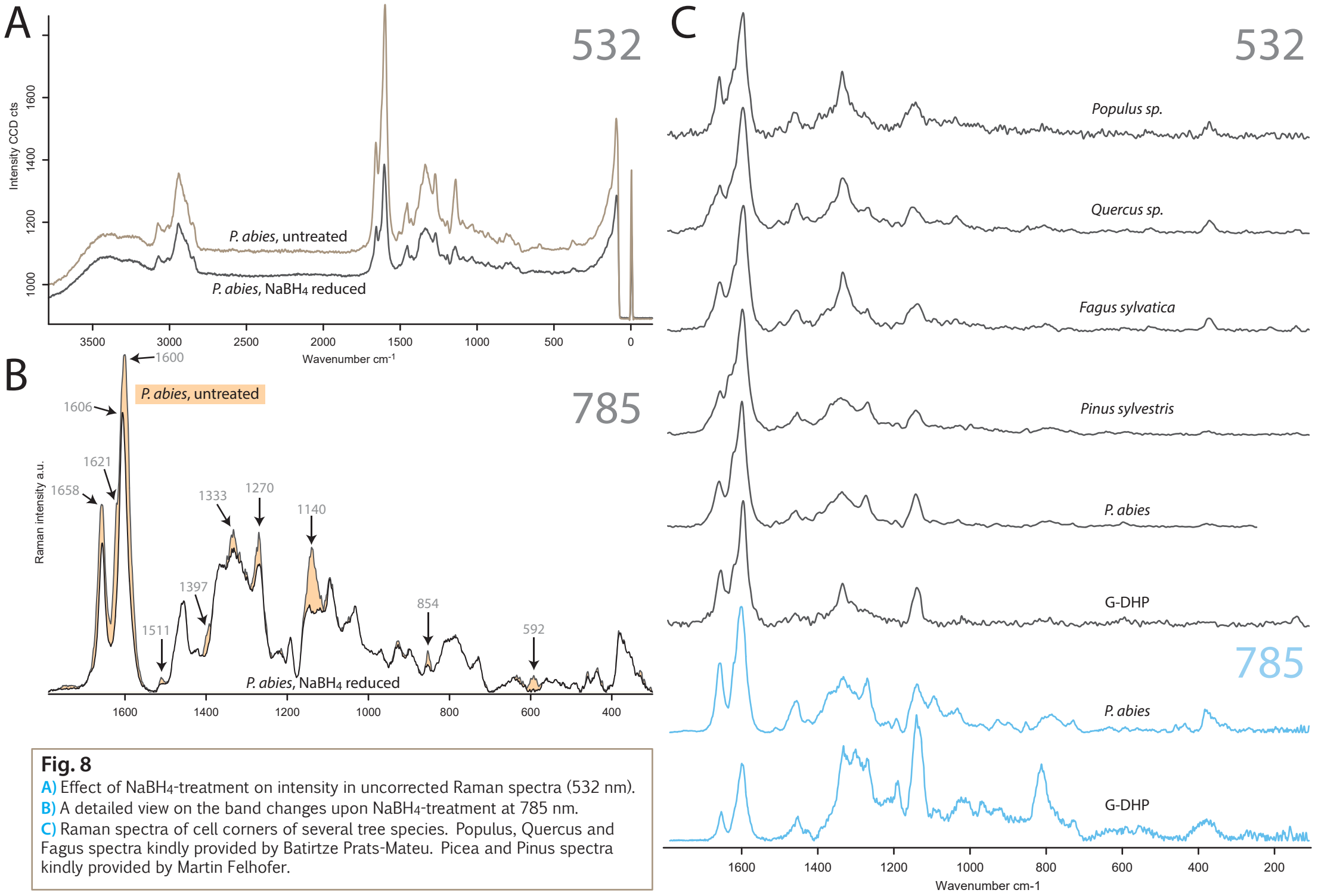

Fig. 8

A) Effect of $NaBH_4$-treatment on intensity in uncorrected Raman spectra (532 nm).
B) A detailed view on the band changes upon $NaBH_4$-treatment at 785 nm.
C) Raman spectra of cell corners of several tree species. Populus, Quercus and Fagus spectra kindly provided by Batirtze Prats-Mateu. Picea and Pinus spectra kindly provided by Martin Felhofer.

3.4. IR AND RAMAN SPECTRA OF G-LIGNIN AND THEIR ASSIGNMENT

The assignment of the lignin spectrum was tackled early by researchers due to being a main obstacle in the interpretation of the spectra of wood. The first systematic survey was probably conducted by Ehrhardt[186], who systematically reviewed earlier IR assignments of Hergert[196,260] and others and compared them with quantum-chemical calculations. The last thorough assignment of the lignin IR spectrum was done by Faix[197]. Raman spectra were first assigned in 1993 by Agarwal and Atalla[163] and later refined[185,193,194]. Apart from that, little has been done to further research its vibrational spectra and reviews keep citing the same few sources[261]. Also the boom of computational methods applied to the vibrational analysis of molecules went past the lignin field without many applications. Although useful, lignin-like structures appeared in literature[187,188,191,262], but only a few studies specifically targeted lignin assignments[186,189,190 192].

The discussion of lignin spectra is further complicated by the fact that the Raman spectrum can differ with respect to the wavelength. Therefore, even with one method, it is possible to obtain different spectra of the same sample. This is explained by individual molecules in the sample responding differently to the excitation wavelength in terms of signal enhancement. It is therefore possible to highlight certain structures at one wavelength but also requires different band assignments.

This work focusses on G-lignins, because they show a rich diversity of molecular structures and results can easily be extrapolated to other lignins, because they have the same linkages, just in different proportions. The following discussion of the vibrational spectra of spruce lignin and G-DHP uses the concepts and considerations discussed in the previous sections. Extension to other lignins will be given in section 3.5.

Wavenumbers given are based on a multitude of reference substances and should represent "typical" modes which fit various lignins. They are accurate to +/- 5 cm^{-1}.

Asym-tri-ring	Asymmetrically trisubstitued ring, i.e. substituted at positions 1,3 and 4.
Asym-tetra-ring	Asymmetrically tetrasubstituted ring, i.e substituted at positions 1,3,4,5.
G-OH	G-ring where position 4 is substituted with an OH-group.
G-OR	G-ring where position 4 is substituted with an oxygen linked to another carbon (ether linkage).
C-X	Substituent mode (see section 3.3.1).
Φ	Ring mode in Wilson/Varsanyi notation[203,244].

3600 - 2700 cm^{-1} X-H stretches

This is the region of O-H and C-H stretches. Overtones of ring modes (Φ8) and C=C/C=O stretches can sometimes be seen in the Raman spectrum as weak bands close to 3200 cm^{-1}. Due to the sheer number of different C-H oscillators and complicated interactions[73,263-265], assignments in this region are difficult. A more extensive discussion can be found in the supplementary material of **Paper IV**.

3600 — 3100 O-H stretch

Broad absorption by all sorts of OH-groups. Hydrogen-bonding shifts the band to lower wavenumbers, high-wavenumber components represent shorter and less H-bondend O-H oscillators[266-268].

3069 C-H stretch Φ2 of rings

In-phase stretch of aromatic hydrogens. All rings have this mode at approximately this wavenumber. Best seen in Raman, in IR often hidden in the broad OH-stretch.

3002 C-H stretch of methoxy groups
C-H stretch of C=C

This band has two components:
At higher wavenumber (~3010 cm^{-1}) trans C=C bonds have two hydrogens, which gives an in-phase and an out-of-phase mode for their stretches. It is reasonable to assume that these C-H bonds are chemically different due to the presence of the ring. Although uncorrected harmonic frequency calculations are relatively inaccurate for modelling C-H modes[264], the results show a qualitative difference between both hydrogens and two individual C-H stretching modes. The C_α-H stretch is continuously calculated at around 40 cm^{-1} lower than the C_β-H stretch. The tentative assignment would then be: C_α-H stretch of C=C. The C_β-H stretch would be somewhere in the complex band <3000 cm^{-1}.
At lower wavenumbers (~3000 cm^{-1}), the methoxy group is found. The presence of oxygen causes the individual hydrogens of the CH_3 group to be unequal. They are effectively split into a single C-H and a CH_2 group. By comparison with anisole[269,270] this band is assigned to the lone-H stretch of the single hydrogen lying in plane with the oxygen atom, consistent with literature[264].

2960 C-H stretch of methoxy groups

This is the anti-symmetric C-H stretching of the CH_2 set of the methoxy group[264].

2940 C-H stretch of methoxy and methylene groups

Has contributions from the symmetric stretch mixed with symmetric bending of the CH_2 set of the methoxy group[264]. The second combination is found at 2845 cm^{-1}.
Also the anti-symmetric stretch of methylene groups appears at this wavenumber. In lignin, this would be mainly CH_2OH moieties.

2890 C-H stretch of methylene groups
Lone C-H stretch?

Symmetric stretch of methylene groups. In lignin mainly from CH_2OH endgroups.
In 1,1-diphenyl propane, the lone C-H stretch was assigned to 2889 cm^{-1} [264]. In lignin, there are several lone C-H oscillators, e.g. in β-β' or β-5' structures. Note, that the aldehydic C-H stretch appears at even lower wavenumbers due to fermi-resonance with its own bending overtone[204].

2845 C-H stretch of methoxy groups

Good marker band for methoxy groups[271]. Caused by the symmetric stretch in fermi-resonance with the umbrella bending[264,265].

1800 - 1500 cm^{-1} C=O, C=C and ring stretches

This is the most important region in lignin diagnostics, because not many, but strong and well described modes appear here. Three main bands can be identified in the IR and two in the Raman spectrum. They are also the the first bands to look at for determining the presence of aromatic rings (Raman: 1600, IR: 1500 cm^{-1}). Furthermore, the Raman intensity of the 1600 cm^{-1} band tells about the conjugation of the aromatic rings. If it is much higher than the bands around 800 cm^{-1}, then the signal is constituted mainly of conjugated rings (that is mainly end groups of lignins), whereas the same or less intensity than the 800 cm^{-1} band means that unconjugated rings (i.e. the bulk of lignin) are observed. By comparing Raman spectra of different excitation wavelengths (e.g. 532 and 785/1064 nm), the ratio of these two bands can be used to draw further conclusions on the type of the conjugated groups (Conjugation and charge-transfer effects are not affected by the wavelength but resonance enhancement is.)

1660 C=O stretch of coniferyl aldehyde
C=C stretch of coniferyl alcohol (Raman only)

The first discernible band in the IR is the band at 1660 cm^{-1}. It represents conjugated carbonyl groups. In lignin, these can stem from cinnamates (1700 cm^{-1}), cinnamaldehydes (1665 cm^{-1}), α-ketones (~1660 cm^{-1}) and p-hydroxybenzoates (1667 cm^{-1}). Note that cinnamyl alcohols do not appear in the IR at this frequency (the C=C stretch of cinnamyl, coniferyl, sinapyl alcohol and their glycosides is weak in the IR. This is logical, because the bond is not polarized). In G-DHP, a shoulder at 1720 can be observed, which must come from unconjuagted carbonyls. In Raman, the band at 1660 cm^{-1} has contributions from both cinnamaldehydes (C=O stretch) and cinnamyl alcohols (C=C stretch). Based on laser degradation experiments (**Paper II**), it can be concluded that roughly one third of the band is caused by cinnamyl alcohols if normalized to 1600 cm^{-1} to remove the different magnitude of enhancing effects.
Spirodienones are also expected to contribute to this band, the magnitude is unclear but seems to be rather minor. The mode probably involves in-phase C=C stretch and produces a band at around 1660 cm^{-1} also (2,6-Di(tert-butyl)-4-hydroxy-4-methyl-2,5-cyclohexadien-1-one: 1667 cm^{-1}; prednisolone: 1654 cm^{-1}).

1620 C=C stretch of cinnamaldeyhdes and cinnamates

In several compounds, the C=C stretch is lowered due to electron-withdrawing groups. Cinnamates have them at 1630 cm^{-1}, cinnamaldehydes at 1620 cm^{-1}. These bands are not resolved in the IR. Conjugated carbonyls may also appear at this wavenumber.

1600 Ring stretch Φ8b of asym-tri rings
Ring stretch Φ8a of asym-tetra rings

The strongest Raman band of lignin is normally the pair of quarter-circle ring stretches Φ8. Although these modes are rather substituent-insensitive[203], it can be observed that their frequency decreases in homologous series of molecules with increasing conjugation, e.g. the frequency decreases in order 2-methoxy-4-propylphenol 1616 cm^{-1}, coniferyl alcohol 1606 cm^{-1}, coniferyl aldehyde 1598 cm^{-1}. *In-situ*, this can be shown by $NaBH_4$-reduction, where conversion of aldehydes to alcohols causes an upshift of 6 cm^{-1} (see Fig. 8A,B). This difference can also be observed in CAD-mutants, which have higher aldehyde levels, thus lower frequencies than the wild type[157,182]. At 532 nm, the 1600 cm^{-1} is predominantly caused by cinnamyl aldehydes and alcohols and to a lesser extent by cinnamates and dibenzodioxocins. At 785 nm, although the resonance enhancement is not that strong, conjugation and charge-transfer still elevate the signal of those structures (see also Fig. 4). It is therefore justified to also say that at this wavelength, the 1600 cm^{-1} band is mainly caused by cinnamyl aldehydes and alcohols. This is also proven by its unchanged frequency, because if the contribution of cinnamaldehydes were less, then the frequency should rise. Also in the IR, this band has a strong contribution from those structures. This can be rationalized when comparing spectra of different substructures (see Fig. 3B). Unconjugated rings tend to have relatively weak bands at 1600 cm^{-1}, whereas especially charge-transfer molecules have very strong bands. Given, that in IR, 1660 cm^{-1} is assigned to cinnamadehydes and considering that their C=O stretch has around the same intensity as their 1600 cm^{-1} ring stretches, it can be concluded that at least half of the IR band at 1600 cm^{-1} can be attributed to cinnamaldehydes.

The use of this band to estimate S/G-ratios as proposed in the literature[175] is not advised.

1500 Ring stretch Φ19b of asym-tri rings
Ring stretch Φ19a of asym-tetra rings

This is <u>the</u> marker band for lignin in IR spectra. It is caused by one member of the half-circle ring stretches, Φ19. Due to the nature of the mode, its Raman activity is only weak but it has excellent IR activity. Faix[197] previously noted that G-rings tend to have higher frequencies than S-rings. This is consistent with model compound spectra: While G-rings do not show a frequency dependence by conjugation or substitution, S-rings do: Replacing the OH-group on C4 by an OR-group lowers the frequency (Sinapinaldehyde 1510 cm^{-1} > (2E)-3-(8-methoxy-2,3-dihydro-1,4-benzodioxin-6-yl)prop-2-enal 1502 cm^{-1}; Sinapyl alcohol 1514 cm^{-1} > eleutheroside B 1509 cm^{-1} = (2E)-3-(8-methoxy-2,3-dihydro-1,4-benzodioxin-6-yl)prop-2-enol 1506 cm^{-1}; 4-hydroxy-3,5-dimethoxy acetophenone 1516 cm^{-1} >

Trimethoxy acetophenone 1502 cm^{-1}). Furthermore, in going from oxygen to carbon at the C5's substituent seems to lower the frequency, while ring strain increases it (see section 3.3.3.). This is consistent with experimental spectra of β-5' (Freudenberg 1960) and 5-5' (**Paper IV**) compounds and enables the distinction between G-rings (at 1510 cm^{-1}), β-5' (1500 cm^{-1}) and 5-5' structures (1485 cm^{-1}). Since S-type-rings occur in G-lignins only in the form of 4-O-5'-linked units, which have an OH-group at C4, they would also be included in the 1510 cm^{-1} band.

1465 C-H bending of methoxy groups

1455

Various C-H bending modes are responsible for this doublet and almost all reference compounds display it. The doublet is not always resolved and contains several bands attributed to C-H bending of methoxy and methylene groups. In lignin, it is mainly caused by asymmetrical bending of methoxy groups.

1425 Ring stretch Φ19a of asym-tri rings
Ring stretch Φ19b of asym-tetra rings

This is the second member of the half-circle ring stretches. Based on reference spectra it seems that G-OR rings have lower frequencies than G-OH rings (~1430 vs ~1420). Aldehydes and cinnamates have their stretch at ~1430 also, regardless of substitution. Also biphenyl rings are found at this frequency. In lignin, the majority of the rings do not have a free hydroxyl group, so the band should be shifted towards lower wavenumber. This is in accordance with the spectra of G-DHP and spruce MWL, where the band is found at 1423 and 1421 cm^{-1}, respectively.
Based on DFT-calculations, C-H bending is also present at this frequency, but with rather low intensity. Φ19 is known for its large dipole moment derivative[73,203] so that this band mainly represents the rings.

1400 C-H bend of cinnamaldehydes (Raman only)

Not resolved in IR, but observable as a shoulder in the Raman spectrum. It is caused by the C-H bending motion of the aldehyde group. It is better visible in CAD-mutants[157] and disappears upon $NaBH_4$ reduction (see Fig. 8A,B).

1365 Ring stretch Φ14 of G-OH rings (IR only)
C-X stretch Φ20a of 5-5' structures
C-X stretch of Φ20a of DBDO (Raman only)

This band has contributions from two different modes:
Coupling of the OH-bending with ring sextant stretching Φ14 causes a medium absorption band in IR. The Raman intensity is weak. In 4-O-linked rings, coupling is not possible and Φ14 is found at lower wavenumbers. The band is therefore specific to phenol endgroups.
The all-in-phase substituent stretch (Φ20a) of 5-5' structures also appears at this frequency. It has medium IR but strong Raman intensity. At 532 nm, mainly dibenzodioxocin (DBDO) structures are responsible for this band, because they benefit from resonance enhancement. This mode seems to be rather stable at 1360 cm^{-1}, whereas Φ14 can also appear up to 10 cm^{-1} higher.
While it is true that C-H bending modes also appear in this interval, they are normally not associated with large dipole moment changes, so in contrast to previous assignments[196,197], this band should be regarded as a representation of rings.

1335 C-X stretch Φ20a of β-5' and 4-O-5' structures
C-X stretch Φ20a of β-5' coniferyl aldehyde and alcohol (Raman only)
C-X stretch Φ20a of 4-O-5' coniferyl aldehyde and alcohol (Raman only)
C-H bending Φ18b of asym-tetra-rings and C=C

The 1335 cm^{-1} band is one of the strongest Raman bands. Its IR activity is rather low and it might not be resolved at all, which could explain its absence in Hergert's review[196]. The band is commonly assigned to the aromatic ring[193,197], as well as to aliphatic OH-bending[194]. The latter assignment is not supported by model compound studies and should be regarded as incorrect. This band is frequently used as a marker band for S-rings[119,177,178,245], although doubts have arisen on its validity[176]. These doubts are justified, because although G-lignins display a very strong "S-band", they contain almost no S-units[68]. As already discussed, G-units indeed can display this band, namely in the cases, where C5 is specifically substituted (see section 3.3.3. for details). There is only one publication acknowledging this[197]. In G-lignins, only β-5' and 4-O-5' structure can produce this band. Since the 532 nm Raman spectrum mainly shows cinnamaldehydes and alcohols (see section 3.1 and **Paper III**), this band has to

be assigned to these structures. Based on reference spectra[184,248] it is likely that it represents β-5'-linked coniferyl aldehyde and coniferyl alcohol.
However, laser degradation studies have shown that in lignin there are coniferyl alcohol moieties with phenolic OH-groups present (**Paper II**). This can be either "free", i.e. unlinked monomers or 4-O-5' linked molecules, because in this linkage the hydroxyl remains. 5-5' coupling is not observed in lignins[58] and therefore disregarded. The results from laser degradation show a small frequency decrease supposedly caused by the removal of 4-O-5' coniferyl alcohol. Free monomers cannot be responsible for this shift because they don't have a band here. On the basis of theses results it can be argued that 4-O-5' linked coniferyl alcohol endgroups are present in lignin, however more experiments are needed to clarify this. Consequently, this also implies that 4-O-5'-linked cinnamaldehydes contribute to this band.
Replacing the 4-OH with a methoxy group (eugenol -> dimethyleugenol) also results in a band at around this wavenumber (see Fig. 7). It is however caused by a specific molecular geometry (both methoxy groups in-plane with the ring and pointed away from each other) and cannot be regarded as a proof for G-rings (asym-tri) causing this band.
C-H bending of asym-tetra-rings (Φ18b) and C-H bending from C=C bonds can also be thought of contributing to this band in the Raman spectrum (sinapapldehyde 1320, (2E)-3-(8-methoxy-2,3-dihydro-1,4-benzodioxin-6-yl)-prop-2-enal 1318 cm^{-1}, abietin, 1325 cm^{-1}). These modes can acquire considerable Raman intensity, but are often coupled to Φ20a of the ring.
Lastly, it has to be noted that Raman spectra of CAD-mutants (tobacco) featuring a strong 1345 cm^{-1} band have been reported[156]. It likey stems from an asym-tetra-cinnamaldehyde as well. CAD-mutants of *Arabidopsis* don't display such a band shift[157].

1305 C-H bending (Raman 785 only, uncertain)

This band is probably caused by C-H bending of a C=C group or an asym-tetra ring. It has been assigned to aliphatic OH bends in the Raman spectrum[193], which is unlikely. Single OH-bending by itself has a low polarizability and is normally not observed in the Raman spectrum. It can however be activated by symmetry and sinapic acid dimers show such a dimer band at 1307 cm^{-1}, which disappears in ethanol.

1275 C-X stretch Φ20a of 5-5' units (IR only) C-H bend (C=C) of β-O-4'-linked coniferyl alcohol and cinnamaldehydes (Raman only)

Only resolved in the Raman spectrum, this band is typically taken as the G-unit

reference band[119,177,178,245], although mode Φ7a does not display much Raman activity. In Raman 532, it must come from a conjugated substructure. Potential candidates in the spectral library are vanillylidenacetone (1274, 1262 cm^{-1}), ethyl-cinnamate (1272 cm^{-1}), 3,4-dimethoxyacetophenone, trimethoxyacetophenone (1277 cm^{-1}), eleutheroside B (1278 cm^{-1}), abietin (1280 cm^{-1}) and methylisoeugenol (1267 cm^{-1}). Some cannot be fitted into the spectrum due to other bands, this leaves the glucosides of coniferyl and sinapyl alcohol (abietin, eleutheroside B) and methylisoeugenol as the only possibilities.

Although being very weak in Raman spectra of CAD-mutants[157], the band is affected by $NaBH_4$-reduction (see Fig. 8A,B). This together with the fact, that the three remaining molecules all have C-O-4 linkages means, that the band has contribution from β-O-4-linked coniferyl alcohol and from cinnamaldehydes. This also fits the observation, that laser degradation does not affect this band (one OH missing).

In the infrared, this band is hidden in a bigger band complex. It contains signal from 5-5' structures (1277 cm^{-1}) as well as G-rings (see next band).

1265 C-X stretch Φ7a of G-rings (IR only)

In IR, this is a broad, featureless yet important diagnostic band of G-rings. At its flanks, 5-5' structures contribute to the signal (1277, 1248 cm^{-1}). The main body incorporates signals of all kinds of asym-tri-G-rings. Erhardt[186] argues, that instead of speaking of "ring breathing modes coupled with CO stretching modes [...] the bands at 1270 and 1230 cm^{-1} [should] be attributed to CO stretching modes coupled with other substituent modes." It is however clear from the literature[203], that these modes are derived from ring breathing modes, because coupling of substituents with ring modes of benzene around 1000 cm^{-1} (these are Φ1 and Φ12) results in two modes each. In every set, one combination acquires more ring breathing character (< 1000 cm^{-1}) while the other has more C-X stretching character (> 1000 cm^{-1}). It is therefore not wrong to speak of "ring breathing" which is also visualized in computations, although the Wilson[244]/Varsanyi[203] notation should be used to avoid confusion.

1215 C-X stretch Φ13 of G-rings (IR only)
C-X stretch Φ13 of β-5' rings (IR only)
O-H bending of G-OH-rings (IR only)

Literature assigns this band to C-C/C-O plus C=O stretching[197] or to C-O stretching of phenols[196] The former assignment is problematic, because C=O stretching definitely does not occur at this frequency. It is very likely that this was an error made by the compression algorithm when scanning this document

because the wrong double bond is repeated several times. The phenol assignment describes the vibrational motion more accurately, because in Φ13, the local coordinate is localized on C1-C and C4-O. This is true for G- and S-rings. A survey on asym-tri- and asym-tetra-rings shows, that asym-tri-rings have their Φ13 around 1225 cm^{-1} regardless of oxygen substitution. In asym-tetra-rings, this holds except for benzodioxane and β-5'-rings, where it is found at 1215 cm^{-1} (increased mass/ring strain).
In addition, OH-bending of phenols, usually found at 1205 cm^{-1}, contributes to this IR band.

1190 C-H rocking of methoxy groups

This band was assigned as a phenol mode[194] and as a methoxyl-derived mode[196]. Calculations and reference spectra support the latter assignment. The phenol mode is the OH-bending around 10 cm^{-1} higher (see previous band).

1140 C-C stretch of cinnamaldehydes
C-H bending of rings
O-CH_3/C-COH stretching of β-5' units

The 1140 cm^{-1} band is an interesting case, because the assignment differs between IR and Raman. Six individual contributions can be identified. The literature assigns the IR band to aromatic in-plane C-H bending and C=O stretching[197] and methoxy vibrations[186], and the Raman band to modes of cinnamaldehydes[194].
Based on spectra of model compounds and DFT calculations (see also **Paper III**, **Paper IV**), which support the assignment to aromatic C-H bending and cinnamaldehydes, the following conclusions can be drawn:
In IR, C-H in-plane bending of rings is responsible for a high wavenumber component. Φ18b of conjugated asym-tri-rings is found at 1160 cm^{-1}, while Φ18b of unconjugated asym-tri-rings is at 1150 cm^{-1}. Φ18a of β-5' structures probably appears at 1145 cm^{-1}. Φ18a of 5-5' structures comes at 1140 cm^{-1} and C-C stretching of cinnamaldehydes is assigned to 1130 cm^{-1}. C-H bending (Φ15) of G-rings at 1125 cm^{-1}. The out-of-phase O-CH_3/C-COH stretching of β-5' units is assigned to 1115 cm^{-1}.
In Raman, one band component 1150 cm^{-1} comes from β-5' and 4-O-5'-linked conjugated rings (Φ18a, 1150 cm^{-1}), another from the C-C stretch of cinnamaldeyhdes (1130 cm^{-1})
The band intensity can be decreased by $NaBH_4$-treatment, which removes the aldehyde contribution (compare Fig. 8) and by laser degradation (Paper II), which probably removes contribution of 4-O-5'-linked coniferyl alcohol (see also discussion in section 3.2). Non-bonded coniferyl alcohol does not have this band. Spectra of CAD-mutants with elevated cinnamaldehyde levels show the whole

band being shifted to 1162 cm^{-1}. There is however no cinnamaldehyde known which has a strong Raman band that high at this wavenumber (cinnamaldehyde 1120 cm^{-1}, o-methoxycinnamaldehyde 1128 cm^{-1}, p-methoxycinnamaldehyde 1125 cm^{-1}, coniferyl aldehyde 1132 cm^{-1}, 4-acetoxy-3-methoxycinnamaldehyde 1128 cm^{-1}, sinapin aldehyde 1134 cm^{-1} and (2E)-3-(8-methoxy-2,3-dihydro-1,4-benzodioxin-6-yl)-prop-2-enal 1121 cm^{-1}). CAD-mutant lignins might however not be a valid comparison, because of an ether linkage on the C=C bond[58] which severely alters the vibrational behavior of this bond.

1097 unassigned

May be related to C-O/C-C stretching of β-5' units (see previous band) or to C-C stretching of side chains (see next band).

1085 C_β-C_γOH stretch
O-CH_3 stretch of 5-5' structures

Many phenylpropanoids have a C-C stretching mode at this frequency, which is located in the side chain. From reference spectra it is noted that all cinnamyl alcohols have a medium to strong IR band here. The Raman intensity is low. Isoeugenol does not exhibit such a band, so an attached oxygen is probably required. This is in accordance with literature[194,196,197].
5-5' structures also have an IR band here, it stems from the in-phase O-CH_3 stretch.

1048 O-CH_3 stretch of 5-5' units
O-CH_3/C-COH stretching of β-5' units

According to reference spectra, the in-phase O-CH_3/C-COH stretch of β-5' units[248] is located higher (1060 cm^{-1}) than the out-of-phase O-CH_3 stretch of 5-5' units (1048 cm^{-1}).

1030 O-CH_3 stretch of G-rings

Strong IR band characteristic for G-rings. Every G-ring has this band. Medium to weak Raman intensity.

967 C-H wag of C=C (IR only)
C-X stretch Φ7a of 5-5' units (Raman 785 only)

One of the bands assigned differently to IR and Raman. In IR, it represents the C-H wag of C=C bonds. These are cinnamyl alcohols, aldehydes and esters. Also stilbenes have this band very strong.
In Raman, the band is only observed at 785 nm, where it is assigned to the in-phase combination of the C-X stretching modes Φ7a of 5-5' structures.

930 C-X stretch Φ7b of G-rings
C-X stretch Φ7b of 5-5' units (Raman 785 only)

Literature assigns this band to C-H out-of-plane bending (of rings)[194,197]. DFT-calculations show in accordance with literature[73,203] that there are indeed C-H modes of rings in at this frequency, but the associated dipole moment change is low (these are high-order standing waves, i.e. Φ5, Φ17 in benzene). G-rings additionally display a weak to medium C-X mode, which is coupled to the symmetric C-O-CH_3 stretch. The IR band is therefore assigned to the latter mode. 5-5' structures have a medium-intense Raman band caused by the in-phase combination of the C-X stretching modes Φ7b.

855 C-H wag Φ10a of G-rings
C-H wag of cinnamaldehydes (Raman only)

Assigned to aromatic C-H out-of-plane modes in literature[186,194,196,197]. Consistent with calculations and theoretical considerations[203]. This is the "lone H wag" of the G-ring. In Raman, the band intensity decreases upon $NaBH_4$-reduction, so contribution of cinnamaldehydes is expected. 4-Acetoxy-3-methoxycinnamaldehyde (846 cm^{-1}) and sinapaldehyde (861 cm^{-1}) show Raman bands at 532 nm, at 785 nm, only sinapaldehyde looks promising.

814 C-H wag Φ11 of G-rings (IR only)
Ring stretch Φ1 of G-rings

Based on reference spectra and calculations, the band is expected to have a high-wavenumber component (Φ11, C-H wag) and a low-wavenumber component (Φ1, ring stretch). Both are observed in the IR spectrum, while the Raman spectrum shows only the totally symmetric ring stretch.
In most cases, this is one of the strongest Raman bands of unconjugated aromatic

asym-tri- and asym-tetra-type rings. It was this observation that led to the conclusion that the Raman 532 nm spectrum shows mainly conjugated structures of lignin, because otherwise this band would be among the strongest (see also **Paper III**).
If there is no deviation from the ideal angle (120°) in benzene, then the frequency is found at 800 cm^{-1} (4-hydroxy-3-methoxy-acetophenone 797 cm^{-1}, 4-hydroxy-3,5-dimethoxyacetophenone 798 cm^{-1}, deviation 0.3° in both cases). This also confirms DFT-calculations, which show the mode to be localized on the light triangle (C2-C4-C6). If the angle deviates from 120°, then the frequency drops (3,4-diemethoxyacetophenone, 766 cm^{-1}, 4,6°). If the substituents are connected, this increases the frequency depending on ring size and strain: 7-Methyl-2H-1,5-benzodioxepin-3(4H)-one (7-membered ring, 744 cm^{-1}) < 6-acetyl-1,4-benzodioxane (6-membered ring, 749 cm^{-1}) < 3,4-methylenedioxyacetophenone (5-membered ring, 812 cm^{-1}).

782 Ring stretch/bending Φ1/12

Structural origin uknown.

770 Ring bending/puckering Φ12/Φ4 of G-rings (IR only)
Ring puckering Φ4 of 5-5' structures

Signal from ring bending and puckering modes. If the second-order substituent is not in plane with the ring (the regular case), Φ12 tends to couple with the nearby ring puckering Φ4. This results in both modes having similar IR/Raman activity.

742 Ring bending/puckering Φ12/Φ4 of G-rings (IR only)
Ring bending Φ12 of DBDO

Based on reference spectra[248], this band is also assigned to β-5' structures. Dibenzodioxocin has an out-of-phase ring bending mode here.

734 Ring puckering Φ4 of G-rings

This band can also be seen in Raman 785.

630 Out-of-plane bending (Φ16a) of G-rings?

Band with broad background in IR caused by OH-torsion modes. May be related to out-of-plane bending of the ring (Φ16a).

598 Ring bending (Φ12/6b) of conjugated β-5'/4-O-5'-structure? Ring/C=O bending (Φ6a) of coniferyl aldehyde

One of the few bands discernible in Raman at 532 nm, this indicates a conjugated structure being responsible for it. Coniferaldehyde shows a relatively strong Raman line at 582 cm^{-1} assigned to Φ6a/C=O bending and the band disappears upon $NaBH_4$-reduction (see Fig. 8A,B). Other cinnamaldehydes do not exhibit this mode that strongly.
The relative symmetrical ring bending Φ12 of asym-tetra rings would also be reasonable.

560 In-phase-C-X bending Φ3 of G-rings?

390 C-O-CH_3 bending C-X bending (Φ9b, 10a) of G-rings

270 Ring bending Φ12 of 5-5' structures (Raman 785 only)

This is the in-phase bending mode (more details in **Paper IV**).

Raman 532

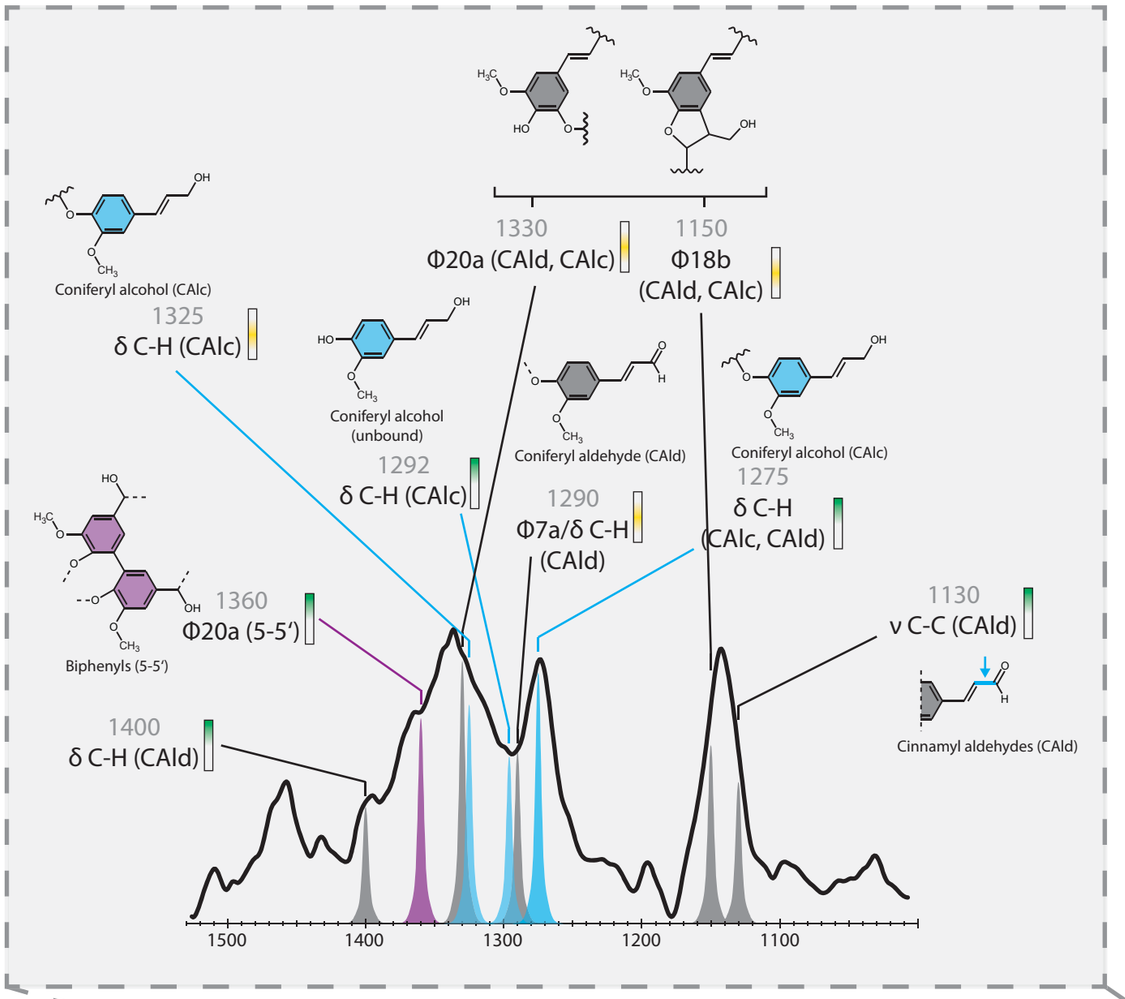

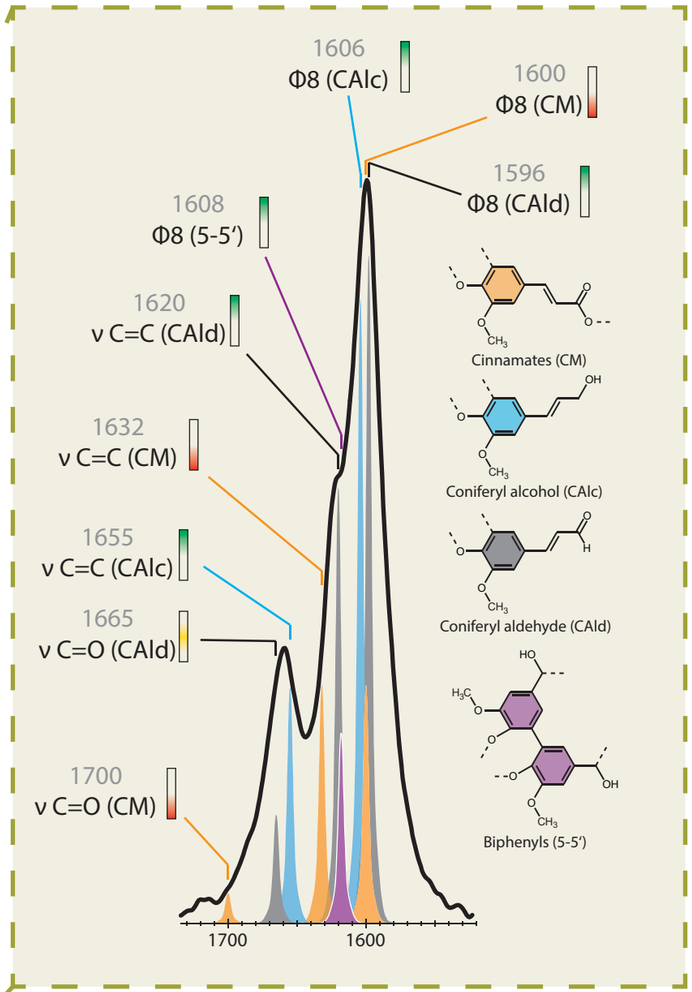

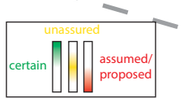

BP.....biphenyl unit
G.....G-ring

Φ.....ring mode
ν.....stretching
δ.....bending
τ.....torsion

s.....symmetric
as.....anti-/asymmetric
=.....in-phase
Λ.....out-of-phase

Bock. P., 2020. The vibrations of lignin. Doctoral thesis. Vienna.

G-DHP kindly provided by Grigory Zinovyev and Hassan Amer. Cell corner spectrum kindly provided by Martin Felhofer.

Raman 785

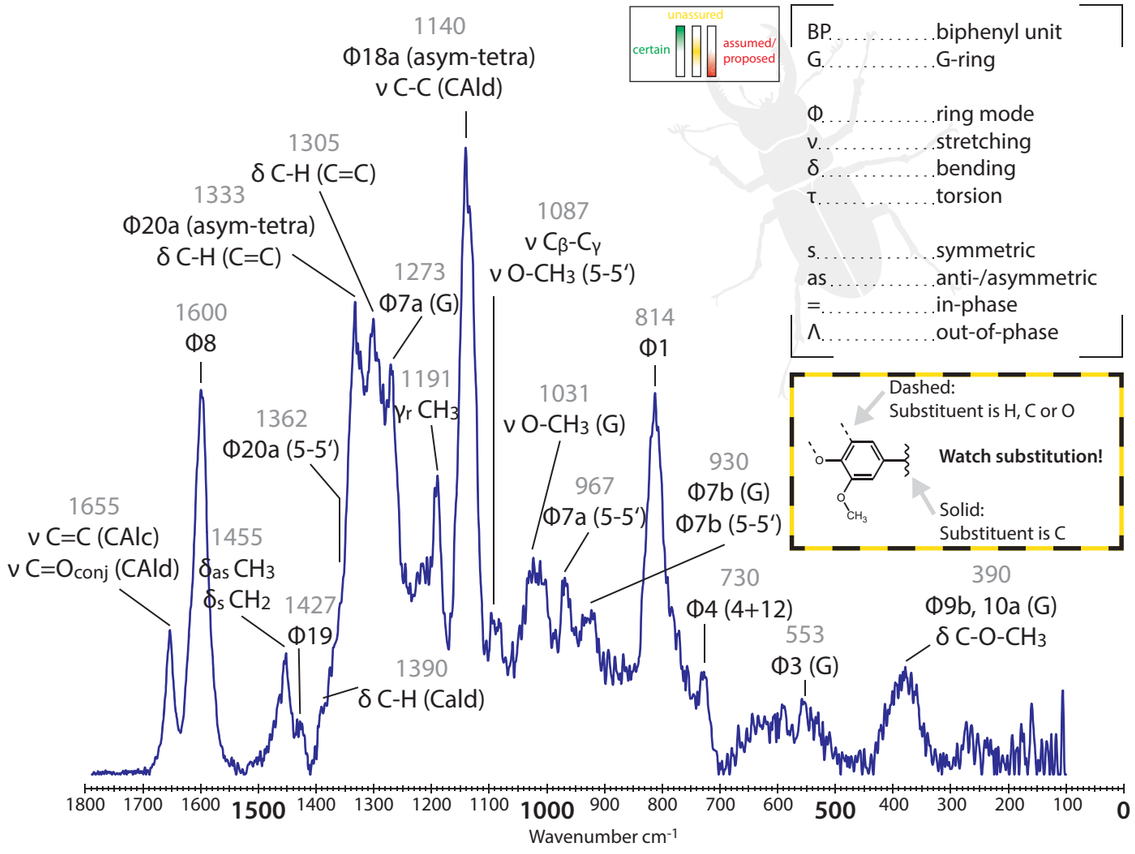

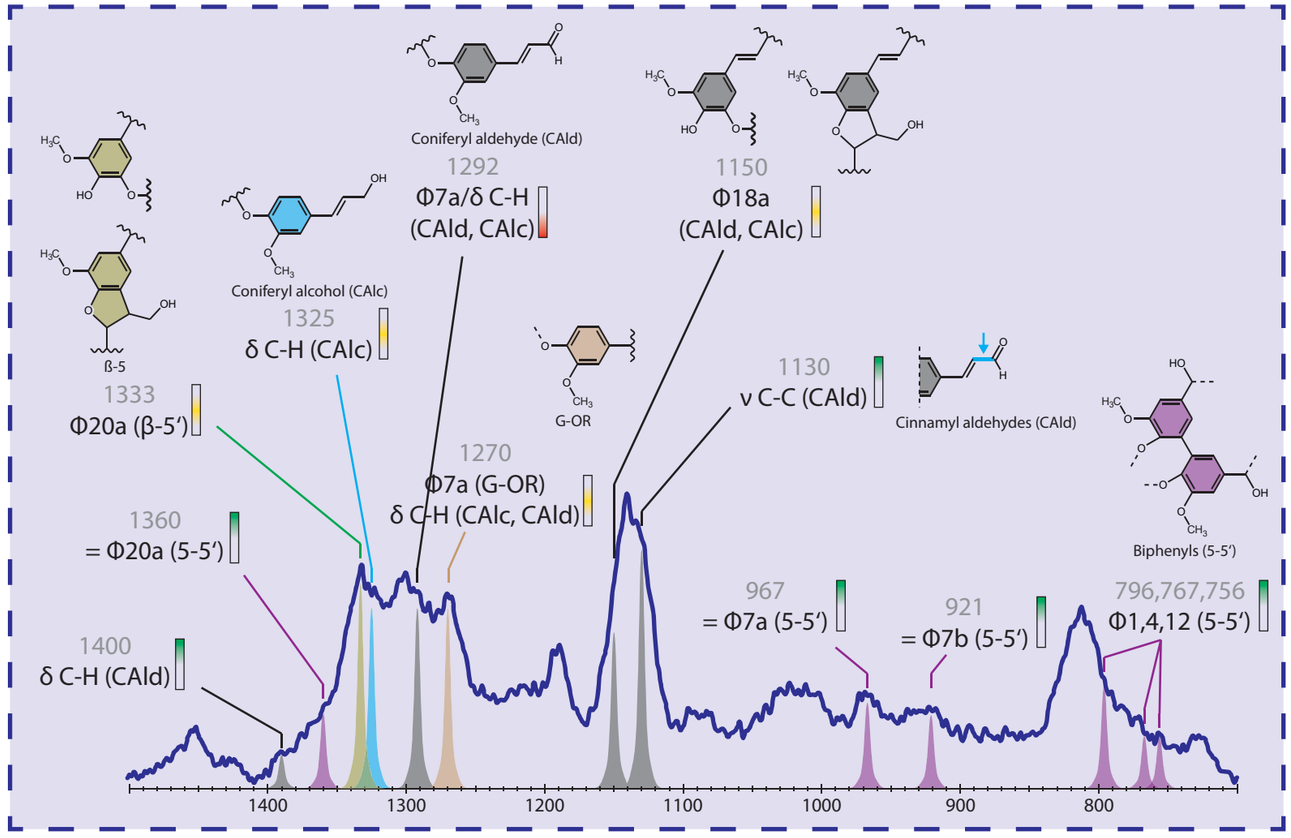

G-DHP kindly provided by Grigory Zinovyev and Hassan Amer.

Bock. P., 2020. The vibrations of lignin. Doctoral thesis. Vienna.

Infrared

BP.....biphenyl unit
G.....G-ring

Φ.....ring mode
ν.....stretching
δ.....bending
τ.....torsion

s.....symmetric
as.....anti-/asymmetric
=.....in-phase
Λ.....out-of-phase

Dashed:
Substituent is H, C or O

Watch substitution!

Solid:
Substituent is C

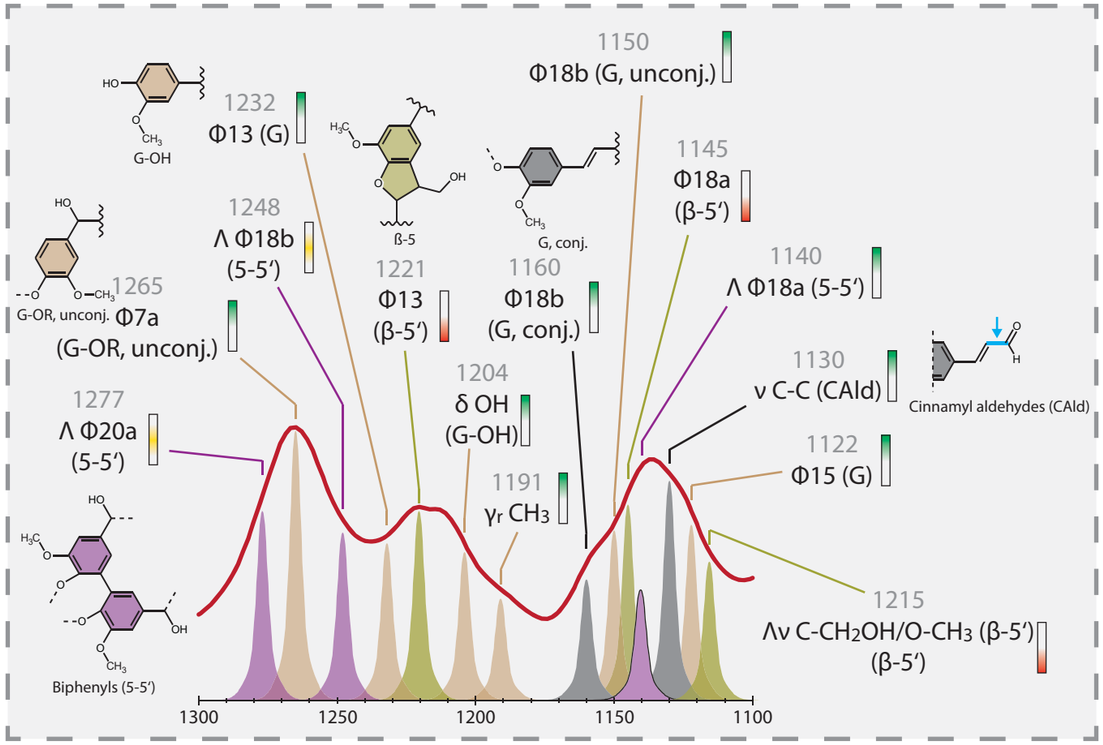

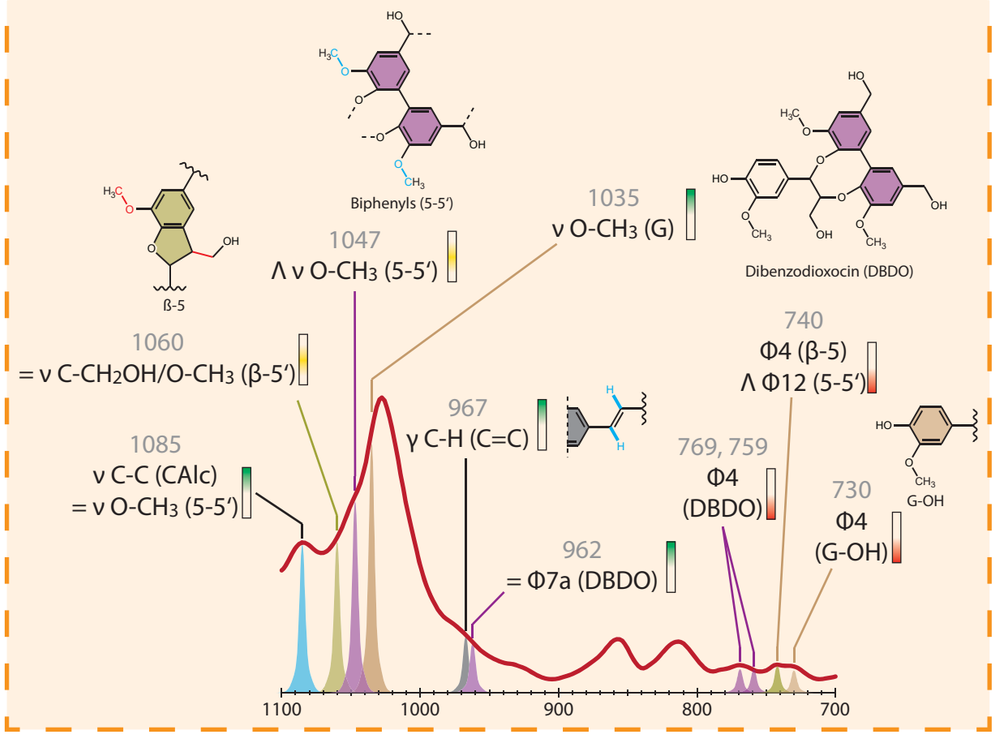

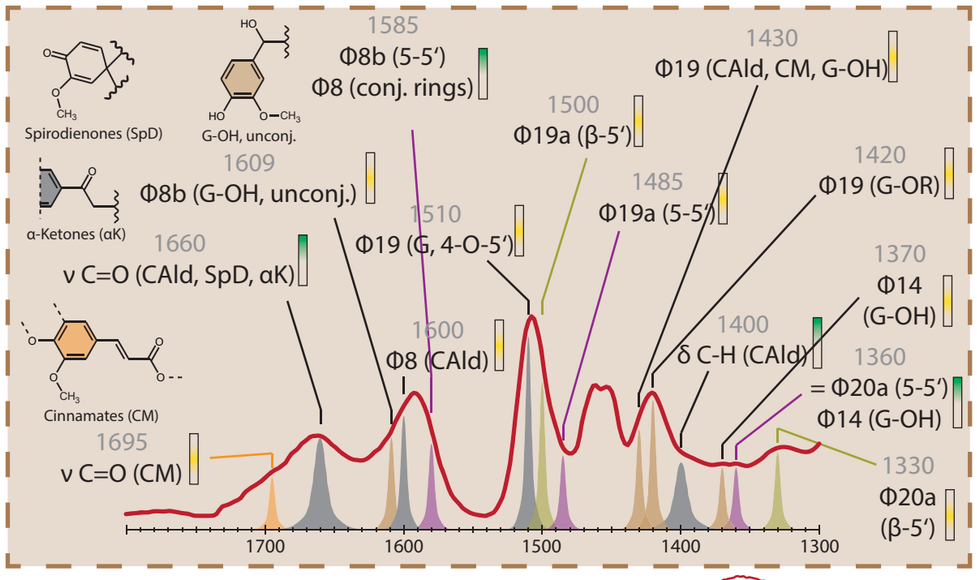

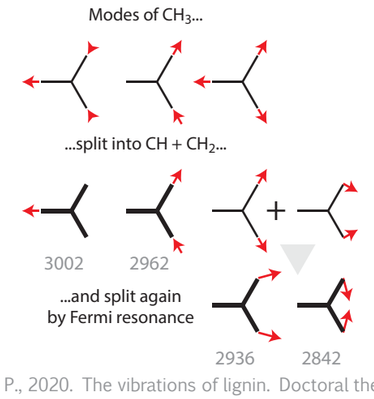

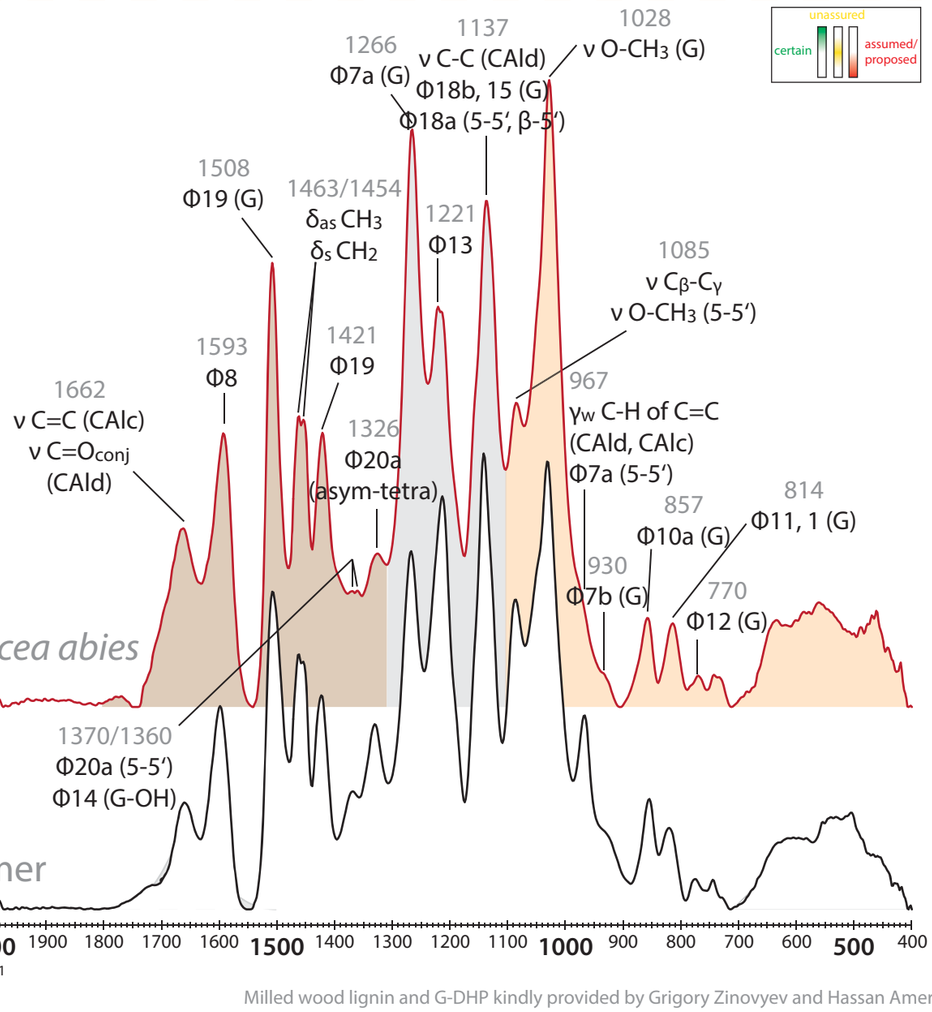

Bock. P., 2020. The vibrations of lignin. Doctoral thesis. Vienna.

Milled wood lignin and G-DHP kindly provided by Grigory Zinovyev and Hassan Amer.

3.5. THE EXTRAPOLATION TO NON-G-LIGNINS

Sections 3.3 and 3.4 dealt with differently linked G-rings and the spectroscopic fingerprint of the resulting lignins. It was noticeble that the number of ring substituents had a greater effect on the spectrum than the type of the substituent. Lignin monomers can therefore be grouped into three types:

1) 1,4-disubstituted rings: H (except for β-3'/4-O-3'/3-3')

2) 1,3,4-asymetrically-trisubstituted rings: C, G (except for β-5'/4-O-5'/5-5'), H (only β-3'/4-O-3'/3-3')

3) 1,3,4,5-asymetrically tetrasubstituted rings: 5H, S, G (only β-5'/ 4-O-5'/ 5-5')

This further results in five different substitution patterns:

1) One carbon, one oxygen: H

2) Two carbons, one oxygen: H (pos. 3)

3) One carbon, two oxygens: C, G

4) Two carbons, two oxygens: G (pos. 5)

5) One carbon, three oxygens: 5H, S

As a result, rings with the same substitution pattern will show similar bands in the spectrum.

In the following, spectral properties of other lignins will be discussed briefly.

H-lignins

p-coumaryl rings differ the most from of the previously discussed rings, because they have only two substituents, thus four hydrogens and the ring falls into the C_{2v} point group. This makes a_1 symmetry species very interesting for the Raman spectrum. The all-in-phase C-X stretch Φ7a (~1250 cm^{-1}), the totally symmetric C-H bend Φ9a (1175 cm^{-1}), ring breathing Φ1 (860 cm^{-1}) all give good Raman signals. The latter frequently enters into fermi resonance with Φ16a to produce strong Raman doublet[272]. Judging from literature[119,122,273], Φ9a seems to be the most useful Raman band.

G-lignins

See sections 3.3. and 3.4.

C-lignins

IR spectra of C-lignins were recently published[274]. Since G- and C-rings have identical first-order substituents, the only difference should arise from C-X-sensitive ring modes and substituent modes. Furthermore, the benzodioxane linkage is not causing enough strain on the ring to significantly shift the wavenumbers (see band 814 cm above).

It was noted that the typical doublet at 1465/1455 cm^{-1} is replaced by a single band at 1440 cm^{-1}. From the structural point of view, this is clear, because the doublet is caused by methoxy groups which do not exist in C-lignin, instead there are only one CH_2 and two single C-H oscillators, which appear a little bit lower than OCH_3 bendings, consistent with standard literature[73,204]. Φ14 is shifted to 1340 cm^{-1} due to the second-order substituent being a carbon (see above discussion of band 1365 cm^{-}

^{1}). Φ7a (1270 cm^{-1}) is at the same position as in G-lignin, Φ18b shows an unexpected upshift (1165 cm^{-1}), which shows that the Varsanyi notation is a better description than "C-H bending of ring", because it considers all substituents. C-lignin shows an additional band at approximately 1090 cm^{-1} and a changed shape of the 1038 cm^{-1} band complex. This is also clear, because there is difference in the C-C/C-O scaffold by definition (3-O-α instead of methoxy group). Φ7b is lowered from 930 cm^{-1} (G) to 870 cm^{-1}, because there is no C-O-CH_3 stretch to couple with. Lastly, the strong band at 814 cm^{-1} is Φ11, with Φ1 as a shoulder (782 cm^{-1}).

S-lignins

S-rings are asym-tetra-rings belonging to the C_{2v} point group. Like for H-rings, this activates a_1-species in the Raman spectrum, which is most useful in the case of substituent modes, e.g. Φ20a (1335 cm^{-1}), in-phase C-O stretching (1040, 960 cm^{-1}) and bending (370 cm^{-1}). Also C-H bending (Φ18a, 1160 cm^{-1}) has notable intensity. In IR, anti-symmetric modes are intensified in a similar way, the strongest band is normally the out-of-phase O-CH_3 stretch (1100 cm^{-1}), which is stronger than the similar mode in β-5' units. Conversly, in IR, Φ20a of S-units is weaker than of β-5'-linked G-units. At 1210 cm^{-1}, Φ13 appears as a strong band.

5H-lignins

Athough lignins of 5H-type have the benzodioxane linkage in common with C-lignins, they have an additional methoxy group which can interact with the C-O oscillators. This causes an IR-active doublet at 1065/1045 cm^{-1} and bands at 955 and 885 cm^{-1}. The Raman activity is low, only the mode at 1065 cm^{-1} acquires some intensity. Other bands are similar to S-units due to similar ring substitution.

4

Conclusion and Outlook

Finis coronat opus.

Ovid

The plant cell wall can readily be investigated with Raman imaging techniques. These allow for chemical analysis at nanometer resolution. This work presented a detailed discussion of the Raman and infrared spectra (IR) of guaiacyl (G) - lignin and discussed the influence of the laser (wavelength) to sample and spectrum.

Specifically, it was found that π-conjugated molecules can be subject to three different enhancing mechanisms. A good indication for the operation of these effects is that the ring stretch at 1600 cm^{-1} is more intense than the ring breathing around 800 cm^{-1}. In addition, conjugation normally increases the Raman cross section which results in disproportionate contribution to the Raman spectrum by such structures. Dibenzodioxocin only profits from resonance enhancement and its signal can therefore be reduced by increasing the excitation wavelength (e.g. 532 --> 785 nm).

Conjugatation- and charge-transfer enhancement cannot be removed this way. In lignin, cinnamyl aldehydes, -alcohols, -acids and -esters show these effects. To remove their contribution from the Raman spectrum, the π-conjugation path has to be destroyed, e.g. by chemical treatment. More generally, this effect also plays a role in non-lignin aromatic compounds and provides high sensitiviy towards stilbenes and those flavonoids where both aromatic rings are connected over a π-system (chalcones, aurones, anthocyanins, flavones). This makes Raman spectroscopy an invaluable tool to track such compounds, which often comprise only small fractions in the cell wall.

Only charge-transfer enhancement plays a role in the IR spectrum, where specific bands are intensified (e.g. the bands >1600 cm^{-1}). The overall contribution, however, is only minor and the IR spectrum of lignin can therefore be regarded a much better representation of the bulk structure than the Raman spectrum.

The effects of 532 nm and 785 nm lasers on the experiments were studied. It turned out that two-photon absorption has to be considered during Raman measurements, given the high laser intensities normally used in Raman experiments. Two-photon absorption at 532 nm matches absorption bands of lignin, creating a possibility for energy transfer to the sample. In lignins it seems that mainly 4-hydroxycinnamyl alcohols are responsible for this absorption band (coniferyl- and sinapyl alcohol: ~260 nm). Subsequent generation of radicals can increase the absorption further if

the generated species have absorption bands matching the laser wavelength. This will cause degradation and ultimate burning of the sample. Immersion in water is an appropriate countermeasure, because it reduces the lifetime of excited species.

Beside generation of radicals it could specifically be shown that cinnamyl alcohols, which possess an OH-group at the para-position of the ring are prone to quinone-methide formation in water, when irradiated with a 532 nm laser. This effect is visible as a decrease of the 1660 cm^{-1} band. One consequence is that care should be taken when using this band for ratios, etc. Another welcome implication is that with this effect, the existence of such molecules can be specifically tested. Given that this intensity decrease is also observed in wood, this implies that some cinnamyl alcohols in wood occur either as unbound monomers or are 4-O-5' linked into the polymer.

In practice, laser-induced effects are mainly an issue when using 532 nm excitation, because 785 nm radiation does not match absorption bands, even when frequency-doubled. Laser susceptibility checks and keeping laser retention times short are measures to assess vulnerabilities and avoid laser damage. The process can also be used to selectively remove susceptible compounds, e.g. laser-delignify a sample.

Extensive measurements on reference compounds and computation of their theoretical spectra resulted in the spectral assignment of guaiacyl (G) - lignin at an unprecedented level of detail. With regard to different excitation wavelengths, many bands of the IR and Raman spectra were reassigned or even assigned for the first time. A detailed discussion of the vibrational modes causing the bands increases the understanding of the IR and Raman spectra of lignin. The spectral footprints of lignin substructures as well as advice on how to extrapolate to other lignins are included in this work.

There is still much to do for future research in this field. Given that reference spectra serve as the basis of any vibrational interpretation, it has to be noted that the available spectra are strongly biased towards the traditional S-, G- and H-monomers. Spectra of other monomers are not available. Furthermore, the reference compounds typically used do not always suit the interpretation. On the one hand, there is a lack of dimers and oligomers to properly assess 3D-structure effects on vibrational modes (e.g. π-stacking) which are necessary on the quest to fully understand the lignin spectrum. On the other hand, many compounds used are in some aspect or the other unrealistic, that is they are only bad representations of lignin. This includes overrepresentation of compounds bearing OH-groups at the para-position of the ring (only a minority in lignin) and ring-substitutions not present in lignin (e.g. ortho substitution). Furthermore, the spectroscopic investigation is challenging as well: Improper account for factor group splitting, dimer formation (acids!), polarization and solvent effects results in reference spectra not reflecting the state of the molecule *in-situ*.

The capability to selectively cause photochemical reactions for a detailed characterization of the sample seems not to be used much in current work. It has to be noted that a lot of information is hidden "between" the spectra, meaning that some insight can only be attained by analyzing differences between spectra of different excitation wavelengths. Also UV-VIS absorption spectra proved valuable for this process.

Since the disproportionate representation of π-conjugated structures in the Raman spectra of lignin is also reflected in the assignment tables, some abundant structural features (β-O-4' linkages, resinol structures) are not included. This makes vibrational spectroscopy of lignins currently lacking behind established methods like NMR, because evaluation and quantification of linkage types is

very important for lignin characterization. While there definitely should be no competition between methods (each method sees different aspects, no one the whole picture), as of today, the potential of IR and Raman imaging on plant cell walls is not fully utilized. Future work should aim to remove these obstacles to facilitate the use and increase the potential of this versatile method.

5

Literature

I asked her for one hair from her golden head.

She gave me three.

Gimli

---

[1] European Commission, *The European Green Deal*, **2019**. Press release, 11 December 2019, Brussels.

[2] European Commission, *Financing the green transition: The European Green Deal Investment Plan and Just Transition Mechanism*, **2020**. Press release, 14 January 2020, Brussels.

[3] M. Aglietta, G. Bai, *Chinas 13th five year plan. In Pursuit of a "Moderately Prosperous Society"*, CEPII, **2016**.

[4] L. Myung-bak, *A Great People with New Dreams*, **2008**. Speech on the 63rd anniversary of national liberation and the 60th anniversary of the founding of the Republic of Korea, 15 August 2008, Seoul.

[5] A. Ocasio-Cortez, *Recognizing the duty of the Federal Government to create a Green New Deal*, **2019**. Resolution H.Res.109 of the 116th Congress of the U.S.A., Washington.

[6] United Nations Environment Programme, *Green Economy*, **s.a.** www.unenvironment.org/regions/asia-and-pacific/regional-initiatives/supporting-resource-efficiency/green-economy [Accessed on 20.02.2020]

[7] H. W. Heldt, B. Piechulla, *Plant Biochemistry*; Academic Press, **2010**.

[8] T. Higuchi, *Biochemistry and Molecular Biology of Wood*; Springer: Berlin Heidelberg, **1997**.

[9] L. Taiz, L. Zeiger, *Plant physiology*; 3rd ed.; Sinauer: Sunderland, **2002**.

[10] G. Henriksson in *Wood Chemistry and Wood Biotechnology*; Ek M, Gellerstedt G, Henriksson G, Eds.; Walter de Gruyter: Berlin, **2009**; Vol. 1.

[11] C. Chio, M. Sain, W. Qin, *Renewable and Sustainable Energy Reviews* **2019**, *107*, 232. 10.1016/j.rser.2019.03.008

[12] W. Schutyser, T. Renders, S. Van den Bosch, S. F. Koelewijn, G. T. Beckham, B. F. Sels, *Chem Soc Rev* **2018**, *47*, 852. 10.1039/c7cs00566k

[13] D. Tarasov, M. Leitch, P. Fatehi, *Biotechnol Biofuels* **2018**, *11*, 269. 10.1186/s13068-018-1262-1

[14] V. K. Ponnusamy, D. D. Nguyen, J. Dharmaraja, S. Shobana, J. R. Banu, R. G. Saratale, S. W. Chang, G. Kumar, *Bioresour Technol* **2019**, *271*, 462. 10.1016/j.biortech.2018.09.070

[15] W. G. Glasser, *Front Chem* **2019**, *7*, 565. 10.3389/fchem.2019.00565

[16] A. J. Ragauskas, G. T. Beckham, M. J. Biddy, R. Chandra, F. Chen, M. F. Davis, B. H. Davison, R. A. Dixon, P. Gilna, M. Keller, P. Langan, A. K. Naskar, J. N. Saddler, T. J. Tschaplinski, G. A. Tuskan, C. E. Wyman, *Science* **2014**, *344*, 1246843. 10.1126/science.1246843
[17] G. Gellerstedt in *Wood Chemistry and Biotechnology*; Ek M, Gellerstedt G, Henriksson G, Eds.; Walter de Gruyter: Berlin, **2009**; Vol. 1.
[18] R. Rinaldi, R. Jastrzebski, M. T. Clough, J. Ralph, M. Kennema, P. C. A. Bruijnincx, B. M. Weckhuysen, *Angewandte Chemie-International Edition* **2016**, *55*, 8164. 10.1002/anie.201510351
[19] N. Gierlinger, *Appl Spectrosc Rev* **2018**, *53*, 517. 10.1080/05704928.2017.1363052
[20] H. Renault, D. Werck-Reichhart, J. K. Weng, *Curr Opin Biotechnol* **2019**, *56*, 105. 10.1016/j.copbio.2018.10.011
[21] R. A. Berner, S. T. Petsch, J. A. Lake, D. J. Beerling, B. N. Popp, R. S. Lane, E. A. Laws, M. B. Westley, N. Cassar, F. I. Woodward, W. P. Quick, *Science* **2000**, *287*, 1630. DOI 10.1126/science.287.5458.1630
[22] J. B. Graham, R. Dudley, N. M. Aguilar, C. Gans, *Nature* **1995**, *375*, 117. Doi 10.1038/375117a0
[23] A. Yeo in *Plant Solute Transport*; Yeo A, Flowers T, Eds.; Blackwell Publishing: Oxford, **2007**.
[24] S. Shabala in *Plant Solute Transport*; Yeo A, Flowers T, Eds.; Blackwell Publishing: Oxford, **2007**.
[25] C. K. Boyce, M. A. Zwieniecki, G. D. Cody, C. Jacobsen, S. Wirick, A. H. Knoll, N. M. Holbrook, *Proc Natl Acad Sci U S A* **2004**, *101*, 17555. 10.1073/pnas.0408024101
[26] L. A. Donaldson, *Iawa Journal* **2002**, *23*, 161. Doi 10.1163/22941932-90000295
[27] J. Ralph, K. Lundquist, G. Brunow, F. Lu, H. Kim, P. F. Schatz, J. M. Marita, R. D. Hatfield, S. A. Ralph, J. H. Christensen, *Phytochem. Rev.* **2004**, *3*, 32. 10.1023/B:PHYT.0000047809.65444.a4
[28] M. Perkins, R. A. Smith, L. Samuels, *Curr Opin Biotechnol* **2019**, *56*, 69. 10.1016/j.copbio.2018.09.011
[29] E. Yi Chou, M. Schuetz, N. Hoffmann, Y. Watanabe, R. Sibout, A. L. Samuels, *J Exp Bot* **2018**, *69*, 1849. 10.1093/jxb/ery067
[30] C. Lion, C. Simon, B. Huss, A. S. Blervacq, L. Tirot, D. Toybou, C. Spriet, C. Slomianny, Y. Guerardel, S. Hawkins, C. Biot, *Cell Chem Biol* **2017**, *24*, 326. 10.1016/j.chembiol.2017.02.009
[31] E. Pesquet, B. Zhang, A. Gorzsas, T. Puhakainen, H. Serk, S. Escamez, O. Barbier, L. Gerber, C. Courtois-Moreau, E. Alatalo, L. Paulin, J. Kangasjarvi, B. Sundberg, D. Goffner, H. Tuominen, *Plant Cell* **2013**, *25*, 1314. 10.1105/tpc.113.110593
[32] R. Vanholme, B. De Meester, J. Ralph, W. Boerjan, *Current Opinion in Biotechnology* **2019**, *56*, 230. 10.1016/j.copbio.2019.02.018
[33] Y. Tobimatsu, M. Schuetz, *Curr Opin Biotechnol* **2019**, *56*, 75. 10.1016/j.copbio.2018.10.001
[34] J. Ralph, G. Brunow, P. J. Harris, R. A. Dixon, P. F. Schatz, W. Boerjan in *Recent advances in polyphenol research*; Blackwell Publishing: Oxford, **2008**.
[35] L. Berstis, T. Elder, M. Crowley, G. T. Beckham, *ACS Sustainable Chemistry & Engineering* **2016**, *4*, 5327. 10.1021/acssuschemeng.6b00520
[36] O. M. Terrett, P. Dupree, *Curr Opin Biotechnol* **2019**, *56*, 97. 10.1016/j.copbio.2018.10.010
[37] H. V. Scheller, P. Ulvskov, *Annu Rev Plant Biol* **2010**, *61*, 263. 10.1146/annurev-arplant-042809-112315
[38] H. Nishimura, A. Kamiya, T. Nagata, M. Katahira, T. Watanabe, *Sci Rep* **2018**, *8*, 6538. 10.1038/s41598-018-24328-9
[39] X. Kang, A. Kirui, M. C. D. Widanage, F. Mentink-Vigier, D. J. Cosgrove, T. Wang, *Nature Communications* **2019**, *10*. 10.1038/s41467-018-08252-0
[40] O. M. Terrett, J. J. Lyczakowski, L. Yu, D. Iuga, W. T. Franks, S. P. Brown, R. Dupree, P. Dupree, *Nat Commun* **2019**, *10*, 4978. 10.1038/s41467-019-12979-9
[41] W. Boerjan, J. Ralph, M. Baucher, *Annu Rev Plant Biol* **2003**, *54*, 519. 10.1146/annurev.arplant.54.031902.134938

[42] J. Ralph, C. Lapierre, F. C. Lu, J. M. Marita, G. Pilate, J. Van Doorsselaere, W. Boerjan, L. Jouanin, *Journal of Agricultural and Food Chemistry* **2001**, *49*, 86. Doi 10.1021/Jf001042+

[43] F. Chen, Y. Tobimatsu, D. Havkin-Frenkel, R. A. Dixon, J. Ralph, *Proceedings of the National Academy of Sciences of the United States of America* **2012**, *109*, 1772. 10.1073/pnas.1120992109

[44] F. Chen, Y. Tobimatsu, L. Jackson, J. Nakashima, J. Ralph, R. A. Dixon, *Plant J* **2013**, *73*, 201. 10.1111/tpj.12012

[45] J. C. del Rio, J. Rencoret, A. Gutierrez, H. Kim, J. Ralph, *Plant Physiology* **2017**, *174*, 2072. 10.1104/pp.17.00362

[46] W. Lan, F. C. Lu, M. Regner, Y. M. Zhu, J. Rencoret, S. A. Ralph, U. I. Zakai, K. Morreel, W. Boerjan, J. Ralph, *Plant Physiology* **2015**, *167*, 1284. 10.1104/pp.114.253757

[47] W. Lan, K. Morreel, F. C. Lu, J. Rencoret, J. C. del Rio, W. Voorend, W. Vermerris, W. Boerjan, J. Ralph, *Plant Physiology* **2016**, *171*, 810. 10.1104/pp.16.02012

[48] W. Lan, J. Rencoret, F. C. Lu, S. D. Karlen, B. G. Smith, P. J. Harris, J. C. del Rio, J. Ralph, *Plant Journal* **2016**, *88*, 1046. 10.1111/tpj.13315

[49] J. C. Del Rio, J. Rencoret, A. Gutierrez, H. Kim, J. Ralph, *J Agric Food Chem* **2018**, *66*, 4402. 10.1021/acs.jafc.8b00880

[50] J. H. Grabber, C. Davidson, Y. Tobimatsu, H. Kim, F. Lu, Y. Zhu, M. Opietnik, N. Santoro, C. E. Foster, F. Yue, D. Ress, X. Pan, J. Ralph, *Plant Sci* **2019**, *287*, 110070. 10.1016/j.plantsci.2019.02.004

[51] T. Elder, J. Carlos Del Rio, J. Ralph, J. Rencoret, H. Kim, G. T. Beckham, *Phytochemistry* **2019**, *164*, 12. 10.1016/j.phytochem.2019.04.003

[52] J. Rencoret, D. Neiva, G. Marques, A. Gutierrez, H. Kim, J. Gominho, H. Pereira, J. Ralph, J. C. Del Rio, *Plant Physiol* **2019**, *180*, 1310. 10.1104/pp.19.00344

[53] H. Önnerud, G. Gellerstedt, *Holzforschung* **2003**, *57*, 165. Doi 10.1515/Hf.2003.025

[54] P. Karhunen, P. Rummakko, J. Sipila, G. Brunow, I. Kilpelainen, *Tetrahedron Letters* **1995**, *36*, 169. Doi 10.1016/0040-4039(94)02203-N

[55] P. Karhunen, P. Rummakko, J. Sipila, G. Brunow, I. Kilpelainen, *Tetrahedron Letters* **1995**, *36*, 4501. Doi 10.1016/0040-4039(95)00769-9

[56] D. S. Argyropoulos, L. Jurasek, L. Kristofova, Z. C. Xia, Y. J. Sun, E. Palus, *Journal of Agricultural and Food Chemistry* **2002**, *50*, 658. 10.1021/jf010909g

[57] F. X. Yue, F. C. Lu, S. Ralph, J. Ralph, *Biomacromolecules* **2016**, *17*, 1909. 10.1021/acs.biomac.6b00256

[58] J. Ralph, C. Lapierre, W. Boerjan, *Curr Opin Biotechnol* **2019**, *56*, 240. 10.1016/j.copbio.2019.02.019

[59] L. M. Zhang, G. Gellerstedt, *Chemical Communications* **2001**, 2744. Doi 10.1039/B108285j

[60] L. M. Zhang, G. Gellerstedt, J. Ralph, F. C. Lu, *Journal of Wood Chemistry and Technology* **2006**, *26*, 65. 10.1080/02773810600580271

[61] M. Sette, R. Wechselberger, C. Crestini, *Chemistry-a European Journal* **2011**, *17*, 9529. 10.1002/chem.201003045

[62] M. Sette, H. Lange, C. Crestini, *Computational and Structural Biotechnology* **2013**, *6*, 7. 10.5936/csbj.201303016

[63] E. A. Capanema, M. Y. Balakshin, J. F. Kadla, *Journal of Agricultural and Food Chemistry* **2004**, *52*, 1850.

[64] L. M. Zhang, G. Gellerstedt, *Magnetic Resonance in Chemistry* **2007**, *45*, 37. 10.1002/mrc.1914

[65] M. Erickson, S. Larsson, G. E. Miksche, *Acta Chemica Scandinavica* **1973**, *27*, 903. DOI 10.3891/acta.chem.scand.27-0903

[66] A. Pereira, I. C. Hoeger, A. Ferrer, J. Rencoret, J. C. del Rio, K. Kruus, J. Rahikainen, M. Kellock, A. Gutierrez, O. J. Rojas, *Biomacromolecules* **2017**, *18*, 1322. 10.1021/acs.biomac.7b00071

[67] J. Rencoret, G. Marques, A. Gutierrez, L. Nieto, J. I. Santos, J. Jimenez-Barbero, A. T. Martinez, J. C. del Rio, *Holzforschung* **2009**, *63*, 691. 10.1515/Hf.2009.070

[68] J. R. Obst, L. L. Laaducci, *Journal of Wood Chemistry and Technology* **1986**, *6*, 311. 10.1080/02773818608085230
[69] I. Cesarino, *Curr Opin Biotechnol* **2019**, *56*, 209. 10.1016/j.copbio.2018.12.012
[70] F. Chen, Y. Tobimatsu, L. Jackson, J. Nakashima, J. Ralph, R. A. Dixon, *Plant Journal* **2013**, *73*, 201. 10.1111/tpj.12012
[71] T. Ikeda, K. Holtman, J. F. Kadla, H. M. Chang, H. Jameel, *Journal of Agricultural and Food Chemistry* **2002**, *50*, 129. 10.1021/jf010870f
[72] M. Schwanninger, J. C. Rodrigues, H. Pereira, B. Hinterstoisser, *Vibrational Spectroscopy* **2004**, *36*, 23. 10.1016/j.vibspec.2004.02.003
[73] N. B. Colthup, L. H. Daly, S. E. Wiberley, *Introduction to Infrared and Raman Spectroscopy*; 3rd Edition ed.; Academic Press Inc.: New York, **1990**, 547.
[74] P. R. Griffiths in *Infrared and Raman Spectroscopic Imaging*; Salzer R, Siesler HW, Eds.; Wiley: Weinheim, **2009**.
[75] N. Gierlinger, T. Keplinger, M. Harrington, *Nature Protocols* **2012**, *7*, 1694. 10.1038/nprot.2012.092
[76] T. X. Huang, X. Cong, S. S. Wu, K. Q. Lin, X. Yao, Y. H. He, J. B. Wu, Y. F. Bao, S. C. Huang, X. Wang, P. H. Tan, B. Ren, *Nat Commun* **2019**, *10*, 5544. 10.1038/s41467-019-13486-7
[77] O. Ilchenko, Y. Pilgun, A. Kutsyk, F. Bachmann, R. Slipets, M. Todeschini, P. O. Okeyo, H. F. Poulsen, A. Boisen, *Nat Commun* **2019**, *10*, 5555. 10.1038/s41467-019-13504-8
[78] A. Baliyan, H. Imai, *Sci Rep* **2019**, *9*, 18241. 10.1038/s41598-019-54770-2
[79] M. S. Dresselhaus, G. Dresselhaus, R. Saito, A. Jorio, *Physics Reports* **2005**, *409*, 47. 10.1016/j.physrep.2004.10.006
[80] T. Hummer, J. Noe, M. S. Hofmann, T. W. Hansch, A. Hogele, D. Hunger, *Nat Commun* **2016**, *7*, 12155. 10.1038/ncomms12155
[81] J. B. Wu, M. L. Lin, X. Cong, H. N. Liu, P. H. Tan, *Chem Soc Rev* **2018**, *47*, 1822. 10.1039/c6cs00915h
[82] C. Neumann, S. Reichardt, P. Venezuela, M. Drogeler, L. Banszerus, M. Schmitz, K. Watanabe, T. Taniguchi, F. Mauri, B. Beschoten, S. V. Rotkin, C. Stampfer, *Nat Commun* **2015**, *6*, 8429. 10.1038/ncomms9429
[83] M. V. Balois, N. Hayazawa, S. Yasuda, K. Ikeda, B. Yang, E. Kazuma, Y. Yokota, Y. Kim, T. Tanaka, *npj 2D Materials and Applications* **2019**, *3*. 10.1038/s41699-019-0121-7
[84] P. Vecera, J. C. Chacon-Torres, T. Pichler, S. Reich, H. R. Soni, A. Gorling, K. Edelthalhammer, H. Peterlik, F. Hauke, A. Hirsch, *Nat Commun* **2017**, *8*, 15192. 10.1038/ncomms15192
[85] A. Paudel, D. Raijada, J. Rantanen, *Adv Drug Deliv Rev* **2015**, *89*, 3. 10.1016/j.addr.2015.04.003
[86] F. G. Vogt, M. Strohmeier, *Mol Pharm* **2013**, *10*, 4216. 10.1021/mp400314s
[87] M. Edinger, D. Bar-Shalom, J. Rantanen, N. Genina, *Pharm Res* **2017**, *34*, 1023. 10.1007/s11095-017-2126-2
[88] L. Nasdala, S. Kostrovitsky, A. K. Kennedy, M. Zeug, S. A. Esenkulova, *Lithos* **2014**, *206-207*, 252. 10.1016/j.lithos.2014.08.005
[89] M. Zeug, A. I. Rodríguez Vargas, L. Nasdala, *Physics and Chemistry of Minerals* **2016**, *44*, 221. 10.1007/s00269-016-0851-4
[90] D. Srodek, M. Dulski, I. Galuskina, *Sci Rep* **2018**, *8*, 13593. 10.1038/s41598-018-31809-4
[91] E. Słaby, A. Domonik, M. Śmigielski, K. Majzner, G. Motuza, J. Götze, K. Simon, I. Moszumańska, Ł. Kruszewski, P. Rydelek, *Contributions to Mineralogy and Petrology* **2014**, *167*. 10.1007/s00410-014-0995-5
[92] M. T. Cicerone, C. H. Camp, *Analyst* **2017**, *143*, 33. 10.1039/c7an01266g
[93] M. S. Bergholt, *Journal of Gastrointestinal & Digestive System* **2013**, *01*. 10.4172/2161-069x.s1-008
[94] M. Jermyn, K. Mok, J. Mercier, J. Desroches, J. Pichette, K. Saint-Arnaud, L. Bernstein, M. C. Guiot, K. Petrecca, F. Leblond, *Science Translational Medicine* **2015**, *7*. 10.1126/scitranslmed.aaa2384

[95] T. Yamamoto, T. Minamikawa, Y. Harada, Y. Yamaoka, H. Tanaka, H. Yaku, T. Takamatsu, *Sci Rep* **2018**, *8*, 14671. 10.1038/s41598-018-33025-6
[96] N. MacRitchie, G. Grassia, J. Noonan, P. Garside, D. Graham, P. Maffia, *Heart* **2018**, *104*, 460. 10.1136/heartjnl-2017-311447
[97] A. Y. F. You, M. S. Bergholt, J. P. St-Pierre, W. Kit-Anan, I. J. Pence, A. H. Chester, M. H. Yacoub, S. Bertazzo, M. M. Stevens, *Science Advances* **2017**, *3*. 10.1126/sciadv.1701156
[98] M. Pilarczyk, K. Czamara, M. Baranska, J. Natorska, P. Kapusta, A. Undas, A. Kaczor, *Journal of Raman Spectroscopy* **2013**, *44*, 1222. 10.1002/jrs.4352
[99] M. Bourbousson, I. Soomro, D. Baldwin, I. Notingher, *J Med Imaging (Bellingham)* **2019**, *6*, 036001. 10.1117/1.JMI.6.3.036001
[100] S. Yang, B. Li, A. Akkus, O. Akkus, L. Lang, *Analyst* **2014**, *139*, 3107. 10.1039/c4an00164h
[101] P. Wang, E. J. D. Anderson, E. A. Muller, F. Gao, Y. Zhong, M. B. Raschke, *Journal of Raman Spectroscopy* **2018**, *49*, 1559. 10.1002/jrs.5419
[102] M. Sharifzadeh, D. Y. Zhao, P. S. Bernstein, W. Gellermann, *Journal of the Optical Society of America a-Optics Image Science and Vision* **2008**, *25*, 947. Doi 10.1364/Josaa.25.000947
[103] P. Arjonilla, A. Domínguez-Vidal, E. Correa-Gómez, M. J. Domene-Ruiz, M. J. Ayora-Cañada, *Journal of Raman Spectroscopy* **2019**, *50*, 1537. 10.1002/jrs.5660
[104] A. Klisińska-Kopacz, K. Lech, J. M. Hoyo-Meléndez, A. Mendys, A. Jaworucka-Drath, B. Łydżba-Kopczyńska, *Journal of Raman Spectroscopy* **2019**. 10.1002/jrs.5710
[105] F. Pozzi, E. Basso, A. Rizzo, A. Cesaratto, J. T. J. Tague, *Journal of Raman Spectroscopy* **2019**. 10.1002/jrs.5585
[106] M. Lopez-Lopez, V. Merk, C. Garcia-Ruiz, J. Kneipp, *Anal Bioanal Chem* **2016**, *408*, 4965. 10.1007/s00216-016-9591-z
[107] K. C. Doty, I. K. Lednev, *TrAC Trends in Analytical Chemistry* **2018**, *103*, 215. 10.1016/j.trac.2017.12.003
[108] A. G. G. de Oliveira, E. Wiercigroch, J. D. Gomes, K. Malek, *Analytical Methods* **2018**, *10*, 1203. 10.1039/c7ay02684f
[109] R. Rosenblatt, L. Halámková, K. C. Doty, E. A. C. de Oliveira, I. K. Lednev, *Forensic Chemistry* **2019**, *16*, 100175. 10.1016/j.forc.2019.100175
[110] G. McLaughlin, I. K. Lednev, *J Forensic Sci* **2015**, *60*, 595. 10.1111/1556-4029.12708
[111] J. Guo, X. Feng, P. Yang, Z. Yu, L. Q. Chen, C. H. Yuan, W. Zhang, *Nat Commun* **2019**, *10*, 148. 10.1038/s41467-018-08118-5
[112] M. Janko, R. W. Stark, A. Zink, *J R Soc Interface* **2012**, *9*, 2581. 10.1098/rsif.2012.0174
[113] R. Georgiou, P. Gueriau, C. J. Sahle, S. Bernard, A. Mirone, R. Garrouste, U. Bergmann, J. P. Rueff, L. Bertrand, *Science Advances* **2019**, *5*. 10.1126/sciadv.aaw5019
[114] N. Gierlinger, M. Schwanninger, *Spectroscopy-an International Journal* **2007**, *21*, 69. Doi 10.1155/2007/498206
[115] H. J. Butler, L. Ashton, B. Bird, G. Cinque, K. Curtis, J. Dorney, K. Esmonde-White, N. J. Fullwood, B. Gardner, P. L. Martin-Hirsch, M. J. Walsh, M. R. McAinsh, N. Stone, F. L. Martin, *Nature Protocols* **2016**, *11*, 664. 10.1038/nprot.2016.036
[116] N. Gierlinger, *Frontiers in Plant Science* **2014**, *5*. 10.3389/Fpls.2014.00306
[117] B. Prats Mateu, M. T. Hauser, A. Heredia, N. Gierlinger, *Front Chem* **2016**, *4*, 10. 10.3389/fchem.2016.00010
[118] R. Wightman, M. Busse-Wicher, P. Dupree, *Micron* **2019**, *126*, 102733. 10.1016/j.micron.2019.102733
[119] P. N. Perera, M. Schmidt, V. L. Chiang, P. J. Schuck, P. D. Adams, *Anal Bioanal Chem* **2012**, *402*, 983. 10.1007/s00216-011-5518-x
[120] A.-S. Jääskeläinen, U. Holopainen-Mantila, T. Tamminen, T. Vuorinen, *Journal of Cereal Science* **2013**, *57*, 543. 10.1016/j.jcs.2013.02.007

[121] Z. Heiner, I. Zeise, R. Elbaum, J. Kneipp, *J Biophotonics* **2018**, *11*, e201700164. 10.1002/jbio.201700164
[122] J. Ma, X. Zhou, J. Ma, Z. Ji, X. Zhang, F. Xu, *Microsc Microanal* **2014**, *20*, 956. 10.1017/S1431927614000658
[123] L. G. Thygesen, N. Gierlinger, *J Struct Biol* **2013**, *182*, 219. 10.1016/j.jsb.2013.03.010
[124] X. Wang, T. Keplinger, N. Gierlinger, I. Burgert, *Ann Bot* **2014**, *114*, 1627. 10.1093/aob/mcu180
[125] N. Zhu, D. Wu, K. S. Chen, *Plant Methods* **2018**, *14*. 10.1186/s13007-018-0328-1
[126] Y. Cai, G. Li, J. Nie, Y. Lin, F. Nie, J. Zhang, Y. Xu, *Scientia Horticulturae* **2010**, *125*, 374. 10.1016/j.scienta.2010.04.029
[127] M. Szymanska-Chargot, M. Chylinska, P. M. Pieczywek, P. Rosch, M. Schmitt, J. Popp, A. Zdunek, *Planta* **2016**, *243*, 935. 10.1007/s00425-015-2456-4
[128] M. Szymańska-Chargot, P. M. Pieczywek, M. Chylińska, A. Zdunek, *Chemometrics and Intelligent Laboratory Systems* **2016**, *151*, 136. 10.1016/j.chemolab.2015.12.015
[129] M. Chylinska, M. Szymanska-Chargot, A. Zdunek, *Plant Methods* **2014**, *10*. 10.1186/1746-4811-10-14
[130] S. Gamsjaeger, M. Baranska, H. Schulz, P. Heiselmayer, M. Musso, *Journal of Raman Spectroscopy* **2011**, *42*, 1240. 10.1002/jrs.2860
[131] N. Gierlinger, L. Sapei, O. Paris, *Planta* **2008**, *227*, 969. 10.1007/s00425-007-0671-3
[132] I. Zeise, Z. Heiner, S. Holz, M. Joester, C. Buttner, J. Kneipp, *Plants (Basel)* **2018**, *7*. 10.3390/plants7010007
[133] G. R. Littlejohn, J. C. Mansfield, D. Parker, R. Lind, S. Perfect, M. Seymour, N. Smirnoff, J. Love, J. Moger, *Plant Physiol* **2015**, *168*, 18. 10.1104/pp.15.00119
[134] S. Richter, J. Mussig, N. Gierlinger, *Planta* **2011**, *233*, 763. 10.1007/s00425-010-1338-z
[135] P. Heraud, M. F. Cowan, K. M. Marzec, B. L. Moller, C. K. Blomstedt, R. Gleadow, *Sci Rep* **2018**, *8*, 2691. 10.1038/s41598-018-20928-7
[136] M. Baranska, H. Schulz, E. Joubert, M. Manley, *Analytical Chemistry* **2006**, *78*, 7716. 10.1021/ac061123q
[137] N. Schreiber, N. Gierlinger, N. Putz, P. Fratzl, C. Neinhuis, I. Burgert, *Plant J* **2010**, *61*, 854. 10.1111/j.1365-313X.2009.04115.x
[138] M. Baranska, R. Baranski, H. Schulz, T. Nothnagel, *Planta* **2006**, *224*, 1028. 10.1007/s00425-006-0289-x
[139] J. C. Huss, V. Schoeppler, D. J. Merritt, C. Best, E. Maire, J. Adrien, O. Spaeker, N. Janssen, J. Gladisch, N. Gierlinger, B. P. Miller, P. Fratzl, M. Eder, *Adv Sci (Weinh)* **2018**, *5*, 1700572. 10.1002/advs.201700572
[140] J. C. Huss, O. Spaeker, N. Gierlinger, D. J. Merritt, B. P. Miller, C. Neinhuis, P. Fratzl, M. Eder, *Journal of the Royal Society Interface* **2018**, *15*. 10.1098/Rsif.2018.0190
[141] E. Kuprian, C. Munkler, A. Resnyak, S. Zimmermann, T. D. Tuong, N. Gierlinger, T. Muller, D. P. Livingston, 3rd, G. Neuner, *Plant Cell Environ* **2017**, *40*, 3101. 10.1111/pce.13078
[142] N. P. Ivleva, R. Niessner, U. Panne, *Anal Bioanal Chem* **2005**, *381*, 261. 10.1007/s00216-004-2942-1
[143] F. Schulte, J. Lingott, U. Panne, J. Kneipp, *Analytical Chemistry* **2008**, *80*, 9551. 10.1021/ac801791a
[144] A. S. Mondol, M. D. Patel, J. Ruger, C. Stiebing, A. Kleiber, T. Henkel, J. Popp, I. W. Schie, *Sensors (Basel)* **2019**, *19*. 10.3390/s19204428
[145] A. Petjukevics, N. Skute, *Biologia* **2017**, *72*, 1017. 10.1515/biolog-2017-0120
[146] N. Altangerel, G. O. Ariunbold, C. Gorman, M. H. Alkahtani, E. J. Borrego, D. Bohlmeyer, P. Hemmer, M. V. Kolomiets, J. S. Yuan, M. O. Scully, *Proc Natl Acad Sci U S A* **2017**, *114*, 3393. 10.1073/pnas.1701328114
[147] M. Rys, M. Szaleniec, A. Skoczowski, I. Stawoska, A. Janeczko, *Open Chemistry* **2015**, *13*. 10.1515/chem-2015-0121

[148] N. Gierlinger, S. Luss, C. Konig, J. Konnerth, M. Eder, P. Fratzl, *Journal of Experimental Botany* **2010**, *61*, 587. 10.1093/jxb/erp325
[149] M. Felhofer, B. Prats-Mateu, P. Bock, N. Gierlinger, *Tree Physiol.* **2018**, *38*, 1. 10.1093/treephys/tpy073
[150] Ö. Özgenc, S. Durmaz, I. H. Boyaci, H. Eksi-Kocak, *Spectrochimica Acta Part a-Molecular and Biomolecular Spectroscopy* **2017**, *171*, 395. 10.1016/j.saa.2016.08.026
[151] T. Belt, T. Keplinger, T. Hänninen, L. Rautkari, *Industrial Crops and Products* **2017**, *108*, 327. 10.1016/j.indcrop.2017.06.056
[152] S. Durmaz, Ö. Özgenc, I. H. Boyaci, U. C. Yildiz, E. Erisir, *Vibrational Spectroscopy* **2016**, *85*, 202. 10.1016/j.vibspec.2016.04.020
[153] N. B. Pedersen, N. Gierlinger, L. G. Thygesen, *Holzforschung* **2015**, *69*, 103. 10.1515/hf-2014-0024
[154] N. Gierlinger, M. Schwanninger, A. Reinecke, I. Burgert, *Biomacromolecules* **2006**, *7*, 2077.
[155] C. Lehringer, N. Gierlinger, G. Koch, *Holzforschung* **2008**, *62*. 10.1515/hf.2008.036
[156] D. Stewart, N. Yahiaoui, G. J. McDougall, K. Myton, C. Marque, A. M. Boudet, J. Haigh, *Planta* **1997**, *201*, 311. DOI 10.1007/s004250050072
[157] M. Özparpucu, N. Gierlinger, I. Burgert, R. Van Acker, R. Vanholme, W. Boerjan, G. Pilate, A. Dejardin, M. Ruggeberg, *Planta* **2018**, *247*, 887. 10.1007/s00425-017-2828-z
[158] T. Kanbayashi, Y. Kataoka, A. Ishikawa, M. Matsunaga, M. Kobayashi, M. Kiguchi, *Journal of Wood Science* **2018**, *64*, 169. 10.1007/s10086-018-1698-8
[159] C. Gusenbauer, E. Cabane, N. Gierlinger, J. Colson, J. Konnerth, *Sci Rep* **2019**, *9*, 18569. 10.1038/s41598-019-54664-3
[160] T. Keplinger, E. Cabane, M. Chanana, P. Hass, V. Merk, N. Gierlinger, I. Burgert, *Acta Biomater* **2015**, *11*, 256. 10.1016/j.actbio.2014.09.016
[161] M. A. Ermeydan, E. Cabane, N. Gierlinger, J. Koetz, I. Burgert, *RSC Advances* **2014**, *4*, 12981. 10.1039/c4ra00741g
[162] R. H. Atalla, *Journal of Wood Chemistry and Technology* **1987**, *7*, 115. 10.1080/02773818708085256
[163] U. P. Agarwal, R. H. Atalla, **1993**, *531*, 26. 10.1021/bk-1992-0531.ch002
[164] U. P. Agarwal, R. H. Atalla, I. Forsskahl, *Holzforschung* **1995**, *49*, 300. DOI 10.1515/hfsg.1995.49.4.300
[165] U. P. Agarwal, S. A. Ralph, *Holzforschung* **2008**, *62*, 667. 10.1515/Hf.2008.112
[166] N. Gierlinger, M. Schwanninger, *Plant Physiology* **2006**, *140*, 1246. 10.1104/pp.105.066993
[167] K. X. Jin, X. E. Liu, K. Wang, Z. H. Jiang, G. L. Tian, S. M. Yang, L. L. Shang, J. F. Ma, *Planta* **2018**, *248*, 849. 10.1007/s00425-018-2931-9
[168] M. Schmidt, A. M. Schwartzberg, P. N. Perera, A. Weber-Bargioni, A. Carroll, P. Sarkar, E. Bosneaga, J. J. Urban, J. Song, M. Y. Balakshin, E. A. Capanema, M. Auer, P. D. Adams, V. L. Chiang, P. J. Schuck, *Planta* **2009**, *230*, 589. 10.1007/s00425-009-0963-x
[169] H. Miyafuji, K. Komai, T. Kanbayashi, *Vibrational Spectroscopy* **2017**, *88*, 9. 10.1016/j.vibspec.2016.10.011
[170] U. P. Agarwal, R. H. Atalla, *Planta* **1986**, *169*, 325. Doi 10.1007/Bf00392127
[171] J. S. Bond, Doctor's Dissertation, **1991**. Available at. Accessed on
[172] B. Prats-Mateu, P. Bock, M. Schroffenegger, J. L. Toca-Herrera, N. Gierlinger, *Sci. Rep.* **2018**, *8*, 1. 10.1038/s41598-018-30096-3
[173] U. P. Agarwal, S. A. Ralph, D. Padmakshan, S. Liu, S. D. Karlen, C. E. Foster, J. Ralph, in *International Symposium on Wood, Fiber and Pulping Chemistry* Vienna, **2015**.
[174] U. P. Agarwal, S. A. Ralph, D. Padmakshan, S. Liu, C. E. Foster, *Journal of Agricultural and Food Chemistry* **2019**, *67*, 4367. 10.1021/acs.jafc.8b06707
[175] M. Takayama, T. Johjima, T. Yamanaka, H. Wariishi, H. Tanaka, *Spectrochim Acta A* **1997**, *53*, 1621.
[176] J. S. Lupoi, E. A. Smith, *Appl Spectrosc* **2012**, *66*, 903. 10.1366/12-06621

[177] J. S. Lupoi, S. Singh, M. Davis, D. J. Lee, M. Shepherd, B. A. Simmons, R. J. Henry, *Biotechnology for Biofuels* **2014**, *7*, 1. 10.1186/1754-6834-7-93
[178] J. S. Lupoi, A. Healey, S. Singh, R. Sykes, M. Davis, D. J. Lee, M. Shepherd, B. A. Simmons, R. J. Henry, *BioEnergy Research* **2015**, *8*, 953. 10.1007/s12155-015-9578-1
[179] L. Sun, P. Varanasi, F. Yang, D. Loque, B. A. Simmons, S. Singh, *Biotechnol Bioeng* **2012**, *109*, 647. 10.1002/bit.24348
[180] T. Hänninen, E. Kontturi, T. Vuorinen, *Phytochemistry* **2011**, *72*, 1889. 10.1016/j.phytochem.2011.05.005
[181] B. Liu, P. Wang, J. I. Kim, D. Zhang, Y. Xia, C. Chapple, J. X. Cheng, *Anal Chem* **2015**, *87*, 9436. 10.1021/acs.analchem.5b02434
[182] M. Ozparpucu, M. Ruggeberg, N. Gierlinger, I. Cesarino, R. Vanholme, W. Boerjan, I. Burgert, *Plant J* **2017**, *91*, 480. 10.1111/tpj.13584
[183] U. P. Agarwal, R. H. Atalla, in *ACS symposium series*; American Chemical Society: Washington, D.C, **2000**; Vol. 742, p 250.
[184] U. P. Agarwal, R. S. Reiner, A. K. Pandey, S. A. Ralph, K. C. Hirth, R. H. Atalla, in *59th APPITA Annual Conference and Exhibition* Auckland, New Zealand, **2005**.
[185] U. P. Agarwal in *Advances in Lignocellulosics Characterization*; Argyropoulos DS, Ed.; TAPPI Press: Atlanta, GA, **1999**, p 201.
[186] S. M. Ehrhardt, Doctoral dissertation, Lawrence University, **1984**. Available at: https://smartech.gatech.edu/handle/1853/5751. Accessed on December 21, 2018.
[187] S. Sebastian, N. Sundaraganesan, S. Manoharan, *Spectrochim Acta A Mol Biomol Spectrosc* **2009**, *74*, 312. 10.1016/j.saa.2009.06.011
[188] H. M. Badawi, W. Förner, *Journal of Molecular Structure* **2011**, *1003*, 62. 10.1016/j.molstruc.2011.07.021
[189] K. L. Larsen, S. Barsberg, *J. Phys. Chem. B* **2010**, *114*, 8009.
[190] K. L. Larsen, S. Barsberg, *J Phys Chem B* **2011**, *115*, 11470. 10.1021/jp203910h
[191] B. Z. Chowdhry, J. P. Ryall, T. J. Dines, A. P. Mendham, *J Phys Chem A* **2015**, *119*, 11280. 10.1021/acs.jpca.5b07607
[192] S. Tong-fu, H. Rong, S. Ya-qiong, Z. Guo-zhong, W. De-yin, W. Jian-an, G. Chang-rong, X. cui-lian, *Spectrochim Acta A* **2015**, *139*, 456. 10.1016/j.saa.2014.12.052
[193] U. P. Agarwal, R. S. Reiner, *Journal of Raman Spectroscopy* **2009**, *40*, 1527. 10.1002/jrs.2294
[194] U. P. Agarwal, R. H. Atalla in *Lignin and lignans: Advances in Chemistry*; C. H, D.R. D, J.A. S, Eds.; CRC Press: Boca Raton, FL, **2010**, p 103.
[195] J. S. Segmehl, T. Keplinger, A. Krasnobaev, J. K. Berg, C. Willa, I. Burgert, *Spectrochimica Acta Part a-Molecular and Biomolecular Spectroscopy* **2019**, *206*, 177. 10.1016/j.saa.2018.07.080
[196] H. L. Hergert, *Journal of Organic Chemistry* **1960**, *25*, 405. Doi 10.1021/Jo01073a026
[197] O. Faix, *Holzforschung* **1991**, *45*, 21. DOI 10.1515/hfsg.1991.45.s1.21
[198] N. S. Zwirchmayr, T. Elder, M. Bacher, A. Hofinger-Horvath, P. Kosma, T. Rosenau, *ACS Omega* **2017**, *2*, 7929. 10.1021/acsomega.7b00874
[199] M. W. Schmidt, K. K. Baldridge, J. A. Boatz, S. T. Elbert, M. S. Gordon, J. H. Jensen, S. Koseki, N. Matsunaga, K. A. Nguyen, S. J. Su, T. L. Windus, M. Dupuis, J. A. Montgomery, *Comput. Chem.* **1993**, *14*, 16.
[200] M. S. Gordon, M. W. Schmidt in *Theory and Applications of Computational Chemistry: the first forty years*; Dykstra CE, Frenking G, Kim KS, Scuseria GE, Eds.; Elsevier: Amsterdam, **2005**, p 1167.
[201] B. M. Bode, M. S. Gordon, *J. Mol. Graphics Mod.* **1998**, *16*, 133.
[202] G. W. T. M. J. Frisch, H. B. Schlegel, G. E. Scuseria, M. A. Robb, J. R. Cheeseman, G. Scalmani, V. Barone, G. A. Petersson, H. Nakatsuji, X. Li, M. Caricato, A. V. Marenich, J. Bloino, B. G. Janesko, R. Gomperts, B. Mennucci, H. P. Hratchian, , A. F. I. J. V. Ortiz, J. L. Sonnenberg, D. Williams-Young, F. Ding, F. Lipparini, F. Egidi, J. Goings, B. Peng, A. Petrone, T. Henderson, D. Ranasinghe, V. G.

Zakrzewski, J. Gao, N. Rega, , W. L. G. Zheng, M. Hada, M. Ehara, K. Toyota, R. Fukuda, J. Hasegawa, M. Ishida, T. Nakajima, Y. Honda, O. Kitao, H. Nakai, T. Vreven, K. Throssell, J. A. Montgomery, Jr., J. E. Peralta, F. Ogliaro, M. J. Bearpark, J. J. Heyd, E. N. Brothers, K. N. Kudin, , T. A. K. V. N. Staroverov, R. Kobayashi, J. Normand, K. Raghavachari, A. P. Rendell, J. C. Burant, S. S. Iyengar, J. Tomasi, M. Cossi, J. M. Millam, M. Klene, C. Adamo, R. Cammi, , R. L. M. J. W. Ochterski, K. Morokuma, O. Farkas, J. B. Foresman, and D. J. Fox; Gaussian, Inc.: Wallingford CT, **2016**.

[203] G. Varsanyi, *Vibrational Spectra of Benzene Derivatives*; 1st Edition ed.; Academic Press: New York, **1969**.

[204] D. W. Mayo, F. A. Miller, R. W. Hannah, *Course Notes on the Interpretation of Infrared and Raman Spectra*; John Wiley & Sons, Inc: Hoboken, New Jersey, **2003**.

[205] D. C. Harris, M. D. Bertolucci, *Symmetry and Spectroscopy - An Introduction to Vibrational and Electronic Spectroscopy*; Dover Publications Inc.: New York, **1989**, 550.

[206] G. Keresztury in *Handbook of Vibrational Spectroscopy*; Chalmers JM, Griffiths PR, Eds.; Wiley: **2002**; Vol. 1.

[207] R. Ikeda, B. Chase, N. J. Everall in *Handbook of Vibrational Spectroscopy*; Chalmers JM, Griffiths PR, Eds.; Wiley: **2002**; Vol. 1.

[208] J. Lee, K. T. Crampton, N. Tallarida, V. A. Apkarian, *Nature* **2019**, *568*, 78. 10.1038/s41586-019-1059-9

[209] J. W. Osenbach, C. A. Jack, D. Singh, G. V. Srinivasan, C. D. Theis, in *54th Electronic Components and Technology Conference*; IEEE: Las Vegas, **2004**.

[210] C. Castiglioni in *Handbook of Vibrational Spectroscopy*; Chalmers JM, Griffiths PR, Eds.; Wiley: **2002**; Vol. 1.

[211] C. Krafft, M. Schmitt, I. W. Schie, D. Cialla-May, C. Matthaus, T. Bocklitz, J. Popp, *Angewandte Chemie-International Edition* **2017**, *56*, 4392. 10.1002/anie.201607604

[212] P. L. Davies, *Transactions of the Faraday Society* **1952**, *48*, 789. Doi 10.1039/Tf9524800789

[213] D. A. Long, *The Raman Effect: A Unified Treatment of the Theory of Raman Scattering by Molecules.*; John Wiley & Sons Ltd, **2002**.

[214] P. P. Shorygin, *Russian Chem. Reviews* **1971**, *40*, 367.

[215] E. D. Schmid, B. Brosa, *Berichte Der Bunsen-Gesellschaft Fur Physikalische Chemie* **1971**, *75*, 1334.

[216] E. D. Schmid, B. Brosa, *Journal of Chemical Physics* **1972**, *56*, 2.

[217] E. D. Schmid, B. Brosa, *Journal of Chemical Physics* **1973**, *58*, 3871. Doi 10.1063/1.1679742

[218] E. D. Schmid, P. Schlenker, R. R. M. Brand, *Journal of Raman Spectroscopy* **1977**, *6*, 314. DOI 10.1002/jrs.1250060610

[219] E. D. Schmid, R. D. Topsom, *Journal of the American Chemical Society* **1981**, *103*, 1628. Doi 10.1021/Ja00397a004

[220] G. Zerbi, C. Castiglioni, M. Gussoni, *Synthetic Metals* **1991**, *43*, 3407. Doi 10.1016/0379-6779(91)91315-2

[221] M. Tommasini, C. Castiglioni, M. Del Zoppo, G. Zerbi, *Journal of Molecular Structure* **1999**, *481*, 179. Doi 10.1016/S0022-2860(98)00915-6

[222] T. Verbiest, S. Houbrechts, M. Kauranen, C. Koen, A. Persoons, *J. Mater. Chem.* **1997**, *7*, 2175.

[223] C. Castiglioni, M. Del Zoppo, G. Zerbi, *Journal of Raman Spectroscopy* **1993**, *24*, 485.

[224] M. Del Zoppo, M. Tommasini, C. Castiglioni, G. Zerbi, *Chemical Physics Letters* **1998**, *287*, 100.

[225] U. P. Agarwal, J. D. McSweeny, S. A. Ralph, *Journal of Wood Chemistry and Technology* **2011**, *31*, 324. 10.1080/02773813.2011.562338

[226] M. Kihara, M. Takayama, H. Wariishi, H. Tanaka, *Spectrochim Acta A Mol Biomol Spectrosc* **2002**, *58*, 2213.

[227] K. Radotic, J. Zakrzewska, D. Sladic, M. Jeremic, *Photochemistry and Photobiology* **1997**, *65*, 284.

[228] K. Radotic, S. Todorovic, J. Zakrzewska, M. Jeremic, *Photochemistry and Photobiology* **1998**, *68*, 703. DOI 10.1111/j.1751-1097.1998.tb02533.x

[229] M. Lukeman in *Quinone Methides*; Rokita SE, Ed.; John Wiley & Sons: Hoboken, New Jersey, **2009**.
[230] K. M. Dyumaev, A. A. Manenkov, A. P. Maslyukov, G. A. Matyushin, V. S. Nechitailo, A. M. Prokhorov, in *Thirteenth Symposium on Optical High Power Lasers*; Bennet HE, Guenther AH, Milam D, Newnam BE, Eds. Boulder, Colorado, U.S., **1981**.
[231] K. M. Dyumaev, A. A. Manenkov, A. P. Maslyukov, G. A. Matyushin, V. S. Nechitailo, A. M. Prokhorov, in *Nineteenth Symposium on Optical Materials for High-Power Lasers*; Bennet HE, Guenther AH, Milam D, Newnam BE, Soileau MJ, Eds. Boulder, Colorado, U.S., **1987**.
[232] S. B. Aziz, O. G. Abdullah, A. M. Hussein, H. M. Ahmed, *Polymers (Basel)* **2017**, *9*. 10.3390/polym9110626
[233] J. C. Scaiano, J. C. Nettoferreira, *Journal of Photochemistry* **1986**, *32*, 253. Doi 10.1016/0047-2670(86)87013-7
[234] J. C. Scaiano, J. C. Nettoferreira, V. Wintgens, *Journal of Photochemistry and Photobiology a-Chemistry* **1991**, *59*, 265. Doi 10.1016/1010-6030(91)87014-M
[235] A. Castellan, N. Colombo, C. Cucuphat, P. F. Deviolet, *Holzforschung* **1989**, *43*, 179. DOI 10.1515/hfsg.1989.43.3.179
[236] J. D. Bhawalkar, G. S. He, P. N. Prasad, *Reports on Progress in Physics* **1996**, *59*, 1041. Doi 10.1088/0034-4885/59/9/001
[237] J. C. Pew, *Nature* **1962**, *193*, 250. Doi 10.1038/193250a0
[238] T. Wismontski-Knittel, T. Kilp, *Journal of Physical Chemistry* **1984**, *88*, 110. Doi 10.1021/J150645a028
[239] J. C. Scaiano, M. K. Whittlesey, A. B. Berinstain, P. R. L. Malenfant, R. H. Schuler, *Chemistry of Materials* **1994**, *6*, 836. Doi 10.1021/Cm00042a023
[240] D. Steele, in *Encyclopedia of Spectroscopy and Spectrometry*; 2nd ed.; Lindon JC, Ed.; Academic Press: Oxford, **1999**, p 1066.
[241] H. G. M. Edwards in *Handbook of Vibrational Spectroscopy*; Chalmers JM, Griffiths PR, Eds.; Wiley: **2002**; Vol. 1.
[242] H. F. Shurvell in *Handbook of Vibrational Spectrosocpy*; Chalmers JM, Griffiths PR, Eds.; Wiley: **2002**; Vol. 1.
[243] F. R. Dollish, W. G. Fateley, F. F. Bentley, *Characteristic Raman frequencies of organic compounds*, **1974**.
[244] E. B. Wilson, *Phys. Rev.* **1934**, *45*, 706.
[245] L. Sun, P. Varanasi, F. Yang, D. Loqué, B. A. Simmons, S. Singh, *Biotechnology and Bioengineering* **2011**, *109*, 647.
[246] H. A. Bent, *Chemical Reviews* **1961**, *61*, 275. Doi 10.1021/Cr60211a005
[247] S. Shaik, A. Shurki, D. Danovich, P. C. Hiberty, *Chemical Reviews* **2001**, *101*, 1501. 10.1021/cr990363l
[248] K. Freudenberg, B. Lehmann, *Chemische Berichte-Recueil* **1960**, *93*, 1354. DOI 10.1002/cber.19600930618
[249] J. Ralph, J. H. Grabber, R. D. Hatfield, *Carbohydr Res* **1995**, *275*, 167. 10.1016/0008-6215(95)00237-N
[250] S. Quideau, J. Ralph, *Journal of the Chemical Society-Perkin Transactions 1* **1997**, 2351. Doi 10.1039/A701808h
[251] W. Shen, C. Collings, M. Li, J. Markovicz, J. Ralph, S. D. Mansfield, S.-Y. Ding, *ACS Sustainable Chemistry & Engineering* **2019**, *7*, 10616. 10.1021/acssuschemeng.9b01166
[252] H. M. Chang, E. B. Cowling, W. Brown, E. Adler, G. Miksche, *Holzforschung* **1975**, *29*, 153. DOI 10.1515/hfsg.1975.29.5.153
[253] A. Rygula, T. P. Wrobel, J. Szklarzewicz, M. Baranska, *Vibrational Spectroscopy* **2013**, *64*, 21. 10.1016/j.vibspec.2012.10.005

[254] C. Corredor, T. Teslova, M. V. Cañamares, Z. Chen, J. Zhang, J. R. Lombardi, M. Leona, *Vibrational Spectroscopy* **2009**, *49*, 190. 10.1016/j.vibspec.2008.07.012
[255] T. Teslova, C. Corredor, R. Livingstone, T. Spataru, R. L. Birke, J. R. Lombardi, M. V. Cañamares, M. Leona, *Journal of Raman Spectroscopy* **2007**, *38*, 802. 10.1002/jrs.1695
[256] N. Sundaraganesan, G. Mariappan, S. Manoharan, *Spectrochim Acta A Mol Biomol Spectrosc* **2012**, *87*, 67. 10.1016/j.saa.2011.11.011
[257] O. Unsalan, Y. Erdogdu, M. T. Gulluoglu, *Journal of Raman Spectroscopy* **2009**, *40*, 562. 10.1002/jrs.2166
[258] M. V. Canamares, J. R. Lombardi, M. Leona, *e-PS* **2009**, *6*, 81.
[259] G. Baranovic, S. Segota, *Spectrochim Acta A Mol Biomol Spectrosc* **2018**, *192*, 473. 10.1016/j.saa.2017.11.057
[260] H. L. Hergert, E. F. Kurth, *Journal of the American Chemical Society* **1953**, *75*, 1622. Doi 10.1021/Ja01103a031
[261] J. S. Lupoi, S. Singh, R. Parthasarathi, B. A. Simmons, R. J. Henry, *Renewable and Sustainable Energy Reviews* **2015**, *49*, 871. 10.1016/j.rser.2015.04.091
[262] E. G. Bakalbassis, A. Chatzopoulou, V. S. Melissas, M. Tsimidou, M. Tsolaki, A. Vafiadis, *Lipids* **2001**, *36*, 181. DOI 10.1007/s11745-001-0705-9
[263] D. C. Mckean, *Chemical Society Reviews* **1978**, *7*, 399. Doi 10.1039/Cs9780700399
[264] E. L. Sibert, D. P. Tabor, N. M. Kidwell, J. C. Dean, T. S. Zwier, *Journal of Physical Chemistry A* **2014**, *118*, 11272. 10.1021/jp510142g
[265] M. Rumi, G. Zerbi, *Journal of Molecular Structure* **1999**, *509*, 11. Doi 10.1016/S0022-2860(99)00207-0
[266] C. M. Altaner, L. H. Thomas, A. N. Fernandes, M. C. Jarvis, *Biomacromolecules* **2014**, *15*, 791. 10.1021/bm401616n
[267] C. M. Lee, J. D. Kubicki, B. Fan, L. Zhong, M. C. Jarvis, S. H. Kim, *J Phys Chem B* **2015**, *119*, 15138. 10.1021/acs.jpcb.5b08015
[268] S. Burikov, T. Dolenko, S. Patsaeva, Y. Starokurov, V. Yuzhakov, *Molecular Physics* **2010**, *108*, 2427. 10.1080/00268976.2010.516277
[269] S. A. Katsyuba, R. Schmutzler, U. Hohm, C. Kunze, *Journal of Molecular Structure* **2002**, *610*, 113. 10.1016/S0022-2860(02)00025-X
[270] L. J. H. Hoffmann, S. Marquardt, A. S. Gemechu, H. Baumgartel, *Physical Chemistry Chemical Physics* **2006**, *8*, 2360. 10.1039/b600438p
[271] I. A. Degen, *Appl Spectrosc* **1986**, *22*, 3.
[272] M. N. Siamwiza, R. C. Lord, M. C. Chen, T. Takamatsu, I. Harada, H. Matsuura, T. Shimanouchi, *Biochemistry* **1975**, *14*, 4870. Doi 10.1021/Bi00693a014
[273] U. P. Agarwal, *Frontiers in Plant Science* **2014**, *5*. 10.3389/Fpls.2014.00490
[274] S. T. Barsberg, Y. I. Lee, H. N. Rasmussen, *Seed Science Research* **2018**, *28*, 41. 10.1017/s0960258517000344

6

Appendix

Schil kurtzt er dich an

Durch wechsel gesigt im an.

Johannes Liechtenauer

Fig. A1 shows a simplified way of obtaining displacement patterns of chemically similar oscillators by applying the standing wave approach.

Fig. A2 shows ring modes of asymmetrically tri- and asymmetrically tetrasubstiuted rings.

Fig. A3 shows selected Raman (532 nm) and infrared spectra of model compounds used for this study.

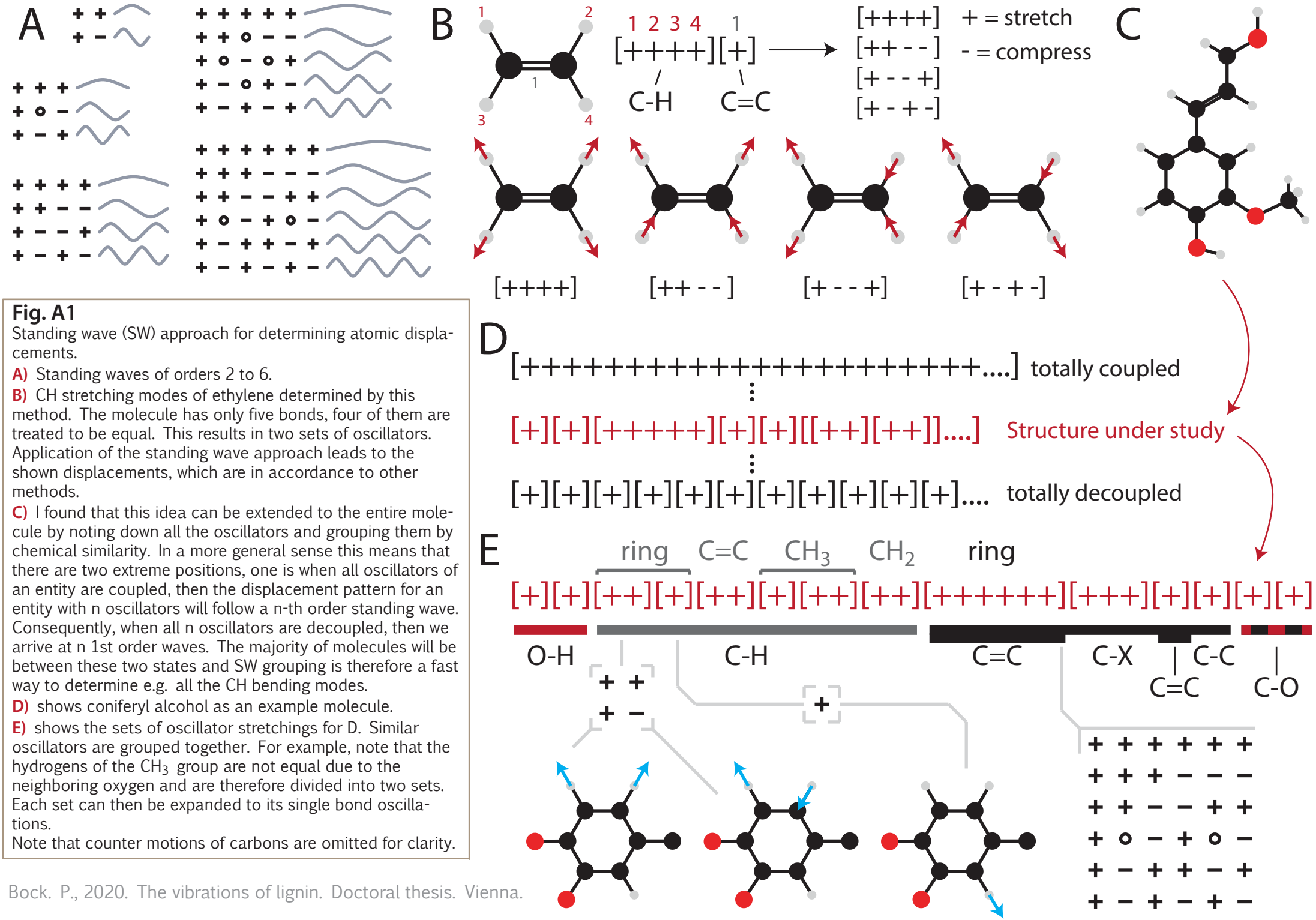

Fig. A1
Standing wave (SW) approach for determining atomic displacements.

A) Standing waves of orders 2 to 6.

B) CH stretching modes of ethylene determined by this method. The molecule has only five bonds, four of them are treated to be equal. This results in two sets of oscillators. Application of the standing wave approach leads to the shown displacements, which are in accordance to other methods.

C) I found that this idea can be extended to the entire molecule by noting down all the oscillators and grouping them by chemical similarity. In a more general sense this means that there are two extreme positions, one is when all oscillators of an entity are coupled, then the displacement pattern for an entity with n oscillators will follow a n-th order standing wave. Consequently, when all n oscillators are decoupled, then we arrive at n 1st order waves. The majority of molecules will be between these two states and SW grouping is therefore a fast way to determine e.g. all the CH bending modes.

D) shows coniferyl alcohol as an example molecule.

E) shows the sets of oscillator stretchings for D. Similar oscillators are grouped together. For example, note that the hydrogens of the CH_3 group are not equal due to the neighboring oxygen and are therefore divided into two sets. Each set can then be expanded to its single bond oscillations.

Note that counter motions of carbons are omitted for clarity.

Bock. P., 2020. The vibrations of lignin. Doctoral thesis. Vienna.

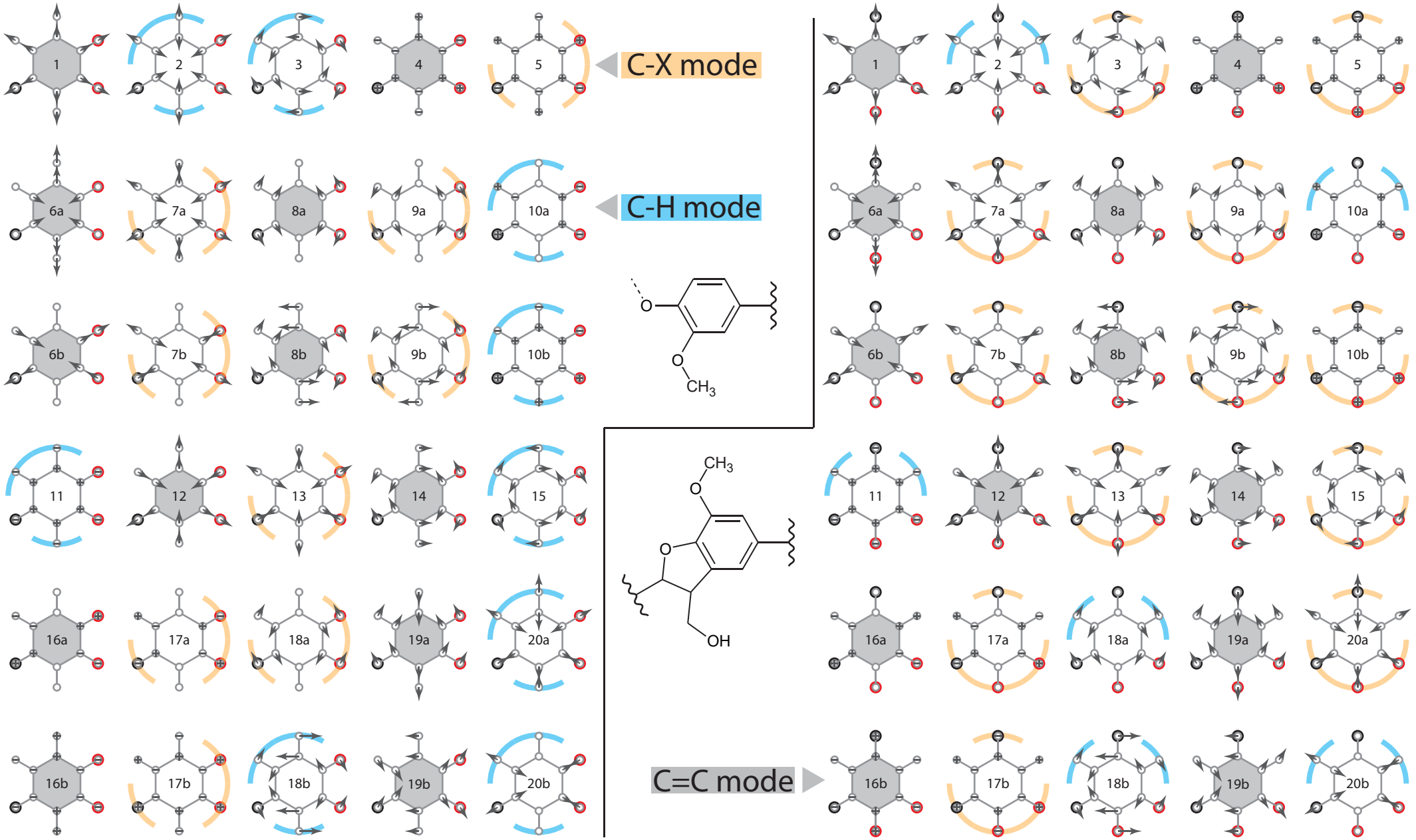

Fig. A2
Vibrational modes in Wilson/Varsanyi notation for asym-tri- and asym-tetra-rings, a β-O-4‘ and a β-5‘ ring are shown as examples. The 30 modes of benzene are divided into 12 ring carbon modes, 6 hydrogen modes and 12 substituent modes. Arrows depict atomic displacements in the plane of the paper and + and – indicate motion out of the paper plane. The magnitude and direction of displacement have only illustrative character. Calculated displacements of actual molecules can considerably deviate from those shown here, although the principal character of the mode can normally still be recognized.

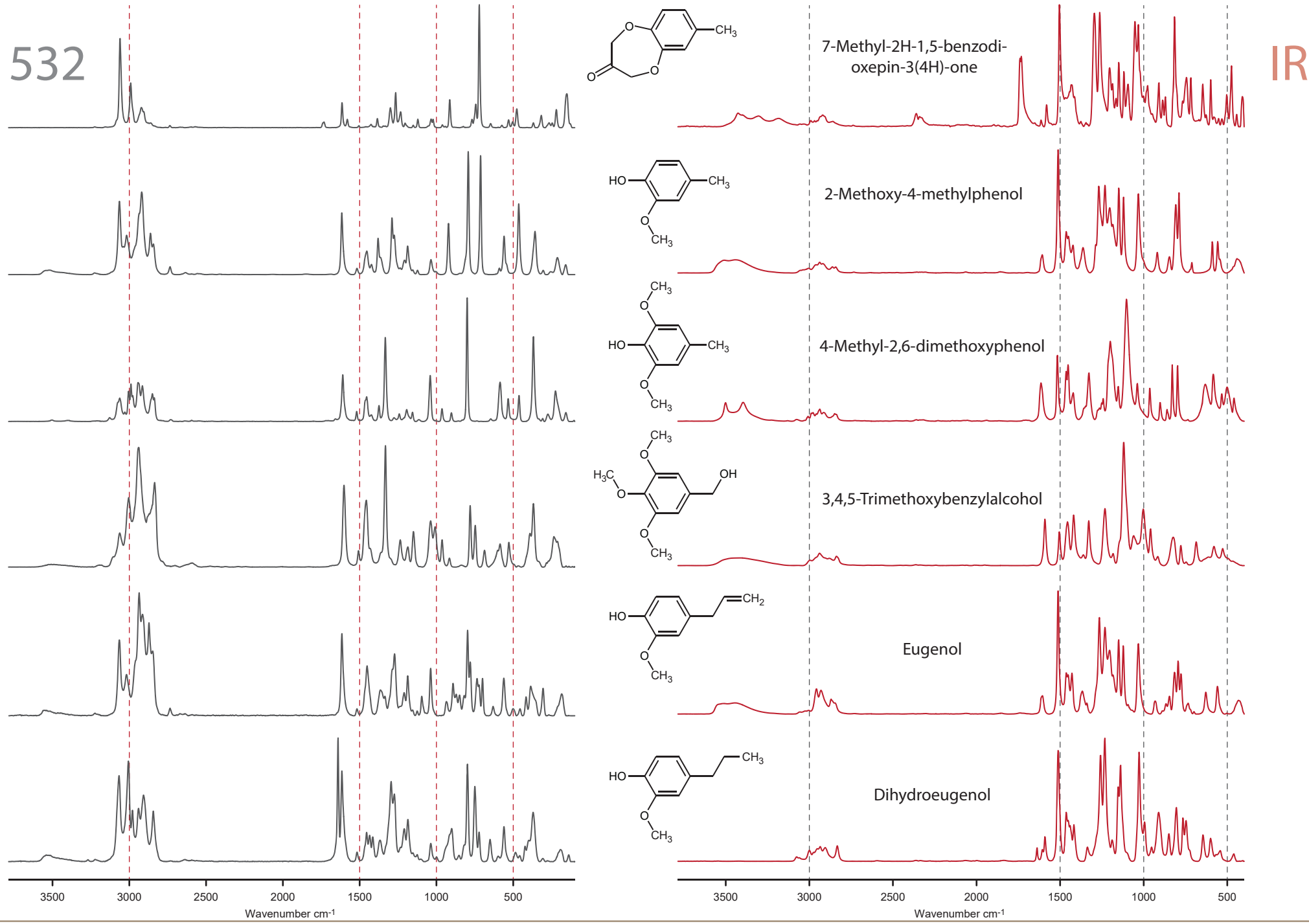

Fig. A3
Raman 532 and IR spectra of selected reference compounds.

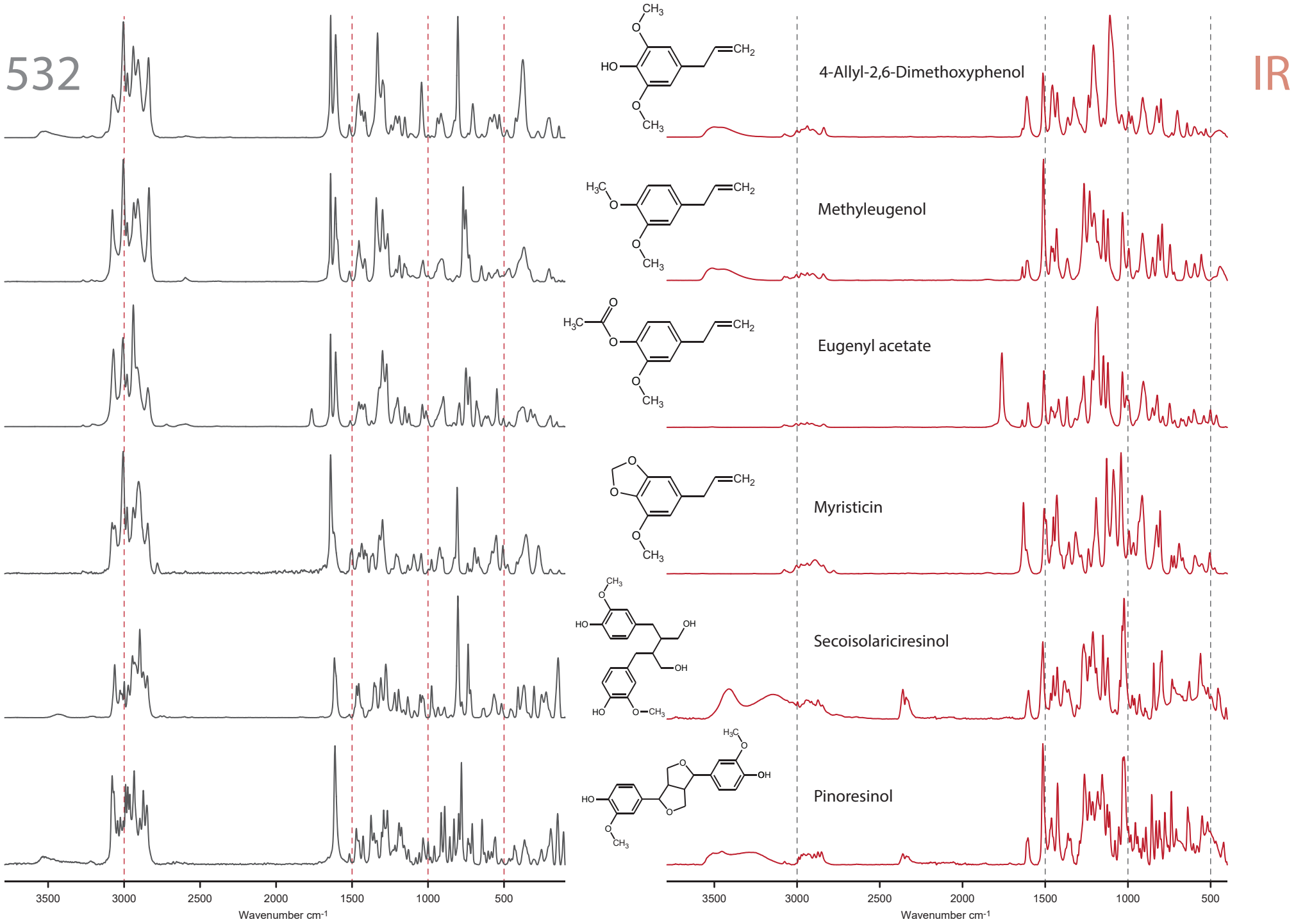

Fig. A3 (continued)

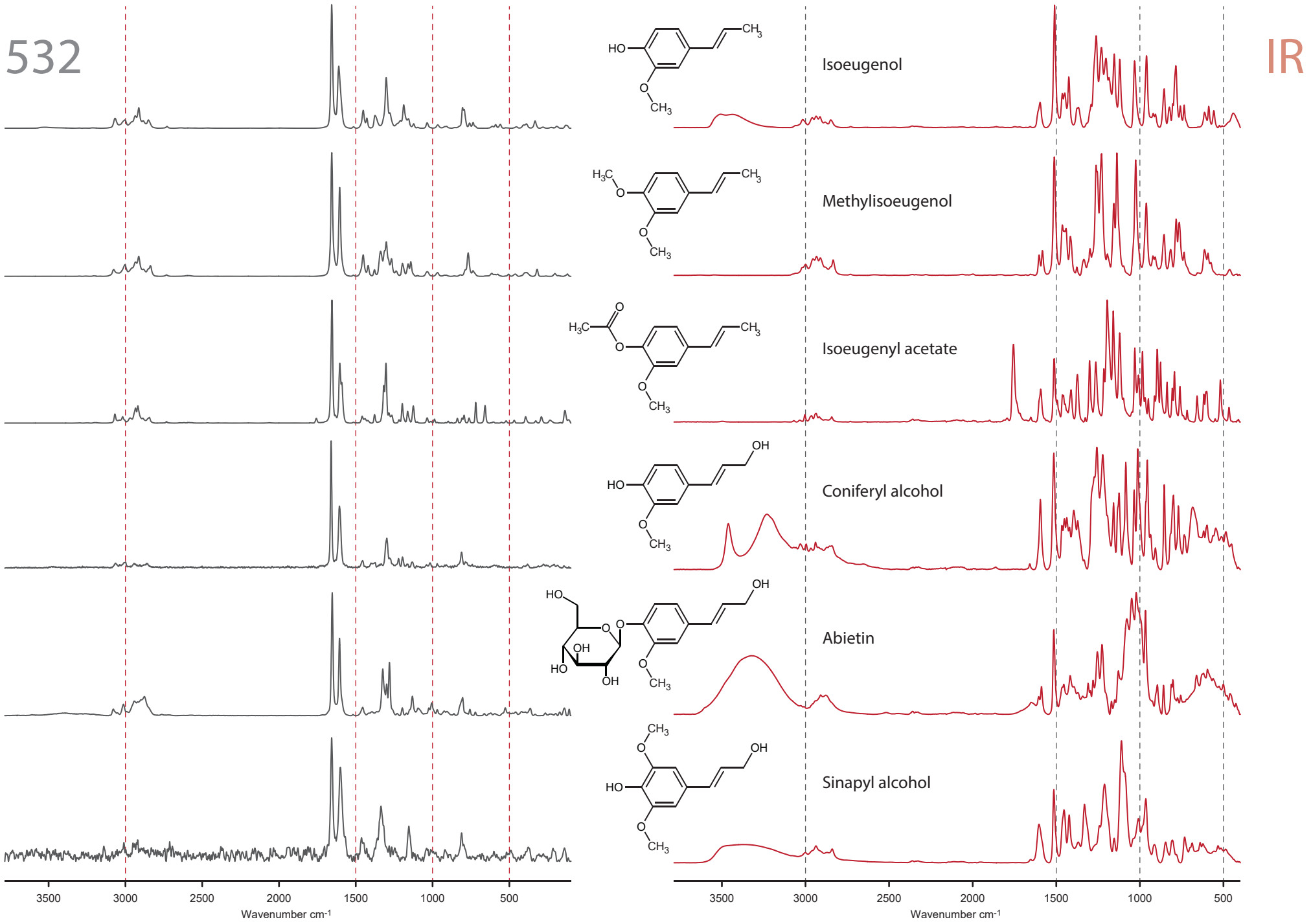

Fig. A3 (continued)

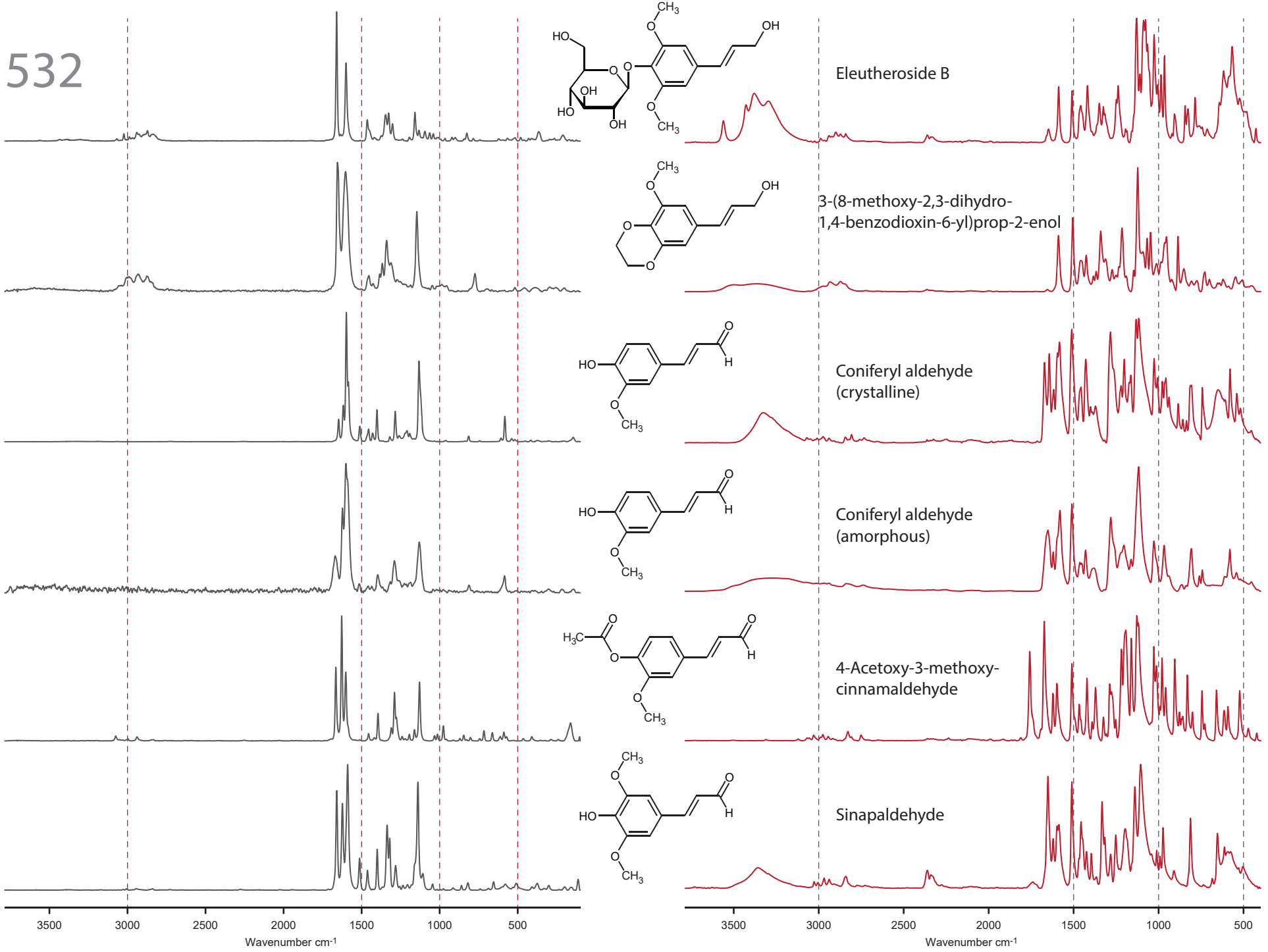

Fig. A3 (continued)

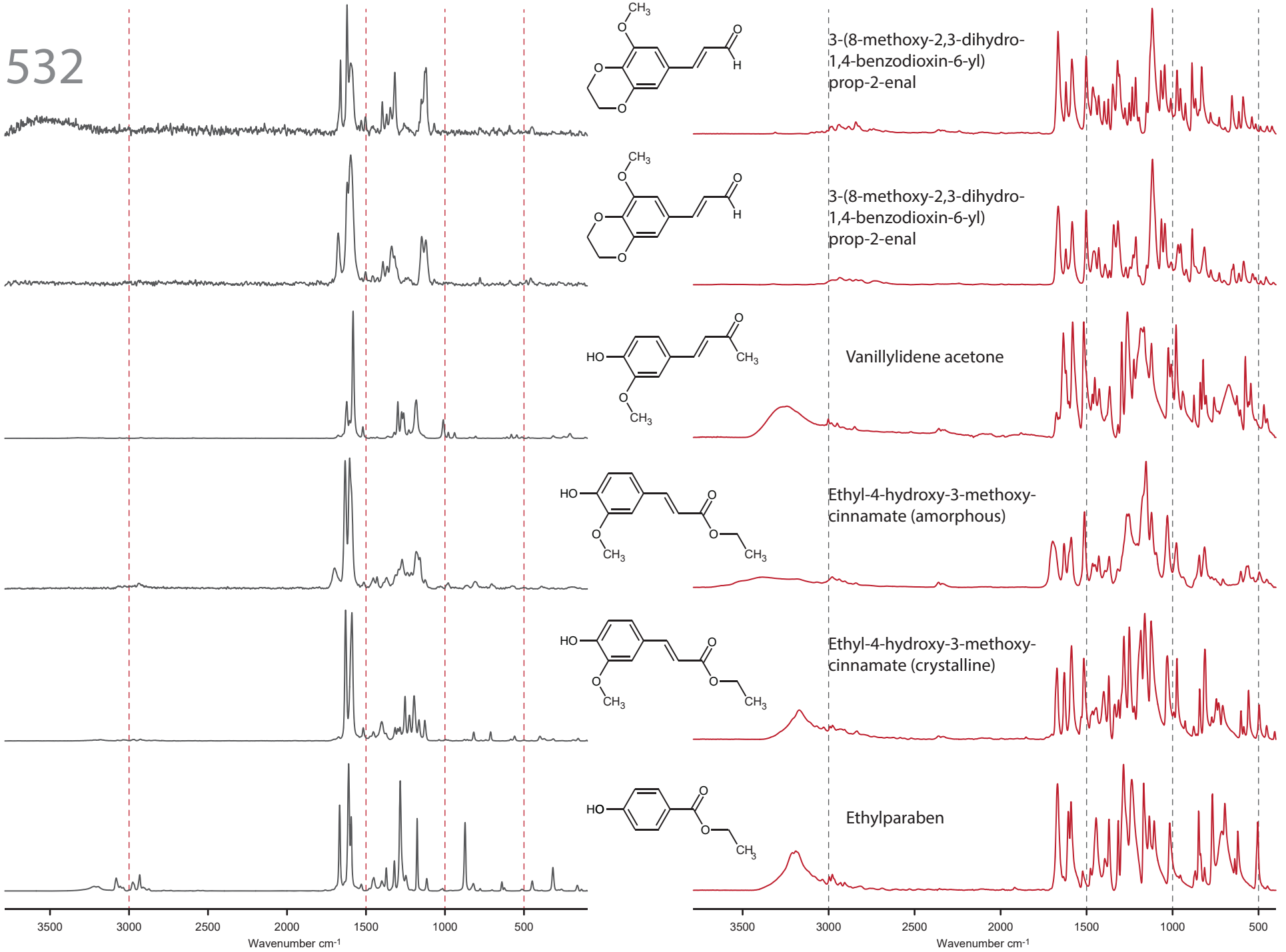

Fig. A3 (continued)

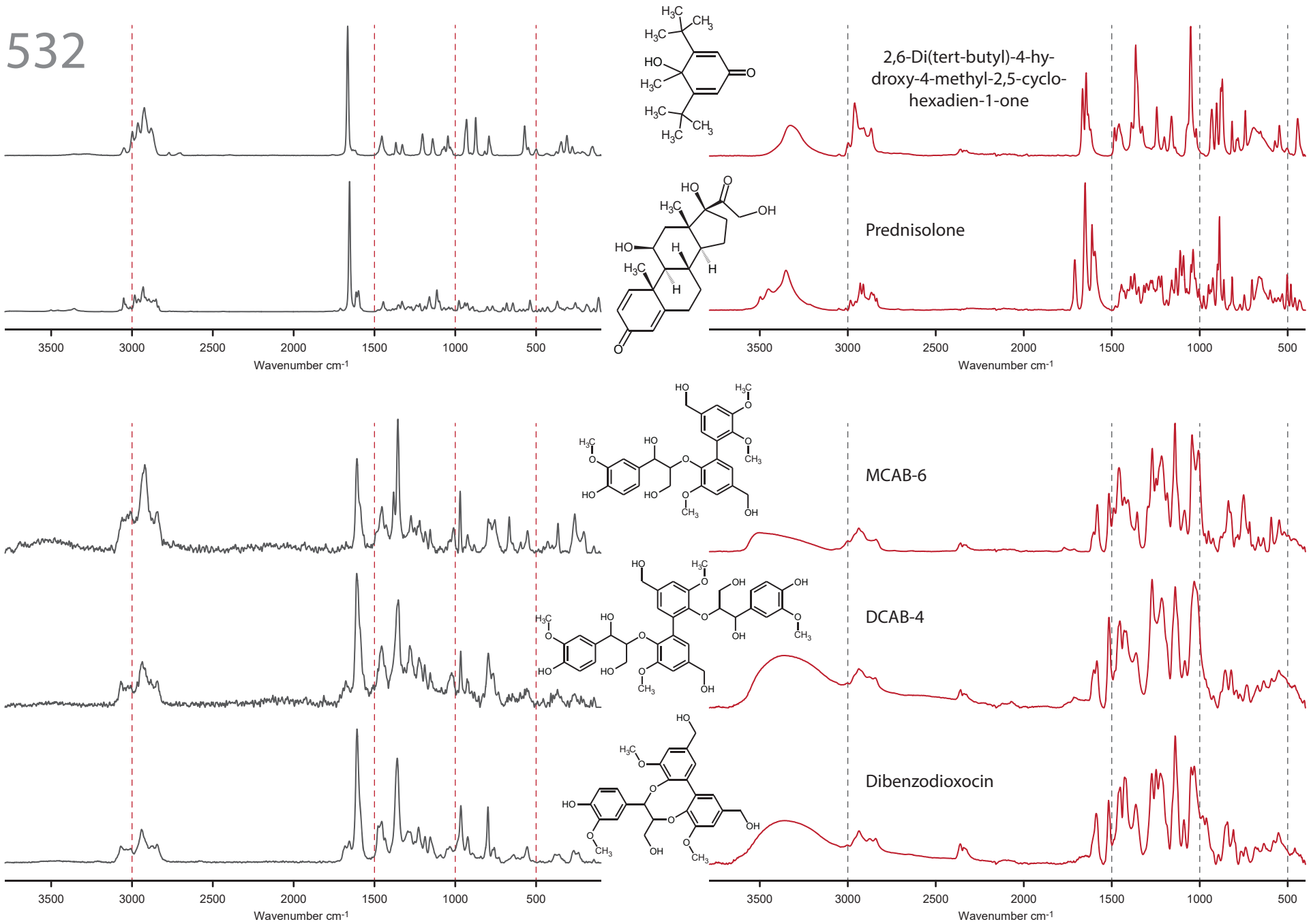

Fig. A3 (continued)

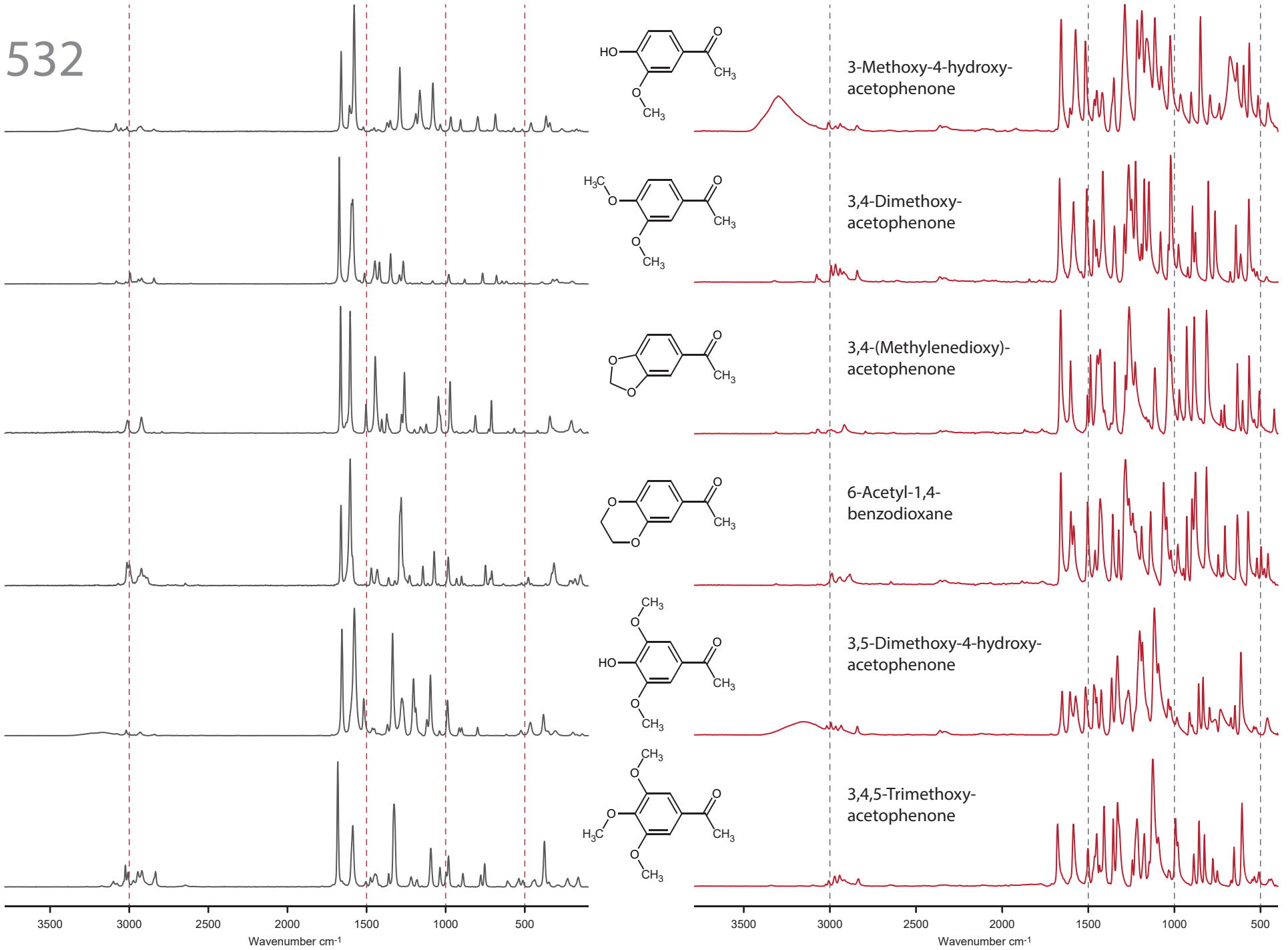

Fig. A3 (continued)

Danksagung

Ich möchte meinen außerordentlichen Dank meiner Chefin, Burgi Gierlinger, die mich vor fünf Jahren mit großem Vertrauen in die Arbeitsgruppe geholt hat. Sie hat in mich vertraut und mir immer freie Hand gelassen, sodas es mir möglich wurde, wertvolle Kenntnisse und Fähigkeiten zu entwickeln. Nicht unerwähnt soll Sabine Rosner bleiben, die mich überhaupt erst in den Universitätsdienst geholt hat und mir schon während des Studiums immer hilfreich zur Seite gestanden ist!

Mein Danke gilt auch José Toca-Herrera, der unermüdlich mit mir fachlich als auch über Gott und die Welt diskutiert hat und dessen Ansichten sehr bereichernd für mich waren.

Antje Potthast sei bedankt, dass sie immer ein offenes Ohr für meine chemischen Fragen hatte und sich bereiterklärt hat, Teil meines Beratungsteams zu werden.

I really want to cordially thank Adya Singh for the time he spent with me and my work and his patience correcting my writing.

I am also very grateful that Tom Elder was always ready to support me with his knowledge about lignin and computational chemistry and that he was willing to correct this thesis. Thanks, Tom!

Herzlich möchte ich mich auch bei Dieter Jäger bedanken, der fürsorglich immer ein offenes Ohr für Anliegen der Kollegen hat und einem große Mühen der Verwaltung abnimmt, die allzu oft den wissenschaftlichen Alltag durchdringen.

Dank gebührt auch Ronald Zirbs, ein Mann, mit dem man tiefgründige Diskussionen über die Dinge führen kann, die die Welt zusammenhalten und der wesentlich zum Funktionieren des Laboralltags beiträgt.

Meinen Kollegen, Bati, Martin, Nadia, Tayebeh, Nannan und Max, stellvertretend für alle anderen, sage ich herzlich Danke dafür, dass sie mir wie eine Familie hilfreich zur Seite standen, im Spiel wie im Ernst. Danke auch Walter Klug, ohne den die IT nicht funktionieren würde und der erst die Erstellung dieser Arbeit im Rahmen der Heimarbeit ermöglicht hat.

Dem anonymen Gutachter Luigi Kaiserschatt sei für die unzähligen kritischen Diskussionen zu meiner Arbeit gedankt, die mir schonungslos die Lücken in meinem Verständnis offenbahrt haben und es mir dadurch erst ermöglicht haben, meine Kenntnisse auf den heutigen Stand auszubauen.

Dass mein Leben nicht ausschließlich aus Arbeit für meine Dissertation bestand, haben folgende Personen zu verantworten: Manu, Walter, Patrick und meine Schwester Julia.

Unglaublich wichtig für mich und immer an der Versorgungsfront eingesetzt waren: Mutti, "die Tant" Trude und Onkel Willi, ohne die ja gar nichts funktioniert hätte.

Zum Schluss sei die wichtigste Person aufgeführt, meine zukünftige Frau 鸡鸡.